INDUCED SEISMICITY STUDY
GEYSERS RECHARGE ALTERNATIVE

SANTA ROSA SUBREGIONAL
LONG-TERM WASTEWATER PROJECT

Prepared for

City of Santa Rosa

and

U.S. Army Corps of Engineers

April 1996

Prepared by

GREENSFELDER & ASSOCIATES

and

PARSONS ENGINEERING SCIENCE, INC.

PLANNING · DESIGN · CONSTRUCTION MANAGEMENT

1301 MARINA VILLAGE PARKWAY, ALAMEDA, CA94501 · 510/769-0100

OFFICES IN PRINCIPAL CITIES

723129/94-16

for

HARLAND BARTHOLOMEW AND ASSOCIATES, INC.

INDUCED SEISMICITY STUDY
GEYSERS RECHARGE ALTERNATIVE

SANTA ROSA SUBREGIONAL
LONG-TERM WASTEWATER PROJECT

Prepared for
City of Santa Rosa
and
U.S. Army Corps of Engineers

April 1996

Prepared by

GREENSFELDER & ASSOCIATES
and
PARSONS ENGINEERING SCIENCE, INC.
PLANNING · DESIGN · CONSTRUCTION MANAGEMENT
1301 MARINA VILLAGE PARKWAY, ALAMEDA, CA 94501 · 510/769-0100
OFFICES IN PRINCIPAL CITIES
723129/94-16
for

HARLAND BARTHOLOMEW AND ASSOCIATES, INC.

TABLE OF CONTENTS

LIST OF TABLES AND FIGURES

1 INTRODUCTION

1.1 GENERAL

The purpose of this report is to evaluate the potential for increased seismicity at the Geysers Geothermal Field that could be caused by proposed subsurface injection of treated wastewater from the City of Santa Rosa. This study was undertaken in response to public concerns that injection induced seismicity could adversely impact neighboring communities.

This study is of one of a series of technical investigations performed to assist in developing the Santa Rosa Subregional Long-Term Wastewater Project Environmental Impact Report (EIR) which is in preparation by Harland Bartholomew and Associates, Inc. (HBA), for the City of Santa Rosa. The EIR utilizes the findings of the various technical studies to analyze potential project impacts, identify populations likely to be affected, assess the significance of impacts, and discuss possible mitigation measures. The Geysers recharge alternative for reuse of treated wastewater is discussed fully in the EIR.

This induced seismicity report was prepared by Greensfelder and Associates in cooperation with Parsons Engineering Science, Inc. Independent technical review of the draft report was performed by Dr. Bruce R. Julian, Seismology Section, U. S. Geological Survey, and by Dr. Ernest L. Majer, Lawrence Berkeley National Laboratory. Administrative oversight and coordination with the EIR was done by HBA.

1.2 PROBLEM STATEMENT

It has been established that geothermal field development activities at the Geysers Geothermal Field, including steam production and injection of water and steam condensate, have been causing microearthquakes. The zone of earthquake occurrence is closely associated with the geothermal field and the maximum magnitude of induced earthquakes appears to be limited to about magnitude (M) 4.5. Repeated low level seismic shaking has been reported in nearby communities of Cobb and Anderson Springs in the Collayomi Valley.

The design injection scenario involves gravity recharge in 10 existing wells in Unocal's lease area and a total water delivery rate to the Geysers of 19.5 million gallons per day based on a projected annual average for the design year. The principal objectives of this report are to predict the anticipated increases in Geysers microseismicity associated with the Santa Rosa wastewater project and to determine whether increased water injection would cause a significant increase in the incidence of felt effects for nearby residents (i.e., a significant impact) through probabilistic forecasts of earthquake intensity levels.

1.3 METHODOLOGY OF INVESTIGATION

The first step in the induced seismicity (IS) study was a review of technical literature regarding seismicity at the Geysers Geothermal Field to evaluate the characteristics and limiting parameters of induced seismicity. Other case history evaluations of vapor-dominated geothermal fields worldwide were examined for occurrences of induced seismicity. Reservoir-induced seismicity was also briefly reviewed.

Secondly, seismicity databases were compiled and precision of earthquake locations and magnitude thresholds for completeness were determined. The principal source of earthquake epicenter information was the Northern California Seismic Network (NCSN) maintained by U.S. Geological Survey (USGS). Data from the local seismographic networks operated by the geothermal power producers were also compared and utilized in detailed area studies.

A third step in the study was the compilation of geothermal field information. Extensive steam production and recharge (injection) well data were provided by Unocal Corporation. Locations of all wells, both producers and injectors, and well bore coordinates in three-dimensions for many injection wells, were compiled. The time histories of average monthly injected water volumes for wells in selected detailed study areas were compiled.

Detailed analysis of induced seismicity was performed for well clusters in four focused study areas. Two approaches were used in order to discriminate injection-related earthquake clusters from production-related earthquakes: 1. spatial correspondence between injection well locations and earthquake hypocenters and 2. time series correlation of injection rates versus earthquake frequency. Data sets that included confirmed induced seismicity were characterized in terms of rate of occurrence versus magnitude and rate of occurrence versus injection rates. A forecast rate of induced seismicity was developed by regression analysis of all earthquakes versus injection rates of all wells in the focused study areas combined.

Finally, maximum probable earthquake intensities (Modified Mercalli Intensity) and accelerations were calculated for a representative nearby community, the town of Cobb. The forecast induced seismicity rates were coupled with a geometric model that includes regional faults and sources of existing and future induced seismicity within the Geysers field. The calculations assumed Poisson distribution of earthquakes over time. An attenuation function appropriate for small earthquakes was utilized to calculate the decay of peak ground acceleration with source to site distance. For expressing site intensity for small earthquake magnitudes as a function of distance, an attenuation relationship was developed based on studies of magnitude versus felt area in California.

1.4 REVIEW OF INDUCED SEISMICITY LITERATURE

1.4.1 General

A review of the literature on induced seismicity in geothermal fields worldwide was conducted in order to better assess parameters which control and limit this phenomenon. The review discussion presents additional information on which to base a forecast of induced seismicity at the Geysers Geothermal Field which may arise from wastewater injection in deep wells. Additionally, reservoir-induced seismicity is reviewed briefly, as it may help illuminate the problem of induced seismicity.

The Geysers is termed a "vapor-dominated geothermal field," meaning that wells produce essentially dry steam which fills fracture porosity in reservoir rocks. However, rock-matrix porosity contains a substantial amount of liquid-phase water, some of which is produced. The only other developed field of this type is near Larderello, Italy. Induced seismicity may depend strongly on changes in pore pressure, and such changes are likely to depend on pre-injection conditions of vapor- or liquid-filled porosity. Therefore, attention is focused on the former. A search of the published literature indicated that a great deal more information concerning induced seismicity is available for the Geysers than for any other geothermal field. Liquid-dominated fields are covered, though briefly, because it is believed that those with saturated steam caps (formed as a result of production) may experience rock mechanical behavior similar to that at the Geysers. Only limited data are available for induced seismicity in this type of field.

While it is known that both production and injection of fluids can cause earthquakes, emphasis is placed on deep-well injection of water because this is the activity of concern in the present EIR/EIS. Production-related seismicity is described in order to assess its relative importance compared with injection-related seismicity, and also to better explain the various proposed causative mechanisms.

Important parameters of induced seismicity include the following: apparent maximum radius of influence of injection; maximum magnitude, magnitude versus frequency-of-occurrence relationships (the "b-slopes" of empirical curves); overall rate of occurrence; focal mechanisms and depths; regional

seismotectonic environment. For injection of fluids, significant parameters include mass flow rates, injection depths, consequent formation overpressures, reservoir properties such as pore pressure, temperature, and mineralogy.

1.4.2 Brief Description of the Geysers Geothermal Field and Its Development

Geological Aspects

The Geysers is located in the northern Coast Ranges of California, in a region characterized by youthful (less than 2 million years old) volcanism (the Clear Lake volcanics), high heat flow, numerous hot springs, active tectonism and moderate seismicity. This high level of geological activity is attributed to plate tectonics, in which the Pacific Plate moves northwesterly against the North American Plate, producing intense crustal deformation under compressive and shear stresses. This crustal deformation takes place mainly along northwest-trending right-lateral faults, many of which are known to be seismically active; the San Andreas fault is the most important of the active regional faults. Net annual right-lateral displacement (Prescott and Yu 1986) across this part of the Coast Ranges has been measured geodetically at nearly 5 cm (2 inches).

Principal rocks of the region are Mesozoic volcanic and sedimentary rocks, most of which belong to the Franciscan formation. These rocks have been intensely deformed (faulted and folded) by ongoing tectonism ever since their deposition more than 100 million years ago, and have been locally intruded by subsurface equivalents of the Clear Lake volcanics.

The Geysers Geothermal Field is positioned in the southwestern part of the Geysers-Clear Lake thermal anomaly, wherein heat-flow exceeds 4 heat-flow units (hfu). Within the Geysers field, heat flow is over 12 hfu (Walters and Combs 1991). For comparison, worldwide average heat flow is about 1 hfu. Most of the area of the thermal anomaly correlates spatially with the Clear Lake volcanic field, although the Geysers is positioned at its southwest margin. Intrusive equivalents (felsites) of the Clear Lake volcanics within the Geysers field have been dated at 1.6 million years in age, which is too old to produce the very high heat flow seen there (Walters and Combs 1991). The elevated heat flow, a pronounced gravity low, and other geophysical information not described here, have led many researchers to infer the presence of a magma body with top about 7 to 10 km (4 to 6 miles) deep beneath the Geysers field (McLaughlin 1981; Walters and Combs 1991).

Rocks of the Franciscan formation, principally greywacke sandstone, outcrop over most of the Geysers area and are present to depths of several thousand feet. At greater depths the aforementioned felsite intrusion is present. The Geysers Geothermal Field is traversed by two northwest-trending faults, the Sulphur Bank and Mercuryville, which appear to be old and inactive. However, two active regional faults, the Collayomi and Maacama, pass within 5 km northeast and 15 km southwest of the Geysers, respectively.

The Geysers Geothermal Field is a vapor-dominated reservoir of nearly dry steam, and has the largest energy production of any geothermal field in the world. The steam is present mainly in fractures (discussed below) and flows into wells which intersect them. The top of the geothermal reservoir has an elevation of -500 to -1,000 feet msl (mean sea level), and the shallowest steam entries run from -1,000 to -3,000 feet msl, all within the greywacke. The bottom of the reservoir is presumed to lie at about -4,200 feet msl, the greatest reported steam entry depth, in felsite (Thompson and Gunderson 1991).

Because of their importance to geothermal steam production, fracture patterns in reservoir rocks have been described by Thompson and Gunderson (1991). Within the greywacke, fractures have nearly random strike but tend to occur in zones with low dip, inherited from Mesozoic (Franciscan) structure. In the felsite, they occur in narrow zones with steep dip, related to recent and present-day strike-slip

tectonism; these fractures trend in all directions, but most abundantly to the northwest, in accord with young regional faulting.

Development History

This history focuses on the leases held by the Unocal-NEC-Thermal (U-N-T) partnership, which accounts for the bulk of Geysers steam and production. It is this area which will take the preponderance of wastewater which would be injected in the EIR alternative. Pacific Gas and Electric Company converts all U-N-T steam output to electric power using turbogenerators in some 16 power plants.

Current large-scale development of the Geysers Geothermal Field began with drilling in 1955, and the first 12 MW power plant came on line in 1960 (Barker et al. 1991). Sustained development began in 1972, with an average rate of power development of 67 MW/year through 1981, which increased to 150 MW/year for the period up to 1989. Steam deliverability on the part of U-N-T peaked in 1987 at about 16 million lbs/hr, and power output peaked at some 1,100 MW. Total production was nearly 30 million lbs/hr in 1987. In 1992, total power output from the Geysers was approximately 1,300 MW. U-N-T has drilled a total of 378 wells, of which 82 have been abandoned. The balance are used either for production, injection, or pressure observation.

It was projected by Barker et al. (1991) that U-N-T production would decline by 50 percent in about 10 years (around 2001). Today, 246 U-N-T wells are in concurrent production (Ed Voge, personal communication 9/12/95). The role of water injection into former production wells is discussed in Section 1.2.3.

Initial steam pressure in the reservoir has been estimated at about 514 pounds per square inch, absolute (psia), but that had dropped to as low as 200 psia in the central U-N-T area by 1988 due to steam withdrawal; field-margin pressures remained relatively high, exceeding 400 psia (Barker et al. 1991). This pressure drop has caused the decline in production seen since 1987. Steam temperatures have apparently not changed much, and run about 240 C (4640 F) (Klein and Enedy 1991).

Water Injection

The decline of steam pressure and production since 1987 is a key factor motivating consideration of the wastewater injection alternative under consideration. The economic objective of injection is to use injected water to transfer heat from hot reservoir rock and to maintain or increase steam pressure, thereby extending the production lifetime of the field, without damaging current production.

In 1969 excess steam condensate from power plants began to be disposed by injection into former production wells, due primarily to regulatory concerns about the impact of land disposal on the quality of surface waters. This was because of the presence of boron and ammonia in reservoir steam and condensate. It was also recognized that injection could improve steam production after several years (Barker et al. 1991). Greatly increased injection volumes have accompanied development of the Geysers Geothermal Field, and long-term injection management has been guided by reservoir performance studies, including injection tests in the areas of greatest pressure decline. Aquifers are protected by federal and State of California agencies.

By 1986 the annual mass of water injected by U-N-T had grown to 19.2 million tons (approximately 12 million gallons/day (mgd) or 8,500 gallons/minute (gpm)), and after a brief decline, this amount was nearly realized again in 1993 (Barker et al. 1991). Since 1980, injection has been augmented with seasonal freshwater runoff collected in Big Sulphur Creek, to the extent of 2 to 8 million tons/year (1 to 5 mgd). Currently, U-N-T uses a total of 26 injection wells, although not all are in service at any given time.

Beginning in 1997, up to 7.8 mgd (5,400 gpm) of wastewater transported by pipeline from the Clear Lake Basin (from Lake County Sanitation District, or LACOSAN) is scheduled to be injected into 15 wells. This water is to apportioned equally among three field operators: U-N-T, Calpine, and NCPA.

A number of studies and large-scale tests of injection have shown that, when cool injectate flows into fractures with superheated surfaces, it will flash to steam which is then produced from nearby wells, and more than 40 percent of injected water is recoverable as steam; in the most depleted portions of the reservoir, steam flow from nearby producers may be greatly enhanced (Barker et al. 1991; Voge et al. 1994; Enedy, Enedy, and Maney 1991). However, if the injectate reaches rock volumes with too little superheat, then liquid "breakthrough" may occur in nearby production wells, which damages production. Avoidance of "breakthrough" (i.e., liquid injectate flowing into production well) is a key concern in the design of injection schemes.

1.5 INDUCED SEISMICITY IN THE GEYSERS GEOTHERMAL FIELD

1.5.1 Overview

A considerable amount of research concerning induced seismicity (IS) in the Geysers Geothermal Field has been accomplished over the past 20 years. Much of the work on induced seismicity is combined with broader studies of earthquake mechanics and reservoir dynamics, including seismic wave propagation velocities. None of these studies attempts to determine the portion of total seismicity which may be induced by exploitation of the geothermal field.

The Geysers is situated in the northern California Coast Ranges, a seismotectonically active region with numerous active faults and a moderate level of historic seismicity. In this chapter, regional seismotectonics are described only as necessary to help interpret induced seismicity, and in a conclusive manner. Detailed presentation of the subject is given in Chapter 7.

Although baseline seismicity at the Geysers is not well documented, it appears that earthquakes began to occur there by the early 1960s, shortly after start-up of the earliest significant steam deliveries (producing 11 MW of electric power) in 1960. Studies of induced seismicity at the Geysers began around 1971. By 1972, regional seismographic capabilities were greatly enhanced, and numerous small earthquakes with epicenters in the Geysers Geothermal Field began to be routinely reported. Since 1975 more than 20,000 microearthquakes, with $0.7 \leq M < 3.0$, have been located in the Geysers area; some 300 earthquakes have had $3.0 \leq M \leq 4.5$. Seventeen earthquakes with $M \geq 2.3$ were felt in the town of Cobb between 1973 and 1985 (the last year of available felt records); many of these shocks were also felt in nearby communities.

Based on the documented parallel increase of seismicity rates and field development, including steam production and steam condensate injection, it is established that these activities trigger earthquakes (these matters are discussed in detail below). A reasonably unambiguous correlation of injection and seismicity (below 2 km) in the central Geysers is revealed by projections of well courses and hypocenters onto lines of section at a 1:1 scale (Unocal internal memorandum, B. Cumming to D. Hackley 1/11/96).

Space-time correlations between steam production and condensate injection in deep wells have been well documented and are described below. It appears that induced seismicity here represents a triggered release of natural tectonic strain present in the earth's crust. Several mechanisms (physical models), described below, have been proposed to explain the generation of earthquakes by fluid injection or withdrawal, but none have been generally accepted as proven for the Geysers.

1.5.2 Studies of Induced Seismicity

Seismicity associated with exploitation of the Geysers was not documented until 1972, because seismographic networks did not then have the capability to detect small-magnitude earthquakes

characteristic of the Geysers. As a result, no adequate baseline exists to identify local microseismicity (microearthquakes with magnitudes less than 3) prior to geothermal development. Because of its critical importance to induced seismicity research, the development of seismographic networks in the region is described.

Before 1972, the only seismographic network in the region was operated by the Seismographic Station of the University of California, Berkeley, with nearest station in Calistoga, about 30 km south of the Geysers. The smallest earthquakes whose epicenters could be located within the Geysers area had magnitudes around 3. However, numerous microearthquakes with magnitudes less than 3 within 60 km of the Calistoga station were recorded at Calistoga from 1962 to 1977. Based on correlative information from the US Geological Survey (USGS) seismographic network from 1972 onward, it is reasonable to conclude that many of the pre-1972 events had epicenters in the Geysers area: the rate of occurrence of events recorded at Calistoga during 1975-77 was nearly twice that during 1962-63, and this was almost certainly related to increased power production in the Geysers Geothermal Field (Eberhart-Phillips and Oppenheimer 1984).

One of the earliest studies used eight portable seismographs to record and locate 53 microearthquakes during a three-week interval in spring 1971 (Hamilton and Muffler 1972). Twenty-two epicenters were concentrated in a narrow zone, 4 km by 1 km, lying along the north side of Big Sulphur Creek, where the bulk of all steam wells (more than 50) and two injector wells were located; earthquake magnitudes were estimated to be mostly less than zero. The authors concluded that the data did not indicate a case of induced seismicity; however, research performed since 1971 suggests that at least some of those microearthquakes were probably induced by steam production, and possibly by condensate injection as well.

By 1972, the regional seismographic network operated by the USGS, then named CALNET and now called NCSN (Northern California Seismograph Network), was routinely providing hypocentral locations for most events with $M \geq 1$ in the Geysers area (Bufe and Ludwin 1980).

A note about magnitudes: the NCSN and other local and regional networks report magnitudes of earthquakes with $M < 3$ using the coda-length magnitude scale, almost exclusively. This scale yields values practically the same as Richter magnitude for $M \leq 4$, and the differences are not significant for the purposes of this study. Hence, the two scales are not distinguished herein, except for discussion of events with $M > 4$.

In 1975, NCSN's capability in the Geysers was greatly increased by the addition of four new stations located at the field's periphery. With this enhancement, NCSN began to provide hypocentral data for *all* events with $M \geq 1.2$ (Oppenheimer 1986). Since 1975, NCSN hypocentral coordinates have typically had a precision of about 0.4 km (1,300 feet) horizontally and 0.6 km (2,100 feet) vertically; horizontal accuracy is on the order of 800 feet or better. NCSN currently incorporates two stations inside the Geysers Geothermal Field and six more within 4 km (2.5 miles) of the field perimeter. Two other networks (one owned by a partnership among Unocal, NEC, and Thermal Power; and another owned by Lawrence Berkeley Lab) began operation after 1988, and are discussed below. Figures 1.1 and 1.2 show the locations of seismograph stations in these three networks.

The first investigators to document features of seismicity in the Geysers area over a long period time, from 1972 to 1980, were Bufe and Ludwin (1980). Their research related thousands of NCSN hypocenter locations to steam pressure conditions and to locations of production and injection wells. They examined the temporal variations and spatial clustering of seismicity, and related these to the onset of production at two power plants. Faulting mechanisms and crustal deformation accompanying seismicity were also examined. Their study reached several interesting conclusions:

1) Two clusters of seismicity persisted through the period 1975-1980, and these coincided with the most heavily exploited area of the steam field (northwest and central part of the Geysers). Steam production and seismicity are spatially correlated. Focal depths ranged from about 0.5 to 4.5 km (1,600 to 15,000 feet) below land surface, and most were between 1.0 and 3.5 km. Slopes ("b" slopes) of magnitude-frequency of occurrence curves were calculated in each 0.5 km depth interval, and ranged from 0.7 to 1.45, averaging around 1.2.

2) The two largest earthquakes between May 1975 and December 1978 had M = 3.1 (12/22/76) and 3.3 (9/22/77), and were centered near the two injection wells (DX-7 and LF-3) most distant from production wells. This suggested a link between fluid injection and larger seismic events, with $M \geq 2.5$.

3) Initiation of steam production for Unit 15 in June 1979 was attended by an increase in seismicity within two weeks. This seismicity occurred in a tight cluster about 0.5 km north of injection well PEC A-6. The area had previously displayed virtually no seismicity.

4) Between 1972 and 1977, the size of the largest annual events increased from M = 3.1 to 3.8, paralleling the increase in steam production.

5) First-motion data suggested a great heterogeneity in the local stress field, although the orientation of maximum and minimum horizontal compressive stress averaged north-northeast and west-northwest, respectively, in accord with the regional pattern.

Many of these conclusions were repeated in a publication of Bufe et al. (1981).

In 1984, a major study was published by Eberhart-Phillips and Oppenheimer, based on data for 7,215 earthquakes recorded during May 1975 to February 1982. Their conclusions follow, and referenced wells and operating unit numbers may be seen in Figure 1.2.

1) Based on spatial and temporal relationships between production and injection wells and attendant mass flows, seismicity in the Geysers area is induced by geothermal production.

2) A significant clustering of seismicity near production wells is apparent, but was not revealed in earlier studies. All clusters are within or below production areas, but not all wells have nearby seismicity clusters. Earthquakes are deepest in the areas of oldest production. Also, aseismic areas within the Geysers field correlate with the local absence of geothermal production.

3) The sharp southwestern boundary of the seismicity appears to be structurally controlled by the northeast-dipping Mercuryville thrust fault.

4) With the increase of power production by some 70 percent in 1979-1980, seismicity developed near the newly producing areas.

5) Seismicity occurs on rock fractures whose length is less than 1 km, and it is more or less continuous in time. That is, seismicity is not time-clustered in "swarms."

6) Statistical cross-correlations for several wells between monthly numbers of events and monthly volumes of steam produced and fluid injected revealed no consistent correlation between injection and seismicity. Nor was there consistent correlation between steam production and seismicity for wells in production longer than 7 years.

Cross-correlations of monthly injection volumes with monthly local seismicity for seven wells, presented by Eberhart-Phillips and Oppenheimer (1984), have been reviewed for this EIR/EIS. Although they did not find consistent correlation of injection and induced seismicity for all (seven) injection wells studied, correlograms presented for three injectors (DX-8, HJ-9, and GDC-5313) show correlation coefficients which exceed their 95 percent significance levels for time lags ranging from 0 to 2 years. The authors reported three cases where the onset or cessation of injection at a particular well had little effect on nearby seismicity and inferred weak or non-existent correlation of injection and induced seismicity. However, in his review of this article, Stark (1990) noted that in all three of these cases injection into the area was simply re-routed to nearby alternate injectors, but not changed significantly; the re-routing of injectate from well LF-3 to LF-23 in 1979 is a good example (this is analyzed in Chapter 4 herein).

The fact that the other four injectors do not show such correlation may be influenced by the manner in which space volumes were defined for selecting earthquakes to be correlated. Epicenters were selected within a 1 km radius of each injection well (presumably the wellhead) and *for all depths*. However, seismicity associated with injection tends to have depths exceeding 2 km (Stark 1990). It is possible that inclusion of seismicity shallower than 2 km may have incorporated production-related seismicity, somewhat confusing the picture, although Eberhart-Phillips and Oppenheimer stated that their correlations for various depth intervals (not presented) were similar to those for all depths.

Correlations were also presented (Eberhart-Phillips and Oppenheimer 1984) for overall production within the Big Geysers and the "Lakoma Fame" area (occupying most of Units 9-10), but not for individual production wells; these did not show significant correlation at the 95 percent confidence level. We suspect that this low correlation may have been related to either the relatively long time after inception of production, or to intermixing of injection related seismicity, in these areas.

Oppenheimer (1986) made some further observations as follows:

For the entire Geysers field during the period 1976-1984, annual numbers of earthquakes with $M \geq 1.2$ are well correlated with the annual mass of steam withdrawn. Earthquake mechanisms show no spatial consistency over short distances, as had been noted by Bufe and Ludwin (1980); they appear to occur on small, randomly oriented, preexisting rock fractures. Nonetheless, the stress field is consistent with regional tectonic strain, with principal extension oriented east-southeast. However, geodetic surveys show that the strain rate in the Geysers area is nearly 50 times larger than in the surrounding region.

In 1990, excellent correlations between injection and earthquakes were reported within the Unocal leasehold (Stark 1990). Stark utilized data obtained with the seismographic network operated jointly by Unocal, NEC, and Thermal Power (U-N-T) and by the NCSN. The U-N-T network began operation late in 1988, and was augmented in September 1989 to its present configuration of 21 stations with average spacing of one mile (see Figure 1.1 for station locations). It locates all earthquakes with $M \geq 0.5$, with an accuracy averaging 0.2 km (700 feet) horizontally and 0.4 km (1300 feet) vertically

Stark (1990) concluded as follows:

1) Earthquake clusters associated with injection wells form a rough three-dimensional image of the injected liquid, and that spatial correlation of earthquakes and injection wells is more apparent for hypocentral depths deeper than about 4,000 feet below sea level, which is about 7,000 feet (2.1 km) below land surface.

2) Temporal correlation between the onset of injection and earthquakes is generally clear, and was observed for 10 injection episodes. (This includes wells LF-3, LF-23, DX-61, GDC-18, GDC-21, GDC-26, and six unnamed wells.) The case of well GDC-18 is interesting, because the NCSN hypocenters deeper than 3,000 feet below sea level also show an excellent space-time correlation with injection rate.

3) Isotopic analysis of produced steam shows that the flashed injectate is heavier than the native steam/water in the rock, and that steam wells producing a significant percentage of heavy steam lie within extended earthquake clusters. Some of these clusters are found in zones where reservoir pressure is higher than in the nearest injection wells. The seismicity appears to occur where the injected water flows as a liquid driven by gravity or hydraulic pressure.

4) Maximum depth of hypocenters is 12,000 feet below sea level (about 5 km below land surface), which suggests the presence of a permeability barrier, and reservoir bottom, at that depth.

5) Not all injection is accompanied by seismicity, and some seismicity, especially the shallower events, does not correlate with injection.

The question of maximum radius of influence of injection (or production) wells for induced earthquakes was not resolved by either Eberhart-Phillips and Oppenheimer (1984) or by Stark (1990). Stark's figures show earthquakes up to about 5,000 feet from nearest injectors, but since the figures do not show production wells, and some of the events were likely caused by production, one cannot judge the maximum radius of influence of injectors.

Lawrence Berkeley Laboratory (LBL), with funding from the U.S. Department of Energy and in cooperation with the geothermal operators, has operated a highly sensitive seismograph network -- in the northwestern Geysers since 1988, and in the southeastern Geysers since January 1994. The threshold for complete detection and reporting of earthquakes is M = 0, and the hypocenter location precision is about 100 m horizontally and 200 m vertically (Art Romero, pers. commun. 5/18/95). This location precision is the best achieved to date in the Geysers area.

Reporting seismic monitoring by LBL, Romero et al. (1994) concluded as follows: "Spatial and temporal patterns of seismicity exhibit compelling correlation with geothermal exploitation. Clusters of seismicity occur beneath active injection wells and appear to shift with changing injection activities." The article presents cross-sections of two clusters (year 1988) around injectors "A" and "B" in the CCPA leasehold (in the northwest Geysers area). These show events at maximum distances some 1/2 km (1,600 feet) from the two injectors, at depths exceeding 1.1 km (3,600 ft) and 1.8 km (5,900 ft) below a datum plane at 0.7 km (2,300 ft) above msl.

A more recent article from LBL concerning the southeast Geysers area (Kirkpatrick et al. 1995) shows earthquakes in cross-section around injection well DV-11 and production wells DV-2, and DV-4. For the three wells, essentially all events lie within 1/4 km (800 ft) horizontally of the wellbores, and at depths from 1.5 km (5,000 ft) to 3.4 km (11,000 ft) below land surface. Hypocenters near DV-11 "exhibit a

striking correlation with movement of injectate and injectate-derived steam." They state that the events are located within the felsite intrusion which underlies most of the Geysers Geothermal Field (although only the top of felsite is indicated in the cross-sections). It is also concluded that the steam reservoir is relatively aseismic at elevations between -1,000 ft and 1,000 ft (-0.3 km to 0.3 km) msl. It was noted that events at DV-11 did not begin until one month after initiation of continuous injection; cessation of injection was followed about one month later by a drop in seismicity.

Kirkpatrick et al. (1995) also compared focal mechanisms (moment tensors) of events near the injector (DV-11) and the producers (DV-2 and -4). Orientations of pressure (P) and tension (T) axes of stress are more clustered for the production-related events than for those which are injection-related, with many P-axes gathered strongly in NE-SW alinement, and some T-axes in north-northwest/south-southeast alinement. This is said to be consistent with orientation of the regional geodetic strain field -- N79°W extension and N11°E contraction (Prescott and Yu 1986) -- and with many of the P and T axes obtained by Oppenheimer (1986). However, it appears that there is a divergence of at least 30 degrees between the these axial clusters and the corresponding geodetic trends. Were this difference in focal mechanisms characteristic of all injection and production related events, it would imply that production triggers release of regional tectonic stress to a greater degree than does injection, and that injection tends to create its own seismic stress perturbations.

The moment-frequency relationship for the southeast Geysers data set was examined by Kirkpatrick et al. (1995), and it was noted that the slope of the curve increases at a moment of 3×10^{18} dyne-cm (or M = 1.7). Their hypothesis was that the larger events have causes related to tectonic stress while the smaller events are related to production, although this theory was not tested.

Greensfelder (1993) reported a correlation between earthquakes and injection in well McKinley-5 (MCK-5), in Unit 13, southeast Geysers area. An abrupt onset of microseismicity near this well early in 1980 follows the initiation of injection by about three months. Until 1986, injection and numbers of earthquakes within 3,000 feet (0.9 km) of MCK-5 appear to be roughly correlated. Following 1986, the correlation disappears, which might be caused by the overall decline of injection volumes to this well.

In reviewing microseismicity related to injection in wells GDC-18 and DX-61, which was first described by Stark (1990), Barker et al. (1995) concluded that the magnitude ceiling for induced seismicity caused by injection appears to be limited to magnitudes less than M = 2.0, as observed at Lardarello, Italy (described later herein).

Summary

On balance, previous studies of induced seismicity in the Geysers Geothermal Field indicate that injection and earthquakes are correlated phenomena, although the relationship appears to be highly variable and poorly understood. The relationship is more evident for some wells, or portions of the Geysers area, than for others, and it appears to vary with time, as well as with detailed temporal variation of injectate flow. Induced seismicity is also related to production, although the correlation is not well resolved. Some or much of this apparent variability may be the result of imprecision in hypocentral data or in analytical procedures, resulting in inadequate resolution of induced seismicity characteristics. As for analytical procedures, it appears that use of time intervals smaller than one month would show more consistent correlation of changes of injection rate with seismicity.

1.5.3 Cause of Induced Seismicity

Several investigations have addressed the causative mechanisms for induced seismicity in the Geysers Geothermal Field, but the subject remains poorly understood. All proposed mechanisms involve a change in the elastic response of reservoir rocks to the ambient tectonic stress and strain fields. They consider the mechanics of existing rock fractures -- how effective and failure stresses, or coefficients of friction, may be

altered by changes in reservoir pressure and temperature, and fluid volumes withdrawn or injected. There is a presumption that, prior to exploitation, the state of stress in reservoir rocks was quite near the failure condition, where earthquakes can be easily triggered.

Allis (1981) presented a concise summary of proposed mechanisms for induced seismicity related to *steam production* at the Geysers. Geodetic studies have demonstrated considerable volumetric contraction in the field, with subsidence and horizontal contraction rates observed to be several cm/year during the 1970s, and that the rate of seismicity is some 35 times greater than in the surrounding region. Also, regional geodetic data confirm ongoing fault creep and tectonic strain accumulation throughout the greater region. He considers three basic possible mechanisms for induced seismicity: thermal contraction, pore pressure changes, and coefficient of friction changes. Thermal contraction is unlikely, because the reservoir temperature has remained essentially constant at about 240ºC. Volumetric contraction due to fluid withdrawal is also a possible cause of induced seismicity. The principal difficulty in choosing among these models concerns initial conditions, prior to exploitation: namely, whether the Geysers field was liquid-dominated or dry-steam dominated.

It seems likely that boiling pore water at production depths is the source of produced steam. This must be accompanied by a decline in rock temperature. According to the thermal contraction model, this temperature decline reduces pore pressure in rock cracks, which may alter shear stresses at the crack tips, and this could trigger earthquakes.

The pore-pressure mechanism relies on an increase in confining pressure (i.e., normal stress across cracks) as pore pressure declines during exploitation. The increase in confining pressure is unknown, but would be much greater (50 to 200 bars) if the Geysers field were initially liquid-dominated, rather than vapor-dominated (perhaps 15 bars). It is believed that the Franciscan terrain of northern California is overpressured (hydrostatic approaching lithostatic pressure), which would favor stable sliding (aseismic slip or creep) over brittle (seismic) failure. A rise of confining pressure should tend to change the response of reservoir rocks from aseismic slip (creep) to stick-slip (brittle fracture).

Coefficient of friction in cracks may be increased by deposition of silica, caused by boiling of water as production continues. This would also have the effect of promoting brittle failure, triggering earthquakes.

It is entirely possible that all three of these mechanisms are to some extent effective in producing earthquakes related to steam withdrawal at the Geysers field.

Concerning induced seismicity due to *injection*, the most likely mechanism is an increase of pore pressure, which will reduce the confining pressure (normal stress) across cracks, effectively decreasing the failure strength of the reservoir rock. This is according to the classical Hubbert-Rubey theory (Hubbert and Rubey 1959). Another possible mechanism is that the increased mass (weight) of water (the injectate) will increase shear stress in underlying rocks. This occurs because deviatoric stress (the differential stress that causes distortion and potential failure) is increased by the rise in vertical compressive stress. Of course, these two mechanisms may operate together for increased overall effect. Some researchers have stated (e.g., Stark 1990) that thermal contraction due to cooling of reservoir rocks by cool injectate may be an important mechanism. It is possible that all three of these mechanisms are less important than the stress changes caused by reservoir compaction associated with matrix pore pressure decline, due to mass withdrawal.

Comparing all of the above-described mechanisms for induced seismicity, it seems that both increases and decreases in rock strength, caused by changes in confining pressure (normal stress across cracks) or in coefficient of friction, may be the principal causes. For steam withdrawal, induced seismicity would seem to be caused by an increase in rock strength, while for injection, induced seismicity should be caused by a decrease in rock

strength (or possibly by vertical mass loading of injectate). These mechanisms may not be contradictory, as they appear to operate independently over distinct reservoir volumes located within 1 km (3,000 feet) of any well. Production-induced seismicity may occur under stresses nearer to regional ambient tectonic conditions than does injection-induced seismicity. This is suggested, but not resolved, by the work of Kirkpatrick et al. (1995), as described above.

1.6 INDUCED SEISMICITY IN OTHER GEOTHERMAL FIELDS

Literature review indicates that research on induced seismicity in geothermal fields, worldwide, is practically insignificant when compared with that for the Geysers Geothermal Field. Larderello (Italy) is the single, and outstanding, exception. Induced seismicity has clearly been triggered in several geothermal fields besides Larderello, but relationships between their induced seismicity and that in the Geysers Geothermal Field do not appear to be particularly instructive.

1.6.1 Larderello, Italy

Induced seismicity in the Larderello, Italy geothermal field is, of all worldwide cases, most relevant to the Geysers field. This is because it, too, is a dry steam field. Batini et al. (1985) conducted and reported a study of induced seismicity at Larderello. In 1985, this field was producing 430 MW of electric power from numerous wells. Seismographic monitoring was initiated in 1978, with two purposes: 1) correlation of seismically active geologic structures with geothermal production; 2) monitoring of seismicity related to geothermal wells, especially with regard to reinjection of condensate. In 1985 there were more than 15 active reinjection wells.

More than 1000 microearthquakes were detected within the Larderello-Travale area between 1978 and 1982, with Richter magnitudes 0.0 to 3.2. Activity was quite scattered, but notable clustering also took place. In general, focal depths were less than 8 km, usually 2 to 6 km. The distribution of magnitudes (magnitude vs. frequency of occurrence) was found to be bilinear, similar to that seen in the Geysers field. The b-slope of the curve is 1.01 for $M < 2.6$, and 1.61 for $M > 2.6$. (At the Geysers, the break in b-slope occurs at $M = 3.3$, and the slope values are very similar). The authors postulated that there exists a limiting magnitude which is "not very high, and is characteristic of the zone." Study of focal mechanisms indicated that compression and tension axes were consistent with the type and orientation of known faults.

Reinjection data available for correlation with seismicity are limited to volumes (actually, average flow rates) injected only during drilling, and there are no data on sudden variations of injection. Therefore, no close correlations with earthquakes can be made. Hence, a more generalized analytical approach was adopted. The frequency of microseismicity increased from 1978 to 1982, during which time the flow of reinjectate increased in all wells. However, the frequency of events with $M > 2$ did not change significantly. They concluded that reinjection either (1) triggers lower-energy events, but not those of higher-energy, or (2) favors release of energy and so "does not permit high tensions to accumulate."

The report of Batini et al. (1985) makes no comment on a relationship (if any) between production and microseismicity.

1.6.2 New Zealand

New Zealand geothermal fields are hot-water dominated, and so induced seismicity there has a questionable relationship to that in the Geysers field.

Induced seismicity associated with reinjection under pressure has been reported in the Wairakei geothermal field, although only very limited data are available. At the nearby Ohaaki field, very brief seismic monitoring revealed no induced seismicity in association with reinjection tests performed.

Wairakei Field

The Wairakei field consists of a 200-m thick steam cap, probably formed as a result of boiling induced by production, overlying a deep liquid zone; the deep-liquid zone has its top at a depth of approximately 350 m.

In 1984, microseismicity was monitored during a six-week-long cold-water injection experiment (Sherburn 1984). Induced seismicity took place, with 90 out of a total of 124 microearthquakes occurring during the nine-day duration of two tests. No simple correlation between the rate of seismicity and the rate of injection (injectivity), wellhead pressure, or step increases of injectivity were observed; however, earthquakes ceased entirely when injection stopped.

The test well had total depth of 1,450 m, and was cased to 80 m. Permeability was low except for a single zone of high permeability at 1,311 m. At this depth, flow was into the deep liquid zone of the reservoir. Injection gauge pressure was 20 bars under an injectivity of 400 tonnes/hr of cold water. Maximum excess pore pressure at 1,311 m was 52 bars. Microearthquakes started 23 hours after start of the first test, and nine hours after start of the second. The delay was thought to be related to a critical volume of water required to develop sufficient excess pore pressure to cause earthquakes.

Only 19 of 124 microearthquakes had their epicenters located, and these were distributed in an elliptical zone, and located as far as 3.3 km from the injection site. Epicenters tended to migrate away from the injection site, suggesting control by pre-existing fractures. The b-slope of the magnitude-frequency data was 0.6. Focal mechanisms agreed with regional tectonic stress patterns of dextral shear in the Taupo fault zone (Sherburn et al. 1990).

Post-test leveling indicated ground uplift had occurred, with a maximum value of 4 cm, and was detectable to a radius of 500 m, at the end of the second test.

Earthquakes had not previously been recorded in association with injection in New Zealand: in 1982, a five-week-long microearthquake survey indicated minor activity along the Taupo fault zone, and it was concluded that production had not caused much change in seismicity.

In 1988-1989, another reinjection test was conducted, and had no associated induced seismicity. The test used a single well, flowing 570 tonnes/hr at a depth of 450 m, under gravity alone, and permeability was much higher in this test than in the 1984 test (Hunt et al. 1990). No induced seismicity was observed.

Ohaaki Field

Ongoing reinjection at this field causes no earthquakes, even though wellhead pressures run 20 to 30 bars, similar to pressures of the 1984 Wairakei test. Formation overpressures were about 25 bars in this test, and 50 bars in the 1984 test. It is thought that the lack of induced seismicity is related to the prevailing natural, essentially aseismic, environment.

1.6.3 Philippines

Philippine geothermal fields are hot-water dominated. Seismic monitoring results published for these fields have been limited to the developmental and early production phases of geothermal exploitation, and really resolves no questions of induced seismicity causation. According to Bromley et al. (1987), the Puhagan field, in southern Negros, is the only Philippine geothermal field exhibiting a clear correlation between increased local microseismicity and the development/early production phases of a geothermal power project.

Tongonan Field

In this field, seismic monitoring for three years revealed a small, localized *reduction* in seismicity within the reservoir (Bromley and Rigor 1983). This suggested that creep was absorbing strain along this segment of the Philippine fault; outside the field, frequent swarms of microearthquakes occur along this fault at shallow depth, and show no correlation with reinjection or production.

Puhagan Field

Swarms of microearthquakes, with $M < 2.5$, appear to be triggered by both production and reinjection; the vast majority of reported events occur in a narrow zone, striking west-northwest, in the production sector of the field, with very little activity in the reinjection sector (Bromley et al. 1987). This narrow zone correlates with a known fault trace, and most events have first motions consistent with normal or oblique slip on steep northwest-trending planes. The b-slope is 1.30.

Prior to start-up of production, the field was essentially quiescent, with less than one event/day. Seismicity began with testing of the power plant, with mass flows of 150 kg/s. During the test period, from May 1983 through April 1984, more than 5,000 microearthquakes were recorded.

Correlograms were computed relating formation water pressures and injected volumes to microearthquake counts. Only pressure was found to be correlated with induced seismicity, and the maximum correlation (correlation coefficient of 0.37) occurred for lag times of 3 days; this correlation disappeared by October 1983, some five months after it began.

The favored theories of induced seismicity causation are: (1) stick-slip movement replaces creep due to increased normal stress, or (2) volume contraction occurs as mass is withdrawn. Note that both of these are production (not injection) effects.

1.6.4 Other Regions

Microseismicity was investigated before and during production and injection tests in the Chipilapa-Ahuachapan, El Salvador geothermal field (Fabriol et al. 1992). No microearthquakes above background levels were detected in association with these tests. The lack of microearthquakes may be due to the low flow rates, 70 tonnes/hr for the production well and 70 or 150 tonnes/hr for the injection well; injection took place under gravity feed.

Seismographic monitoring does not appear to have been conducted specifically to investigate induced seismicity in geothermal fields other than those described above.

Important producing geothermal fields where induced seismicity has not been reported by existing seismographic networks include the following: Cerro Prieto, Mexico; Olkaria, Kenya; Krafla and Svartsengi, Iceland; Otake and Hatchobaru, Japan. Principal reasons that induced seismicity has not been observed in these areas are: (1) they are areas of high natural seismicity, such that low levels of induced seismicity would easily be masked; or (2) reinjection has either been very limited or occurs within highly permeable formations, involving little formation overpressure.

1.7 RESERVOIR-INDUCED SEISMICITY

Reservoir-induced seismicity was reported with a fair degree of confidence during and after filling of at least nine reservoirs, worldwide, by a panel of the National Academy of Sciences/National Academy of Engineering (NAS/NAE 1972): Lake Mead (USA), Kariba Lake (Rhodesia-Zambia border), Koyna Reservoir (India), Kremasta and Marathon Lakes (Greece), Monteynard and Grandval Lakes (France), Vogorno Lake (Switzerland), and Qued Fodda Reservoir (Algeria). Largest magnitudes are reported for

the first five reservoirs listed, and range from 4.9 to 6.4 (Koyna). Other cases reported by the panel include: reservoirs north of Lerida, Spain; Lake Meredith (Texas); Bileca Reservoir (Yugoslavia). Conclusions concerning the existence of reservoir-induced seismicity are tentative in all of these cases, because knowledge of seismicity prior to filling is scanty. However, in virtually all instances, the evidence indicates that earthquake frequency and magnitude rise rapidly after initial filling of the reservoir, then decline over a period of several years.

Reservoirs where induced seismicity has been sought but not identified include Oroville Reservoir (California) and various other dam sites located in the western U.S. and Europe.

In addition, Talwani (1981) reported continuous induced seismicity (M = 2 to 4) at two reservoirs in South Carolina, Lake Jocassee and Monticello Reservoir (described below).

According to the NAS/NAE panel report (1972), induced seismicity at Lake Mead (behind Boulder Dam) has been cited by some workers as a classic example. Filling of the lake began in 1935, and maximum lake level was attained in 1941. Though seismographic evidence was unavailable, the region was considered aseismic prior to construction of the dam. The first seismograph was installed near the lake in 1938, following the earliest phase of felt shocks in 1936, during the annual peak of lake level. The largest earthquake to date (occurring in 1939) had M = 5.0, when the reservoir had reached 80 percent of capacity and smaller shocks with epicenters distributed around the lake have been felt since then. A large number of unfelt events with $M \geq 3$ has been recorded, and these show a clear correlation with periods of higher lake level. Extensive geologic study of the Lake Mead area was conducted prior to construction of Boulder dam, and the entire region was found to be broken by myriad minor faults, none of which was considered active. Reservoir-induced seismicity was attributed to reactivation of some of these faults.

1.7.1 Lake Jocassee, South Carolina

As noted above, Talwani (1981) reported continuous induced seismicity (M = 2 to 4) at two reservoirs in South Carolina, Lake Jocassee and Monticello Reservoir. His paper deals almost entirely with detailed studies aimed at understanding reservoir-induced seismicity mechanics and discovering earthquake precursors at Lake Jocassee. It may be the most detailed analysis of reservoir-induced seismicity ever made, and so is worthy of brief review here.

The dam is 177 m (580 feet) high and the reservoir was first filled in April 1974. Situated in the Piedmont region of the southeastern U.S., the area had been regarded as aseismic until a Modified Mercalli intensity III-IV shock took place near the dam in October 1975. This was followed by several felt events and an M = 3.2 shock on November 25, 1975. Seismicity was locally and continuously monitored since that time, using three to seven portable seismographs, augmented by three permanent stations operated since January 1979. The threshold for locatable events is M = -0.6, and some 800 microearthquakes were

recorded between 11/75 and 12/79. These are concentrated within a 100 square km (39 square miles) area including the lake, and are shallower than 5 km.

Seismicity is concentrated in a densely fractured gneiss. In situ stress measurements indicate that the largest principal stress is horizontal, measuring up to 250 bars at shallow depth (236 m). Composite fault plane solutions of the microearthquakes indicate that strike-slip faulting predominates at depths to 2 km. Correlation of lake levels and seismicity indicates that periods of larger seismic energy release follow episodes of rapid sustained rise in lake level. This observation, together with analysis of stress and focal mechanism data, and detailed mapping of surface fractures, led to this conclusion: seismicity is induced by pore-pressure changes (caused by lake level fluctuations) in the highly pre-stressed metamorphic basement rock (the Henderson augen gneiss); it involves rock rupture along existing fractures, rather than new breaks.

The nature of the seismicity changed with time. It began at shallow depths and spread laterally with time, apparently associated with abundant fractures in the Henderson gneiss; large b-values (up to 1.4) were observed. Later, the reservoir-induced seismicity deepened and became less frequent: this was attributed to a decrease in available fractures with increasing depth. Ultimately, the earthquakes are depth-limited by an impermeable layer of Brevard phyllites; thus, it is contained within a bowl-like structure of the fractured gneiss.

1.7.2 Mechanism of Reservoir-Induced Seismicity

Two mechanisms have been proposed for reservoir-induced seismicity, and both depend on reservoir loading. One mechanism (the "pore-pressure" model) involves a triggered release of pre-existing tectonic strain along pre-existing faults or fractures, due to an increase of pore pressure in rock beneath the reservoir associated with an increasing head of water (Hubbert-Rubey model); the pore-pressure increase may be caused directly by hydraulic communication between the reservoir and earth's crust, or indirectly by litho-static loading. The other mechanism involves release of strain energy in the earth's crust, not necessarily along pre-existing faults, generated during its depression under the lithostatic load of the reservoir (the "lithostatic" model). The former model is much more widely accepted, although the latter has been shown to be feasible in terms of strain energy considerations.

Only the pore-pressure model appears to fit the observations of (1) generally close association of reservoir-induced seismicity with known faults or fracture systems and (2) universal decay of reservoir-induced seismicity with time. The latter factor is crucially important. These relationships indicate that reservoir-induced seismicity is caused by the release of stored tectonic strain in a single epoch, usually with a mainshock and a series of smaller ones; while this epoch may last many years, the rate of strain energy release decreases (with earthquake magnitude and frequency) very rapidly within a few years following the first reservoir filling. This behavior is not explained by the lithostatic model, wherein one cannot expect to see what is always observed: rapid decline in reservoir-induced seismicity with repeated fillings of the reservoir.

1.7.3 Relationship of Reservoir-Induced Seismicity to Injection-Induced Seismicity

Near particular wells in the Geysers Geothermal Field, induced seismicity seems to decline over periods of a few months following the initial increases which usually accompany major injection surges (described with the analyses presented in Chapter 4). But no long-term (several-year-long) decrease of seismicity for high injection rates is apparent, and none has been described in the literature reviewed. This suggests that tectonic strain energy stored in reservoir rocks, which is the presumed energy source for induced seismicity in the Geysers Geothermal Field, may not be declining at a noticeable rate. Based on worldwide experience with reservoir-induced seismicity, described above, it is considered likely that induced seismicity near particular injectors will decline very gradually over periods of many years as tectonic strain energy is released in their immediate vicinities. However, injection-related seismicity for the entire Geysers field is likely to increase in the near future in proportion to any increases of injection.

It is not feasible to predict long-term declines of induced seismicity which may be caused by the ongoing release of tectonic strain in the Geysers Geothermal Field reservoir.

2 STATISTICAL COMPARISON OF SEISMICITY DATABASES

Information presented in this chapter is fundamental to understanding the limits of interpretation of earthquake data as to induced seismicity (IS) and its relationship to water injection in geothermal wells. Chapter 4 presents new analyses of the correlation between induced seismicity and injection, which guide this impact assessment for the proposed wastewater scenario.

2.1 OVERVIEW OF SEISMOGRAPHIC DATABASES

Seismographic data gathered by the USGS Northern California Seismographic Network (NCSN) provide the longest good-quality record of seismicity in the Geysers Geothermal Field (since 1975). However, because of NCSN's relatively wide station spacing, nearly one-half of all events with $M < 1.4$ in the Geysers field have hypocentral standard errors greater than those for $M \geq 1.4$; for $M \geq 1.4$, these errors are 0.4 km in plan and 0.6 km in depth. Systematic location errors have been estimated to be on the order of 1/4 km (800 feet), based on mislocations of underground explosions in the immediate Geysers area (Eberhart-Phillips and Oppenheimer 1984). The threshold of complete hypocenter reporting is said to be $M = 1.2$ (Oppenheimer 1986). However, NCSN provides locations for numerous events with $0.7 \leq M \leq 1.2$.

A partnership among Unocal, NEC, and Thermal Power has operated a seismographic network (U-N-T net) in the Geysers field since 1985. Since September 1989, this network has comprised 21 stations with an average spacing of about 1 mile, and has located some 20,000 events/year, with threshold $M = 0.5$. Stations are mostly one-component (vertical), but some are three-component, and recording is analog. The network appears to have provided high-precision hypocentral data for $M \geq 0.7$ since November 1988, with "inaccuracies" averaging 700 ft horizontally and 1300 ft vertically (Stark 1990).

Lawrence Berkeley Laboratory (LBL) has operated one net in the northwestern Geysers area from 1992 to 1994, and a second net in the southeastern Geysers since January 1994 (operation in late 1993 was conducted jointly with Lawrence Livermore Laboratory (LLNL), providing data with timing mismatches). The northwest LBL net does not provide data for the Unocal lease area.

The southeast LBL net comprises 13 three-component stations on the land surface within portions of the Calpine, U-N-T, and Northern California Power Agency (NCPA) leases; this overlaps the southeastern portion of the U-N-T network and has station spacing from 3000 to 7000 feet. Between January and July 1994, this net located over 1000 hypocenters within the U-N-T lease area, many of which were not located by the U-N-T net because of its lower sensitivity (Kirkpatrick et al. 1995). The magnitude threshold for complete detection and location of hypocenters is about $M = 0.0$; the estimated hypocenter location error is about 100 meters horizontally and 200 meters vertically (Art Romero, pers. commun. 5/18/95).

2.2 HYPOCENTRAL PRECISION RELATED TO MAGNITUDE

Hypocentral precision as a function of magnitude, and magnitude threshold of complete reporting, ought to be characterized for each network in order to most effectively interpret hypocentral data from these different sources with regard to induced seismicity. However, only the NCSN catalog provides calculated standard errors (horizontal and vertical) for each hypocenter. Hypocentral precisions for the LBL and U-N-T catalogs have been characterized only generally, as noted above (Section 2.1).

Each NCSN hypocenter report includes estimates of standard errors in its horizontal and vertical position. The entire NCSN dataset covering the Unocal area has been analyzed for average values of these standard errors, in magnitude intervals with width of 0.2 from M 0.7 to 3.7. Results are shown in Figure 2.1, with magnitude-interval midpoints shown (0.8, 1.0, etc.). Both horizontal and vertical standard errors are seen to decrease rapidly as magnitude increases from 0.8 to 1.8, then slowly for M > 1.8. The horizontal standard error is about 1,600 feet at M = 0.8, but only about 800 feet at M = 2.0, a factor-of-two improvement; vertical standard error also decreases by nearly the ratio in this magnitude interval. This behavior is explained by the fact that the precision of P-wave first-arrival times increases with the signal-to-noise ratio of the first arrival, which increases with magnitude; also, because the number of stations recording any event increases with event magnitude, which provides better constraint on hypocenter location. Smaller-magnitude microearthquakes have weak first-arrivals, which are often not much larger in amplitude than background noise on the seismogram; this explains the NCSN cutoff for hypocenter reporting at M = 0.7.

Based on this information, one might suppose there would be an advantage, when correlating induced seismicity with geothermal wells, in using only M≥ 1.8. However, as explained in the next section (on magnitude-frequency relationships), such a procedure would reduce the numbers of events available for correlation, to the point of greatly diminished usefulness.

2.3 MAGNITUDE THRESHOLD OF COMPLETE REPORTING BY NORTHERN CALIFORNIA SEISMIC NETWORK

In order to estimate the magnitude threshold for complete detection and reporting of earthquake hypocenters by the NCSN, graphs showing numbers of reported hypocenters versus magnitude have been prepared. Magnitude data are not available in either the LBL or U-N-T catalogs, but threshold magnitudes for them are described in Chapter 1.

Based on observations worldwide, numbers of earthquakes are expected to increase exponentially with decreasing magnitude, exhibiting a linear relationship between the logarithm of event counts and magnitude. Where counts for the smallest magnitudes reported by a particular network fall below the straight-line fit to higher-magnitude counts, one presumes that some fraction of these smallest magnitude events is not being reported. The largest magnitude showing this "deficit" is taken to be the threshold of complete reporting.

Figure 2.2 shows the frequency (total numbers) of reported hypocenters in magnitude intervals of 0.2, from M = 0.7 to 4.7, for the entire Unocal area for the period January 1976 through May 1995. It also shows a straight line fit by eye to data from M = 1.4 to 3.4. One sees that the line lies progressively further above reported data as M decreases from 1.4: thus M = 1.4 is the threshold of complete detection and reporting.

Because the NCSN station complement has changed with time within and near the Geysers Geothermal Field, the variability of earthquake detection rates for M < 1.3 was checked. As can be seen in Figure 1.1, five stations which once existed have ceased operation: GBO, GFT, GCM, GMM, and GSM. The first two were removed in 1982, and the last three in 1986. Later, during 1986 to 1989, three new stations were added: GAC, GCR, and GGP. In the east-central portion of the Unocal area, it was found (not surprisingly) that abandonment of the three close-in stations in 1986 caused a drop in the rate of detection and reporting of earthquakes with very low magnitude compared to those with larger magnitude. Later addition of the three new stations did little to raise the reporting rate of very small earthquakes, because the three stations removed in 1986 were much closer to the Geysers Geothermal Field than were those added later. As a quantitative assessment, we compare numbers of reported events in two magnitude intervals: the quotient of the number with $0.7 \leq M < 1.1$ divided by the number with $1.3 \leq M < 1.5$ decreased by two-thirds after 1986. The quotient of events with $1.1 \leq M < 1.3$ divided by events of $1.3 \leq M < 1.5$ dropped by one-half. Thus, the preponderance of the change in detection rate was for M < 1.1.

Data for M > 3.4 do not show linear behavior, and fall below the fit line for M ≥ 3.4. It appears that numbers of earthquakes with M > 3.4 decline much more rapidly with magnitude than for 1.4 < M < 3.4. This suggests some difference in seismic strain release mechanism above and below M = 3.4. Such a break in slope was recognized for the Larderello field, at M = 2.6 (Batini et al. 1985).

There are too few earthquakes with M > 3.8 to be sure of magnitude-frequency behavior for M > 3.8. Earthquakes with M = 4.1 to 4.5 have not been reported, while just two have been reported in adjacent magnitude intervals (one event M = 3.9 to 4.1 and another one M = 4.5 to 4.7).

Figure 2.3 shows the *cumulative annual* frequency of earthquakes vs. magnitude, in magnitude intervals of 0.2. This parameter is calculated by summing all events from the largest observed (M = 4.6) down to and including those in the magnitude interval of interest, and dividing the sum by the number of years of record (19.4 years in this case). The cumulative data do not reveal as much detail of the magnitude distribution as do the interval data. The straight-line fit to the data for $1.3 \leq M \leq 3.3$ (by least squares) is shown, and the b-slope is 1.07. The line plotted for M > 3.3 represents a guess concerning possible future behavior.

Further discussion of Figure 2.3, particularly of the straight-line fits shown, is deferred to Sections 4.41 and 7.1.2.

3 COMPILATION OF INJECTION WELL DATA

Monthly volumes (in barrels [bbls]) of injectate and depth intervals of injection have been compiled in order to conduct the analysis of Chapter 4. The highest priority has been those wells which have been injectors and have suspected induced seismicity, based on preliminary examination of epicenter maps and published studies. Eight wells have been identified in this category, and their data have been obtained and examined. They are GDC-18, GDG21, GDC-26, DX-61, LF-3, LF-23, DV-11, and BEF42-B33.

Locations of these injection wells, as well as all other Unocal injection and production wells and Santa Rosa Wastewater Project (SRWW) injection scenario injectors are shown in Figure 3.1. Wells which are the subject of analyses in Chapter 4 have their names shown.

Shut-in (i.e., out-of-service) dates since 1990 for all production wells of interest were obtained, and this record is examined with reference to induced seismicity related to nearby injectors. Ideally, complete production histories would be obtained and examined for all production wells near enough to an injector under study to cause ambiguity of induced seismicity correlation. However, the scope of this work has to be carefully limited, because of the very large amount of data which is potentially involved. Therefore, this task was limited to a review of production from a few wells near injectors of interest.

4 NEW ANALYSES OF INDUCED SEISMICITY WITHIN THE UNOCAL LEASEHOLD

New analyses of induced seismicity have been conducted for five injector wells (DX-61, LF-3, LF-23, GDC-18, and GDC-21) which appear to have spatially associated induced seismicity, using the NCSN hypocenter catalog. These five wells are shown with a special symbol in Figure 3.1. Wells LF-3 and LF-23 are especially pertinent because there are no production wells within 2,000 feet of LF-3, and only one within 1,000 feet of the latter. Hence, earthquakes located near these two wells provides a good opportunity for observing relatively unambiguous correlation with injection.

It was planned to analyze induced seismicity in association with wells GDC-26, DV-11, and BEF42-B33, but these wells were not studied for the following reasons: well GDC-26 is located amongst a large number of production wells, such that distinction of induced seismicity related to production and injection would be extremely difficult; wells DV-11 and BEF42-B33 and associated induced seismicity have already been analyzed by Kirkpatrick et al. (1995), using the LBL hypocenter database, obviating the need for new work.

Originally, it was hoped to make considerable use of hypocentral data from the U-N-T catalog. However, most of that catalog is comprised of hypocenter locations based on machine-picked P-arrival times, which Unocal judges to be imprecise; hand-picked P times are available for only very limited space-time windows (generally for a few days very near a single well). Magnitudes are included only in small portions of the catalog. Generally speaking, it appears that the U-N-T data are not useful for purposes of this study. However, one hand-picked U-N-T data set exists for the vicinity of wells LF-23 and LF-3, for the period March 16 to July 16, 1992. It was obtained because analysis using NCSN data suggested that greater hypocentral precision would be useful. Spatial and temporal correlation of earthquakes with injection are discussed separately because the latter is considerably more definitive than the former. It is convenient and useful to keep the temporal analyses in one section of the study.

4.1 PRELIMINARY DISCRIMINATION OF INDUCED SEISMICITY

Initial identification of possible injection-related induced seismicity has been based on planimetric map study and review of published articles described in Chapter 1 and a review of production/injection status of so-called injection wells. Many wells have served as both producers and injectors, and it has been necessary to determine if and when any of the five study wells listed above were producers: of the five, only GDC-18 had production prior to 1994.

Clusters of epicenters lying within 1,000 feet of an injection well were tentatively identified as possible instances of induced seismicity. This criterion was used to allow for systematic NCSN epicenter location error estimated to be about 800 feet (Chapter 2), and to limit the likelihood that the induced seismicity was caused by nearby producing wells.

Figure 4.1 shows epicenters of $M \geq 2.0$ events in relation to the three detailed study areas discussed below (Figures 4.2 to 4.9). Figure 3.1 shows injection wellheads and wellbores, and production wellheads, in relation to these same study areas. It was not possible to show wells and epicenters on the same map because the epicenters are so dense that they would obscure many wells. Figure 4.1 reveals that seismicity has been most abundant in the northwestern portion of the Unocal leasehold, most particularly within Units 7-8 and 1-6. This area was not examined for induced seismicity because it is characterized by

relatively close proximity of production wells to injection wells, making discrimination between production- and injection-induced seismicity more difficult.

Study area 1-2 (for well DX-61) is situated in the northeasternmost portion of this seismicity. Area 2-3 (wells LF-3 and LF-23) is located in an area of moderately dense seismicity, and area 3-1 (well GDC-18) includes a small but dense cluster of events.

4.2 SPATIAL DISCRIMINATION OF INDUCED SEISMICITY

Spatial relationships of hypocentral locations and wellbores are presented in Figures 4.2 through 4.9. Considerable vertical compression (factor of 10) was employed, in order to fit vertical-plane projections beneath plan views; this causes wellbores to appear to have small plunge angles, but causes no loss of information.

4.2.1 Vicinity of Well DX-61

A catalog search found 883 events for the period 1 July 1986 to 30 May 1995 in area 1-2, vicinity of DX-61. Injection at DX-61 began in September 1986, after many years of production. Figures 4.2 and 4.3 are a plan view with vertical-plane projections of hypocenters and wellbores (the projections run east-west in 4.2 and north-south in 4.3) for this study area; included in the plots are production wells DX-55, DX-56, and DX-62, which have operated since March 1982 (DX-55, DX-56) and since March 1985 (DX-62). The plan view shows a weak tendency for the largest events (M = 3 to 4) to group near and eastward from DX-61, away from the production wells.

Hypocentral depths between 10,000 feet and 12,000 feet are sparsely populated, which could represent a segregation of production- and injection-related earthquakes into shallower and deeper zones; however, a cross-correlation of injection volumes with the deeper events (see Section 4.3.1) indicates this is not the case. There is a weak suggestion in the vertical-plane projections of Figures 4.2 and 4.3 that DX-61 has more associated shallow induced seismicity than do the three production wells; however, the north-south projection shows very few hypocenters beneath the lowermost one-third of the DX-61 wellbore. This suggests that deeper earthquakes are not better correlated with injection than are shallower events, for this well. However, it is possible that the apparent bimodal depth distribution is an artifact of systematic biases in computed depth, perhaps related to which station groups provided data to locate each event. Systematic azimuthal variations in the P-wave propagation velocity, which are known to exist, may have played a role.

4.2.2 Vicinity of Wells LF-3 and LF-23

A catalog search found 1580 events in study area 2-3 for the period 1 April 1979 to 30 May 1995. Injection first took place in this area at well LF-3, beginning September 1973, and LF-23 came on line in June 1979. These two wells have served principally as injectors.

Figures 4.4 and 4.5 are hypocenter plots for study area 2-3, vicinity of injection wells LF-3 and LF-23; production well LF-24 is also shown. The plan view shows more seismicity in the area of LF-23 than around LF-3 or LF-24. The vertical-plane projections show depths which are more constrained than around DX-61: the vast majority lie between 2,000 and 9,000 feet, with a strong concentration from 6,000 to 9,000 feet. These plots do not show several producing wells located about 1,000 feet southerly of LF-23, and they may contribute to the induced seismicity seen.

A plot of epicenter northing (mean monthly positions) versus date is shown in Figure 4.23. This reveals a southerly progression of epicenters from 1,500 feet north of LF-3 to 4,000 feet south of it, between 1976 and the end of 1983, and the progression became rapid in June 1979, when injection at LF-3 was virtually terminated and that at LF-23 was initiated (after this date LF-3 saw only five periods of continuous

injection that lasted more than two months). The overall trend is in the direction of several producing wells south of LF-23, and probably marks the progression of the injectate boiling front, as documented in several instances (Stark 1990). Epicenters shifted abruptly north in early 1984, by nearly 2,000 feet, when LF-23 resumed injection after 10-months' hiatus. No explanation can be found for this behavior, nor for the very limited southward progression that took place while LF-3 was active.

Additional analysis of events around LF-23 has been made using U-N-T hand-picked hypocentral data for the period March 10 through July 16, 1992, which includes 138 earthquakes. Hypocenter plots are shown in Figures 4.6 and 4.7. The plan view shows weak clustering of epicenters near the wellbore of LF-23, and very few epicenters near LF-24. These data seem to show somewhat stronger clustering than the NCSN hypocenters, as expected considering their smaller location errors.

It is noted that LF-24 was producing nearly continuously during this period (3/10/92 to 7/16/92), with only 18 days of reduced steam flow. The east-west vertical-plane projection also shows that most earthquakes occurred beneath and west of the wellbore of LF-23. Thus, it is concluded that production from LF-24 may characteristically have had little effect on overall seismicity within study area 2-3.

4.2.3 Vicinity of Well GDC-18

A search was performed in the immediate area of GDC-18 (area 3-1), revealing 988 events for the period 1 January 1983 to 30 May 1995, shown in Figures 4.8 and 4.9. Most seismicity is located in the area of wells GDC-18 and GDC-24, and Figure 4.9 indicates that more seismicity is located near GDC-18 than GDC-24. A dense cluster is located just above and east of the bottom of GDC-18.

GDC-18 also has been a producer, with steady production from July 1987 to February 1991, followed by production in three periods of four to seven months' duration until October 1994. GDC-24 began production in February 1985 and had no major shut-in periods until January 1995, when it was off-line for 10 days.

4.2.4 Vicinity of Well GDC-21

A search was performed in the immediate area of GDC-21 (area 4-1), revealing 174 events for the period 1 January 1985 to 30 May 1995.

This represents insufficient data for a useful correlation analysis, and no further work was performed for this well.

4.3 TEMPORAL DISCRIMINATION OF INDUCED SEISMICITY

For this study, confirmation of injection-related induced seismicity in a spatial cluster is based on temporal relationships between injection and seismicity, using monthly counts of injected volume (bbls) and earthquakes. The analysis has relied on time-series plots of earthquakes and injection for visual correlation, and on computation of the lagged cross-correlation function, also termed the normalized cross-covariance function, described by Bendat and Piersol (1966). Lag times were chosen to run from 0 to 12 months following injection.

The cross-correlation function is a statistical method which measures the similarity, or relative variation, of two series of observed data (usually time series). It was used by Eberhart-Phillips and Oppenheimer (1984) in their analysis of induced seismicity in the Geysers field. The cross-correlation function is analogous to the better known correlation coefficient from the method of linear regression. The function (termed "rho") yields a scalar quantity that can vary continuously from -1 to 1. A rho-value of 1 indicates exact proportional correspondence of all variations in the two series being compared, and a rho-value of -1 indicates exact inverse proportional correspondence (i.e., positive and negative changes are exactly

correlated). Rho of zero indicates no correlation whatsoever. The degree of correlation increases in proportion to the absolute value of rho. Values of rho at the 5 percent significance level (95 percent confidence level), called the 5% points, for any number of data (note that the lag time effectively determines the number of data being compared) are to be found in standard statistical tables for the correlation coefficient (e.g., Crow, Davis, and Maxfield 1960). The 5% point is the smallest absolute value of rho for which the null hypothesis (stating that the two series are correlated) may be true at the 5 percent significance level (i.e., have a 95 percent probability of being correlated). For example, if rho is .235 and the 5% point is .220, the series are judged to be correlated at the 5 percent significance level.

Making a decision as to confirmation of injection-related induced seismicity is necessarily subjective, as there are no standards from which to work. In this study several episodes of obvious correlation, each lasting perhaps a few months, were considered to be reasonable confirmation. Cross-correlation functions which peak strongly at a given lag time are also confirmatory.

Variability in rate of detection and reporting of events with $M < 1.3$ was discussed in Section 2.3, for the east-central portion of the Geysers field (Area 2-3). It was pointed out that the rate of reporting of these smaller events dropped by factors from one-half to two-thirds, compared with the rate for $M > 1.3$, after three NCSN stations within and at the margin of the Geysers field were abandoned in 1986. Nonetheless, this effect is not evident in monthly earthquake counts, which are for all events with $M \geq 0.7$, presented below. These counts show wide variation in most years, and no overall decline in counts after 1986, which appear unrelated to injection, can be seen. This is clearly so for Area 2-3, and appears to be so for Area 3-1. Area 1-2 is described only after 1985, so that a reporting-rate effect would not be seen there.

4.3.1 Well DX-61

Figure 4.10 plots monthly counts of earthquakes (bar graph) against monthly injection volume (millions of bbls) for area 1-2 (vicinity of DX-61), at all depths, for the period July 1986 through May 1995. One clear episode of correlation may be seen: in late 1986 injection rose sharply (to more than 1.5 million bbls/month), followed within two to three months by a sharp increase in seismicity; the ensuing abrupt decrease in injection in early 1987 was accompanied by a major drop in seismicity. Thereafter, correlation is not obvious, though a few suggestions of it may be seen.

The cross-correlation of monthly earthquake counts and injection volume (Figure 4.11) was computed and shows a correlation coefficient (rho) maximum at a lag of zero months (rho = 0.375), decreasing only gradually for lags out to several months. With a 5% point of 0.195, this correlation is significant.

Considering the bimodal depth distribution noted above, a cross correlation was also performed for only those events deeper than 10,000 feet. It showed much weaker correlation, with rho maximum of 0.128 at zero lag, which is below the 5% point.

It is concluded that induced seismicity around well DX-61 is moderately correlated with injection, and might be better correlated with production from the nearby "DX" wells.

4.3.2 Wells LF-3 and LF-23

Figure 4.12 plots monthly counts of earthquakes (bar graph) against monthly injection volume for area 2-3 (vicinity of LF-3 and LF-23), at all depths, for the period April 1979 (onset of injection in LF-23) through May 1995. This is a rather impressive picture, as one can see many points of correspondence between peaks in earthquake counts and injection, at least for times as late as 1989. There is a fall-off in correlation after 1989, and during some intervals one sees negative correlation. We have no explanation for this.

Figure 4.13 presents cross-correlograms for combined injection at both wells against earthquake counts, for two periods of time: April 1979 to May 1995 and April 1979 to March 1986. The longer period shows weak correlation, as was expected based on Figure 4.10; the shorter period has much stronger correlation, with rho of 0.50 at zero lag, and decreasing steadily with increasing lag time, reaching nearly zero at four months. The 5% point for this correlation is 0.21.

Considering the shape, maximum value, and significance level of this correlation, it does appear that induced seismicity is well correlated with injection at LF-3 and LF-23, from the onset of injection in LF-23 until early 1986.

4.3.3 Well GDC-18

Figure 4.14 shows monthly counts of earthquakes against monthly injection volume for area 3-1 (vicinity of GDC-18), at all depths, for the period January 1983 through May 1995. The onset of injection was in January 1984, and production in nearby wells (on the same wellpad) did not begin until December 1984 (GDC-19). Two major spikes of injection, lasting a few or several months, took place in early and late 1984; they were accompanied by similar spikes (more than doubling) in local seismicity rates. These events occurred prior to any production from nearby wells.

GDC-18 also has been a producer, with steady production from July 1987 to February 1991, followed by production in three periods of four to seven months' duration until October 1994. Seismicity remained very low from mid-1987 to early 1991, while GDC-18 was producing, and increased when injection resumed in February 1991 (Figure 4.14). Intervals of production in late 1992, late 1993, and in 1994 were periods of low seismicity, while adjacent time intervals of injection were accompanied by higher seismicity; one exception to this occurred in early 1993, when seismicity did not increase during a spike of injection. This information demonstrates that, at least in this area, injection causes much more induced seismicity than production does.

Figure 4.15 presents a cross-correlogram for injection at well GDC-18 against earthquake counts, for the period January 1983 to May 1995. Rho is 0.57 at zero lag, and decreases almost steadily with increasing lag time, reaching nearly zero at six months. The 5% point for this correlation is 0.166. Considering the shape, maximum value, and significance level of this correlation, it appears that induced seismicity is well correlated with injection at GDC-18 throughout its history.

4.4 CHARACTERIZATION OF CONFIRMED INDUCED SEISMICITY

In order to assess the impact of expected new induced seismicity on surrounding communities, confirmed induced seismicity must be characterized in terms of rate of occurrence, maximum magnitude and b-slope, as well as associated injection and reservoir parameters.

The rate of occurrence and magnitude distribution of induced seismicity in relation to the rate of well injection has been developed on the basis of data presented in Figures 4.16 through 4.21. These present magnitude-frequency distributions (4.16 to 4.18) and rates of earthquake occurrence in relation to injection volume (4.19 to 4.21) for the vicinities of wells DX-61, LF-3 and LF-23, and GDC-18.

4.4.1 Magnitude vs. Frequency of Occurrence

Magnitude-frequency data in Figures 4.16 to 4.18 have been fit by linear regression for $M \geq 1.10$, as lower magnitudes appear not to be reported completely, with regression lines shown. These show fairly consistent parameters among the areas of the four wells: slopes ("b-slopes" in standard parlance) range from -0.96 to -1.09; the annual numbers of events with $M \geq 2.0$ run from 5.9 to 9.6. The average b-slope is -1.01 and average frequency of $M \geq 2.0$ is 7 per year. Figure 4.16 (DX-61 area) shows no break in slope for M between 3 and 4; Figure 4.17 (LF-3 and LF-23) shows a break in slope at M = 2.5, and Figure

4.18 (GDC-18) may be showing one at M = 3.3. However, the statistical significance of these apparent slope breaks is low due to the small numbers of events with M ≥ 2.5.

However, magnitude-frequency data for the entire study area (Unocal leasehold), presented in Figure 2.3, show a clear and definite break in slope at M = 3.3. Because this figure incorporates vastly more seismicity data than do those for the small study areas, the slope break at M = 3.3 is considered representative of induced seismicity. The slope for M < 3.3 is -1.07, and this is also considered more representative than the small-area results. For M > 3.3, the slope is not well determined but appears to be about -1.83 (note the visually determined fit-line in Figure 2.3). This break in slope is a well-known feature of induced seismicity in the Geysers Geothermal Field, and has also been observed for the Lardarello, Italy geothermal field. It has yet to be explained, but does strongly suggest that induced seismicity has maximum magnitudes much smaller than does natural tectonic seismicity, for which there are no clear slope breaks in magnitude-frequency data.

It might be argued that the slope information in Figure 2.3 represents induced seismicity caused by both injection and production, and therefore is not injection-specific. The response to such an assertion is that available data do not permit distinction of magnitude-frequency relationships on this basis. The plots of small study areas around injection wells also include much seismicity that is certainly a result of production. The only way to avoid this problem would be to analyze only seismicity which is clustered definitively at injection wells. However, insufficient data of this definitiveness are available for development of injection-specific magnitude-frequency curves.

4.4.2 Rates of Induced Seismicity and Injection Volume

Figures 4.19 through 4.21 relate the frequency of induced seismicity to injection for all reported magnitudes (above M = 0.7), using monthly counts, for the three local study areas (DX-61, LF-3 and LF-23, GDC-18). They are surprisingly revealing, and allow reasonable conclusions. Figures 4.19 and 4.20 exhibit clear trends for upper bounds of earthquake frequency in relation to injection volume; similar "critical" monthly injection volumes above which induced seismicity always occurs (annotated as "IS assured"). "Background" levels of induced seismicity are here defined as numbers of events which occur in months with no injection. It must be understood that the existence of background induced seismicity levels does not imply a lack of correlation between induced seismicity and injection, because injection which took place one or a few months earlier (before any particular month in which earthquakes and injection were counted and plotted in Figures 4.19 through 4.21) has a lingering effect. This phenomenon is clearly evidenced in Figures 4.10 through 4.15 (presenting temporal relationships and cross correlations of earthquakes and injection). The "IS assured" marker was identified simply as the minimum injection rate for which the monthly number of earthquakes is always above the maximum background level.

Figure 4.21 does not show these relationships distinctly, most likely because GDC-18 saw a long period (nearly four years) with no injection. However, it does show a general increase in induced seismicity with rate of injection.

Taken together, these three plots indicate the following:

1) injection at rates over one million bbl/month (1.38 mgd) in a given well is virtually certain to cause earthquakes; injection at rates of 0.5 to 1.0 million bbl/month (0.69 to 1.38 mgd) has a good chance of causing induced seismicity;

2) for injection rates over one million bbl/month (1.38 mgd), one may expect induced earthquakes (M ≥ 0.7) at rates of about 10 to 30 per month;

3) the incremental (over background) rate is about 10 events per month ($M \geq 0.7$) for injection of one million bbl/month (1.38 mgd), increasing proportionately with greater injection.

For the purpose of objectively predicting rates of induced seismicity for scenario injection, a linear regression analysis was performed using all of the data shown in Figures 4.19 through 4.21. The simplest mathematical function which could reasonably represent the data was chosen as a model equation, namely, a third-order polynomial. Induced seismicity rates predicted by the model equation are shown in Figure 4.22, together with all data used to derive it. The equation is as follows:

$$N = 5.01 + 1.86\ V + 4.75\ V^2 - 1.15\ V^3 \pm 4.75$$

where N is the monthly number of events with $M \geq 0.7$ and V is injection rate in millions of bbls/month. The standard error of estimate is 4.75.

For the southeastern Geysers area, where LACOSAN injection is to take place, a separate analysis was made using data for injection well McKinley-5 (ESA 1994). Total injection is planned at 5,400 gpm (7.8 mgd), to be distributed among 15 wells. Using the method just described, the rate of induced seismicity ($M \geq 0.7$) was estimated to be about 11 events per year for the entire scenario.

5 FORECAST OF INDUCED SEISMICITY FROM SCENARIO INJECTION WELLS

5.1 SANTA ROSA WASTEWATER SCENARIO

Induced seismicity expected to occur as a result of wastewater injection in the scenario has been characterized based on the results of Chapter 4, above, and expected mass flows.

Total injection in the Santa Rosa wastewater scenario is expected to have an average annual volume of 19.5 mgd, equivalent to 14.1 x 10^6 barrels (bbl)/month (with 1 bbl = 42 gallons) distributed rather evenly among 10 wells in the Unocal leasehold. The average amount per well is therefore 1.95 mgd or 1.41 x 10^6 bbl/month. It is noted that this would cause total injection to be almost three times estimated current injection of 11.5 mgd in the Unocal leasehold, converted from a reported mass flow of 18 million tons/year (Barker et al. 1995).

The expected numbers of induced earthquakes can be predicted from the empirical equation found by linear regression of earthquakes vs. injection rate presented in Chapter 4. For an injection rate of 1.41 million bbl/month (1.95 mgd), the predicted median induced seismicity rate for each scenario well is 13.85 events ($M \geq 0.7$) per month, with a standard error of estimate (SEE) of 4.74 events/month. The 95 percent confidence interval for the prediction is the predicted median plus or minus 2 SEE, which extends between limits of 4.37 and 23.33 events per month. The upper limit is more than five times the lower one, which expresses the large uncertainty in the predicted median value. For all ten wells injecting together, the rate of predicted induced seismicity is 138.5/month or 1662/year. Using the SEE, the 95 percent confidence range for the predicted annual number of events ranges from 524 to 2796.

It is noted that the planned average injection rate of 1.41 million bbl/month (1.95 mgd) per well is clearly within the field of "assured IS," meaning induced seismicity is predicted to be above the "background" level, discussed previously (section 4.4.2). This requires that the lower-bound induced seismicity rate be no less than the average level for zero monthly injection, which is 5.01 events/month per well ($M \geq 0.7$), given by the constant in the regression equation of Section 4.4.2. This value slightly exceeds the lower 95 percent confidence limit of 4.74 stated above. It is considered that a predicted lower bound of 5 events per month per well has a confidence level higher than 95 percent, as the linear regression procedure cannot incorporate the "assured seismicity" observation from the data. Therefore, the lower-bound (95 percent confidence level) predicted induced seismicity rates stated above should probably be at least 5 percent greater than those stated. However, the difference is unimportant in the following assessment of predicted seismicity, because the predicted median level of induced seismicity was utilized.

The annual number of $M \geq 2.0$ earthquakes for the entire scenario is estimated using the magnitude-frequency curves and data described. The average ratio of numbers of $M \geq 0.7$ to $M = 2.0$ events is 10. Thus, for $M \geq 2.0$, scenario seismicity is predicted to have a median level of 16.6 events/year per well, or a total of 166/year for ten wells. The 95 percent confidence interval for the annual total ranges from 52 to 280. Reiterating the caution stated above, this forecast is considered to have 50 percent uncertainty. The forecast scenario induced seismicity rate of 167/year with $M \geq 2.0$ is to be compared with the observed average historical (past 20 years) rate of seismicity for the entire Geysers area, about 155/year with $M \geq 2.0$.

Implicit in the preceding discussion is an assumption that all subareas of the Unocal leasehold will respond similarly to comparable rates of injection in any injector well. It is likely that significant

differences in induced seismicity potential of injection exist within the Unocal leasehold; this is suggested by the much lower rates of induced seismicity observed in the southeastern Geysers (see next section).

However, present analyses are limited to four injection wells and do not support such distinctions.

The magnitude distribution of induced seismicity is forecast to be identical to that described in Section 4.4.1. Table 5.1 lists expected frequencies and b-slopes for forecast induced seismicity, together with those for average historical induced seismicity.

5.2 LACOSAN WASTEWATER SCENARIO

In order to develop a complete understanding of the relative impact of the Santa Rosa wastewater injection scenario, it is also necessary to consider induced seismicity expected as a result of the LACOSAN wastewater injection scenario, to be implemented using 15 wells in the southeastern Geysers area (ESA 1994). As described in Chapter 4, induced seismicity of 11/year for $M \geq 2.0$ is expected for total scenario injection (7.8 mgd or an average of 0.52 mgd per well). Per unit of injection volume, this rate is just 13 percent of that forecast for the Santa Rosa scenario. This is expected, and recent studies in the southeastern Geysers area have shown much less induced seismicity near individual injection wells than observed in the central Geysers area: for example, only a few dozen very small earthquakes (recorded by LBL with magnitude threshold of $M = 0.0$) occurred during the first eight months of injection into NCPA well C-11 (Enedy, Enedy, and Maney 1991).

The b-slope in the magnitude-frequency distribution for the southeast Geysers area was evaluated for the area around well McKinley-5, and found to be 1.28, which is significantly larger than for the central Geysers area (1.06). This means that the frequency of "larger" earthquakes, with $M \geq 3$, is very much smaller than in the central Geysers area. This information is included in Table 5.1.

6 POTENTIAL FOR TRIGGERED EARTHQUAKES ON REGIONAL ACTIVE FAULTS AS A RESULT OF INDUCED SEISMICITY

6.1 PRINCIPLES

Recent articles in the geophysical literature have addressed static stress changes which accompany moderate and large earthquakes, and their potential to trigger seismicity on nearby faults (e.g., King et al. 1994). These stress changes are given in terms of the Coulomb stress change, defined as a change in effective shear stress acting along a chosen fault surface (with particular orientation and sense of slip). This effective shear-stress change ([f) is calculated as a change of shear stress (\) less a frictional stress:

$$[_f = \ - T([- p),$$

where T is the coefficient of friction, [is the normal stress, and p is the pore pressure; all of these stresses act parallel or perpendicular to the chosen fault surface. The sign is important in the context of the expected sense of rupture, e.g., right-lateral, left-lateral, etc. An increase in [f promotes rupture in this sense; a decrease inhibits failure.

6.2 CASE STUDY IN THE MOJAVE DESERT AREA

The paper by King et al. presents an extensive treatment of recent earthquakes in the Mojave desert region of California, and includes maps of Coulomb stress changes accompanying the Homestead Valley earthquake sequence of 1979 (M = 4.8 to 5.2) , and the Joshua Tree (M = 6.1), Landers (M = 7.4), and Big Bear (M = 6.5) events, all occurring in 1992. It is shown that aftershocks were largely confined to areas where the Coulomb stress due to these events increased by more than 0.3 bar. Smaller stress increases had little correlation with aftershock activity. The Big Bear earthquake took place in the middle of the most pronounced stress-increase lobe (+2 to +3 bars) produced by the Landers earthquake, and just 3.5 hours after the Landers event. From these results we conclude that static stress changes exceeding 0.3 bar, caused by moderate and large earthquakes, are an important determinant of aftershock locations, and sometimes may trigger a nearby event of sizable magnitude. The critical presumption is, of course, that the affected areas were already in a near-failure stress condition, as seems to have been the case for the Mojave Desert area. King et al. go on to interpret these results in terms of a timing advance for the Big Bear event: its occurrence was hastened by the shift of regional stress caused by the Landers event.

6.3 APPLICATION TO THE GEYSERS GEOTHERMAL FIELD

From the work of King et al. (1994), it was evident that Coulomb static stress changes from a relatively large shock in the Geysers field would be very small, less than 0.1 bar, at distances of only a few kilometers. Hence, only the nearest active regional fault, the Collayomi fault, needed to be considered. It was decided to model an M = 4.5 event with focal depth of 5 km, located near the center of the distribution of scenario injection wells, located some 5 km southwest of the Collayomi fault. M = 4.5 is just slightly larger than the largest Geysers shock to date. Other model parameters include the following:

Source fault in the Geysers field

rupture area: circular, diameter 4.4 km
slip: tapered with 1 cm maximum at center
strike: N 370 W
seismic moment: 5.8 x 10^{22} dyne-cm (for M = 4.5)

Collayomi fault
Poisson's ratio: 0.25
shear modulus: 3 x 10^{5} bars
coefficient of friction (T): 0.4
strike: N 370 W
rake direction: 1800 (for right-lateral slip)

Computer codes for these calculations are cumbersome and not readily available. However, Dr. Robert Simpson of the U.S. Geological Survey (personal communication 9/6/95), who has extensive experience with calculations of this type, assisted by running a calculation for the model described.

Figure 6.1 presents positive and negative Coulomb stress changes, contoured in plan view at a depth of 5 km. It can be seen that the greatest positive change (a positive change tends to promote fault rupture) along the Collayomi fault is 0.045 bar.

The significance of this result may be assessed in terms of the hastening of stress build-up along the Collayomi fault. The shear-strain rate in the greater Geysers region was 0.39 microstrain/year for the period 1972-1982 (Prescott and Yu 1986), oriented approximately parallel to this fault. The rate of accumulation of regional shear stress is found by multiplying 0.39 microstrain/year by the shear modulus (3 x 10^{5} bar), yielding 0.12 bar/year. Hence, a stress increase of 0.045 bar due to an M = 4.5 event in the Geysers represents approximately 4-1/2 months of natural stress build-up. Considering the above, a stress change of 0.045 bar must be judged as insignificant.

7 EXPECTATION OF FELT AND DAMAGING GROUND SHAKING

7.1 SEISMICITY MODEL

Expected recurrence intervals and maximum probable values for Modified Mercalli intensity and peak horizontal ground acceleration have been projected for induced seismicity expected to accompany implementation of the Santa Rosa wastewater injection scenario and of the Lake County Sanitation District (LACOSAN) injection scenario, which is scheduled to begin in 1996.

Generally, earthquake hazard assessments rely on assessment of ground acceleration, and not intensity. This is because intensity is a rather crude, quasi-quantitative assessment of felt and damage effects, divided into 12 grades; it is not a well defined, continuous variable that can be measured with seismographic instruments; it is what is known as a "state variable."

The projection has been made in the context of current natural regional seismicity and current induced seismicity at the Geysers. Santa Rosa wastewater injection and LACOSAN effects have been reckoned incrementally with respect to regional and Geysers seismicity, in terms of incremental effects on recurrence intervals and maximum probable values for ground shaking. The location of Cobb has been used as the representative receptor site for seismic effects. Cobb is the settlement nearest the predicted Santa Rosa wastewater injection scenario seismic source, and can be expected to see maximum effects.

7.1.1 Region

The project region is taken to include that part of the Coast Ranges which extends from San Pablo Bay on the south to Laytonville on the north, and from the coast as far east as Lake Berryessa. Natural seismicity of the region has previously been modeled in terms of geological slip rates of known active faults, but it was realized that this procedure yields a seismicity level far above (about 8 times) historic experience, and well above that which is reasonable to expect over the coming few decades (ESA 1994). Part of the reason for this discrepancy is related to the seismic cycle, estimated to have a periodicity of about two centuries in Northern California (USGS 1990; Ellsworth 1990). The 1906 earthquake marked the culmination of the last seismic cycle, which had seen a high and increasing level of seismicity in northern California during the 19th century. The 1906 event was followed by almost five decades of low seismicity, up until the early 1950s, when seismicity began to pick up throughout the region. Thus, regional seismicity now appears to be in a phase of intermediate and increasing activity, perhaps similar to the early part of the 19th century. The Loma Prieta earthquake of 1989 (M = 7.1) has been the largest regional event since 1906.

The model of regional seismicity was selected as a compromise between the too-high levels estimated from fault slip rates and the (likely) too-low levels estimated from historic seismicity. It was considered prudent to double the rates of historic seismicity observed on regional faults for the period since 1950. This allows for an expected overall increase in regional seismicity over the coming few decades, although the factor-of-two change is certainly arguable. Nonetheless, in view of the four-times larger seismicity level that would result from adoption of a fault-slip based model (which is commonly used in engineering for earthquake resistance), this procedure seems moderate indeed. Actual historic (post-1950) seismicity levels for regional faults were assigned on the basis of reported epicenters of earthquakes of $M \geq 4.0$ found in the University of California Seismographic Station catalog for the years since 1950.

Figure 7.1 is a map showing important active (Holocene) and potentially active (Late Quaternary and Quaternary) faults, along with epicenters for the period 1808-1987. One can see high levels of seismicity

at the Geysers and along the Konocti Bay, Maacama, and Rodgers Creek faults. Figure 7.2 shows microseismicity in much the same region, recorded by the NCSN from March 1972 to December 1983, which shows, in addition, considerable activity along the Bartlett Springs - Green Valley fault trend.

In addition, a search was made of the NCSN catalog for micro-seismicity along the Collayomi fault, and the events found were used to estimate the activity parameters for it. It is noted that the Collayomi fault is reported to have ruptured sympathetically with the San Andreas in 1906.

Table 7.1 lists important parameters of the regional fault model derived from the procedure just outlined. These parameters, plus additional geometric considerations, were used to compute the effect of regional seismicity.

7.1.2 Geysers Geothermal Field

The current activity of the Geysers source was determined from the magnitude- frequency analysis of Figure 2.3. Important model parameters are shown in Table 7.1; it can be seen that the number of earthquakes expected annually with magnitude $M \geq 2.0$ is 146, and for $M \geq 3.3$ the number is 6. The Geysers Geothermal Field is modeled geometrically as two annular sectors (areas) centered on Cobb; induced seismicity is assumed to occur randomly within these sectors. The cumulative frequency-magnitude graph of Figure 2.3 show two straight line segments which represent a continuous distribution of magnitude. The upper-left line segment fits magnitudes 2.0 to 3.3, and has a slope of -1.07. In seismological terminology, these slopes are referred to as "b-slopes," referring to their use in the standard log-linear frequency-magnitude relationship, expressed by

$$\log N = A - b M,$$

where N is the annual number of events of magnitude M or greater and A is the intercept of the straight line. The line segment on the right is a rough estimate for the poorly behaved data with magnitudes from 3.3 to 4.5, and has a slope of -1.83.

Frequencies in the magnitude interval 3.3 to 4.5 appear to represent a transition between induced and regional tectonic seismicity. The estimated b-slope in this interval is -1.83, which is much steeper than is ever observed for either natural seismicity or for well-behaved (linearly distributed) induced seismicity. The peculiar frequency behavior is judged to be an artifact of a transient and unnatural phenomenon, namely, the temporary imposition of induced seismicity upon regional seismicity. It cannot persist very long: induced seismicity will eventually subside, and is expected to disappear altogether when geothermal exploitation ceases.

The maximum magnitude of induced seismicity in the Geysers Geothermal Field is tentatively assessed at 5.0. This is 0.4 to 0.8 magnitude units greater than the largest earthquake recorded to date, depending on the type of magnitude calculation employed. This shock took place on May 29, 1982, with a NCSN coda-magnitude of 4.6, and an NCSN amplitude-based magnitude of 4.3; its Richter magnitude (using the Wood-Anderson instrument at U.C. Berkeley) was 4.2. Using this information, the best-estimate magnitude for this event is M = 4.3. It is uncertain whether this earthquake was an instance of induced seismicity or was a natural tectonic event which might have occurred with no history of geothermal exploitation. However, given the lack of known active faults in the Geysers area, and the apparent historical absence of felt earthquakes there prior to geothermal development, it is reasonable to surmise that it does represent an instance of induced seismicity. It is possible that the event is related more to long-term contraction of the reservoir than to injection, but there is no way to distinguish these causes.

M = 5 is some 2/3 magnitude unit over the largest Geysers shock recorded to date. It would be very unlikely for any induced seismicity event in the Geysers field to exceed a best-estimate magnitude of 4.5. It is vital to point out here that assumption of a higher maximum magnitude would make very little

difference in any of the calculations which follow, because the rate of occurrence of M = 4.5 or greater in the Geysers field must be extremely low (based on the b-slope discussion above).

7.1.3 LACOSAN and Santa Rosa Wastewater Injection

Predicted seismic effects of induced seismicity caused by the LACOSAN and Santa Rosa wastewater injection scenarios (Chapter 5) are described in the following sections. The induced seismicity is modeled as randomly distributed in annular sectors centered on Cobb. As shown on Figure 7.3, these sectors closely bound the planned well locations for the two scenarios. More definitive specification of induced seismicity source locations was not appropriate for three reasons: (1) wells actually employed in the two scenarios may vary; (2) induced seismicity may occur at varying distances from each well; (3) model results are not sensitive to the positional uncertainties involved, which are not more than 1 km (0.6 mile).

Important parameters of model induced seismicity for the LACOSAN and Santa Rosa wastewater scenarios are given in Table 7.1. Model rates of induced seismicity shown in Table 7.1 are subject to about 50 percent uncertainty, as discussed in Chapter 5.

It can be seen that the numbers of earthquakes expected for these two sources are very different from those of the Geysers area (current induced seismicity activity). The LACOSAN source is projected to have a low induced seismicity rate because of the relatively low frequency and high b-slope (1.28) which characterize induced seismicity in the southeastern Geysers area (see Chapter 5). The Santa Rosa wastewater injection source has high activity because of abundant induced seismicity and lower b-slope which characterize the central Geysers area (see Chapter 5).

7.2 ATTENUATION OF GROUND SHAKING

In order to calculate the ground-shaking effect of an earthquake at a given place, one needs to predict the ground shaking in terms of the earthquake's magnitude and epicentral distance. Many empirical formulas have been developed by numerous researchers over the past 50 years for that purpose, and these mainly predict peak ground acceleration. A few have been prepared for Modified Mercalli Intensity, which is a semi-quantitative measure of ground-shaking effect, but practically none of these formulas uses magnitude as source descriptor. The empirical formulas evaluated as most appropriate were selected for the present study. Practically all published formulas are based on earthquakes with M > 5 (i.e., the larger, generally damaging shocks), and so are not appropriate for the smaller magnitudes associated with induced seismicity.

The practical necessity of using earthquake intensity is that this study is concerned with felt and damage effects, mainly of small events, and it is not possible to estimate either of these effects for small earthquakes (M < 5) from peak acceleration reports. This is described further in Section 7.2.1. Although small events may have sizable acceleration, the *duration* of strong shaking is extremely brief. For example, an M = 3 shock may produce a peak ground acceleration up to 0.3 g (rather strong), but lasting a fraction of a second, and therefore incapable of causing damage or of being strongly felt. On the other hand, an M = 6 shock with the same peak ground acceleration has potential for major damage, by virtue of its much longer duration (hence energy).

Published relationships between peak ground acceleration and Modified Mercalli Intensity are all based on shocks with M > 5, with significant durations and real damage potential; these relationships are simply invalid at much smaller magnitudes — one might easily predict an intensity two grades too high from an acceleration value given for an M = 3 earthquake: the published work *assumes* higher magnitude, hence much higher duration and energy for any acceleration value, and these don't at all characterize small events.

7.2.1 Peak Ground Acceleration

Campbell (1989) has developed a peak ground acceleration (PGA) attenuation formula for small events (M = 2.5 to 5); it also appears to represent M > 5 earthquakes fairly well. His formula has been employed herein. It is given by the equation

$$\log PGA = -1.086 + 0.271 M_L - \log(R + 7.28),$$

where M_L is local (Richter) magnitude.

7.2.2 Modified Mercalli Intensity

For Modified Mercalli Intensity (MMI), no attenuation formula was found representing smaller events (M < 5), and it became necessary to develop one. This was based on the work of Toppozada (1975), which developed equations to compute local magnitude from areas felt with intensities of I, V, VI, VII, and VIII. These have the form

$$M = C_k + B_k \log A_k,$$

where C and B are linear regression coefficients, A is felt area, and the subscript k refers to one of the intensities listed above.

His study appears to be the best available information for predicting intensity as a function of the logarithm of epicentral distance and magnitude, I(M, log R), for any magnitude greater than 2, because it incorporates felt-data for shocks with magnitudes as small as 4.1.

Curves I(log R) were plotted for each integer magnitude (running from M = 2 to 8) by assuming that felt areas are circular (a rough approximation of reality), so that the area (A) could be converted to radius, i.e. epicentral distance (R). At short epicentral distances, from less than 3 to less than 16 km as a function of magnitude, these curves predict intensity which is larger than observed, and it was necessary to fix maximum intensity at maximum epicentral levels, using data of Gutenberg and Richter (1956). The resulting set of curves is shown in Figure 7.4. A computer code was written to interpolate these curves by magnitude, and this was incorporated into the probabilistic ground shaking code described below.

7.3 PROBABILITIES OF GROUND SHAKING

7.3.1 Methodology

Probabilistic analysis of earthquake ground shaking for a given location (that of Cobb was used herein) begins with definition of best-estimate seismicity rates (magnitude-frequency characteristics) and geometries of fault or area sources with respect to the site of interest (altogether these data are termed the "source model"). Table 7.1 lists fault and area source-parameters used for calculations herein; it does not list detailed geometric parameters of the sources. Figures 7.1 and 7.2 show the more important (larger, more active) faults listed in Table 7.1. Figure 7.3 depicts the geometry of the area sources used to model induced seismicity. Results include the annual rate of exceedance, and probabilities of exceedance during specified exposure intervals, of site ground motions which exceed each one of a series of specified test values (e.g. for peak ground acceleration we might select 0.1 g, 0.2 g, etc.). Calculations were made by a computer program which uses standard numerical methods for this type of calculation, as outlined below.

The ground-motion parameter (log(PGA) or Modified Mercalli Intensity) is assumed to have a log-normal distribution about its predicted median value. Times and positions of earthquakes are assumed to be uniformly distributed for/in each source; therefore, the number of events in any given time interval is Poisson-distributed. For each source, the annual rate of exceedance of each ground-motion test value is

found by numerical integration over the source dimensions and magnitude range. Rates of exceedance for the total model are found by summing over all sources, and probabilities of exceedance for given exposure periods are found directly from these rates. The recurrence interval, utilized in the following discussion, is simply the reciprocal of the rate of occurrence. Probabilities of exceedance are calculated using a simple exponential equation (Benjamin and Cornell 1971). The standard deviation of the ground-motion parameter is an important element of the numerics: it is well established for the peak ground acceleration attenuation function used, but not for intensity (see discussion in next section).

It must be stressed that the procedure is *non-historical in nature*. That is, the prediction period represents an arbitrarily chosen interval with no particular place in historical time. This is because seismicity is assumed to have a uniform random distribution of interoccurrence times. The concept of a seismic cycle is not represented in this methodology: the model does not take into account that the site of interest lies in a region of rising seismicity. Hence, regional background sources were assigned activities twice their historical level since 1950 in order to account for an expected rise of seismicity. This approach was explained previously, in Section 7.1.1.

7.3.2 Model Calibration for Modified Mercalli Intensity

Because the standard deviation (SD-I) of Modified Mercalli Intensity from the relationship developed in Section 7.2.2 is not known, it was necessary to adjust it to yield reasonable results. SD-I was set at 0.5 intensity unit because this produced a fairly good fit of model to data (see comparison in Section 7.3.3); smaller SD-I values caused predicted rates of intensity occurrences to be too low, and larger values did not seem reasonable. Intensity data are summarized here.

Felt reports (intensity occurrences) were obtained from the USGS for Cobb, for the period 1906-1985 (later reports are unavailable), and sorted according to their source category, either regional or Geysers. The coverage period extends from 1906 to 1985. The data are given in Table 7.2, and mean recurrence intervals of intensity are shown to the right of the data. For regional events, it is seen that only two earthquakes (1906 and 1938) were felt at Cobb before 1954; beginning in 1954, felt reports for regional events have an average interval of 2.5 years, reflecting the ongoing rise of regional seismicity. Felt Geysers events were first reported in 1973, and 17 felt reports were found for the period 1980 to 1985, making an average interval of 0.3 years. The period 1973-1979 is not used in recurrence calculations because Geysers seismicity had not yet attained the levels seen from 1980 to present. A comparison of these reported intensity data with model predictions is made in the next section of the report.

It is necessary to point out that assignment of Modified Mercalli Intensity (MMI) to a locality for any given earthquake is always approximate. For the lower intensity grades of interest here (III to V), reports of earthquake effects, according to the intensity grade descriptions (see Table 7.4), are gathered by means of a questionnaire sent to postmasters by the U.S. Geological Survey (USGS), and perhaps from newspapers; no field investigation is conducted by trained personnel (as would be done for damaging earthquakes). The postmaster (or postal employee) incorporates his own experience and verbal reports from others in completing the questionnaire. Researchers at the USGS then compile and examine all reported effects, eliminating any which are clearly incompatible with the bulk of information received. Individual reports from a locality may vary by about two intensity grades, depending on the following factors, each of which may vary — sometimes greatly: local geology and soil conditions; type, quality, and age of building construction; stability of household furnishings; untrained observers making the report. Assignment of intensity to a town involves choosing what appears to be the modal (most frequent) intensity grade reported. The procedure is subjective, and is often thought to have a likely error of plus or minus one intensity grade.

7.3.3 Results

Table 7.3 presents a summary of important predicted ground-shaking parameters calculated for the model seismicity. Part A lists mean recurrence intervals for intensity and peak acceleration. The first column ('R') is for regional seismicity not including the Geysers (current induced seismicity); the four columns to the right of 'R' represent cumulative effects, first adding Geysers current induced seismicity ('R+G'), then adding LACOSAN ('R+G+L') or Santa Rosa wastewater injection seismicity ('R+G+S'), and finally including all sources ('R+G+L+S').

Part B lists probable maximum values read from probability-of-exceedance curves, Figures 7.4 and 7.5, at a probability of 63 percent (by standard statistical theory, this is the most probable value: Gumbel 1958). A description (abridged) of the Modified Mercalli Intensity (MMI) Scale of 1931, helpful in interpreting these intensity data, is given in Table 7.4.

Looking at Table 7.3-A, one sees that induced seismicity has a major effect for intensities up to V: adding the Geysers ('G') source reduces regional background ('R') recurrence intervals by factors from 15 (MMI = III) to nearly 2 (MMI = V); the LACOSAN source ('L') makes little difference due its low activity; the Santa Rosa wastewater injection source ('S') further reduces those recurrence intervals by factors of nearly 2.3 (MMI = III) to 1.7 (MMI = V). At MMI = VI to VIII, the induced seismicity sources have little or no effect, due to the high b-slope (rapid fall-off in frequency) for M≥ 3.3. For peak ground acceleration, one can see similar behavior, although induced seismicity makes significant contributions up to 0.40 g. The fractional error in these predicted recurrence intervals is estimated at about ± 30 percent, and is caused mainly by errors in rates of model seismicity for the various sources, with estimated ± 30 percent fractional error. The uncertainty in comparative (ratios of) recurrence intervals for different source combinations in Table 7.3-A would then be about ± 40 percent. Another source of error lies in the attenuation relationships (peak acceleration or intensity), but this should not have much impact on comparative (ratios of) recurrence intervals.

The following discussion compares these predictions with the historic record for Cobb (Table 7.2). The cumulative numbers of events for grades equal to or greater than a given intensity level in Table 7.2 reveal that intensities II and III are quite under-reported, as we would expect to see an approximate five-fold increase in the cumulative numbers of reports with each unit decrease in intensity (based on magnitude-frequency and magnitude-intensity relationships). Based on their relative cumulative frequencies, it looks as though intensities IV and V might be reported rather fully. For regional events, the historic data indicate an average recurrence period for intensity V or larger of 16 years. Table 7.3-A indicates that regional events may cause intensity V or larger every 3.6 years. When the model is adjusted to reflect historic seismicity since 1954 (recall that it was constructed to double the actual seismicity of this period), it predicts about 7 years for intensity V or larger, which is approximately one-half the reported interval (16 years). For intensity IV or larger, the agreement is about the same: the record indicates a 5-year interval, and the adjusted prediction is 2.8 years (2 x 510 days). These comparisons indicate substantial and adequate agreement of predicted regional-source intensity recurrence with that for the historic record.

For the Geysers source, the historic record (1980-1985) for Cobb indicates a recurrence interval of one year for intensity IV or larger, and two years for intensity V or larger. The model for regional background plus Geysers seismicity predicts recurrence intervals of 73 days for intensity IV or larger and 1.6 years for intensity V or larger ('R+G' in Table 7.3-A). Removing the effect of regional background (i.e. 'R+G'-'R') yields 85 days for intensity IV or larger and 2.9 years for intensity V or larger. Thus, the model predicts 50 percent longer recurrence for intensity V than reported, but considerably shorter recurrence for intensity IV (factor of four) than reported. It is certain that many intensity II to III occurrences have not been reported, considering the large number of Geysers earthquakes (with M≥ 2.0) that must have caused such effects; it seems likely that a few intensity IV events have also gone unreported.

Table 7.3-B presents most probable maximum intensity and peak ground acceleration. For intensity, induced seismicity has significant impact only for the shortest listed recurrence intervals, 1 year (and for comparable periods of time). At longer intervals, the intensity levels are limited by the high b-slope for M ≥ 3.3 for induced seismicity sources. For peak ground acceleration, induced seismicity effects are strong for all three listed recurrence intervals.

In the following two paragraphs, probability-of-exceedance curves are presented and discussed. Each of these curves is drawn by manually plotting and fitting a curve through several data points, each relating ground motion to probability for the selected arbitrary exposure interval (here selected to be 1, 10, and 50 years). The data points are calculated from annual rate-of-exceedance data.

Figure 7.5 presents Modified Mercalli Intensity versus probability of exceedance for arbitrary periods of 1, 10 and 50 years, for regional background seismicity (REGION), regional background plus Geysers existing seismicity (REGION + GGF), and regional background plus Geysers plus Santa Rosa wastewater injection-induced seismicity (REGION + GGF + SRWW). The effect of LACOSAN wastewater injection is not plotted because it is very small and cannot be easily distinguished in this type of plot. It is seen that the greatest effect of induced seismicity is over short periods, represented by the 1-year interval shown. The curves on Figure 7.5 for 'REGION + GGF' and 'REGION + GGF + SRWW' merge at low probabilities (intensity VI). For 50 years, the curves are virtually merged for all probabilities less than about 99 percent (largest shown); ultimately, they must separate for larger probabilities (over about 99.99 percent), not shown.

Calculations indicate that errors in probability are greatest for centrally located values, say for probabilities between 40 percent and 60 percent. Based on the estimated fractional error (30 percent) in recurrence intervals, probability error in this range might amount to ± 12 percentage points. Error decreases moving toward very large or very small probabilities. The merging of the probability curves for intensity over V reflects the fact that intensities > V are produced almost entirely by regional (REGION) earthquakes, while intensities due to magnitude-limited induced seismicity sources are virtually limited to intensity V to VI.

Figure 7.6 is like 7.5, but for peak ground acceleration instead of intensity. The curves are well separated for all probabilities, which reflects the fact that peak ground acceleration can be high for small earthquakes, while intensity cannot.

As a final note, it is important to point out that the assessment of intensity has been made independently from that of peak acceleration. In Table 7.3-B, for recurrence intervals of 10 and 50 years, maximum probable peak accelerations of 0.11 g to 0.30 g are associated with maximum probable intensities of V to VI. However, published direct relationships between peak ground acceleration and intensity (e.g., Trifunac and Brady 1975) indicate that these acceleration levels correspond to intensities from VII to VIII, some two grades higher than we have found. This is explained by the fact that the published studies do not include earthquakes of magnitude less than about 5.5, i.e., the smaller magnitudes characterizing the induced seismicity of concern at the Geysers. These smaller shocks may indeed have large accelerations, but their intensities are small because durations (hence energies) are small.

Incremental induced seismicity resulting from the Santa Rosa wastewater injection scenario would be felt at low Modified Mercalli Intensity grades (II to VI-), but would do no significant damage (intensity grade VII or higher).

8 CONCLUSIONS

The following conclusions were derived principally from the analyses described in Sections 4 through 7.

Steam production and, frequently, water injection can produce microearthquakes at the Geysers Geothermal Field. For the Geysers Geothermal Field wells studied, induced seismicity appears to be very likely above a water injection rate of about 1.4 mgd per well.

Each scenario injection well is forecast to produce induced seismicity at an annual rate of about 166 earthquakes with M > 0.7, equivalent to a total injection scenario rate of 1660 earthquakes for 10 wells. Total scenario injection is forecast to generate approximately seven earthquakes of M > 3.3 per year. However, these figures are subject to considerable uncertainty.

The planned injection for this project is likely to increase the incidence of earthquakes with Modified Mercalli Intensity V and less in nearby communities as indicated in Table 7.3. Intensity V felt effects are predicted to increase from about one per 1.6 years to about one per year (approximately 38% more frequent). The analysis predicts a small increase in the rate of intensity VI earthquakes (slight damage), but that increase is of marginal reliability given the level of uncertainties in the model and that no instances of intensity VI due to Geysers induced seismicity have been documented.

For the studied wells, well behavior generally changed with time. As shown in Figures 4.10 through 4.15, correlations between induced seismicity and injection rate were generally strongest for the first few years following initiation of injection, but became weaker in later years. This observation indicates that induced seismicity may decline with time following initial injection. However, a reliable quantitative assessment of the rate of decline could not be made on the basis of the available data, so it is not accounted for in the forecasts given here.

The calculation model was constructed to be appropriately conservative and as realistic as possible. The model was calibrated by matching regional background and existing Geysers seismicity with reported earthquake effects in the community insofar as possible. However, it remains that cases of intensity VI effects due to Geysers induced seismicity have not been documented.

Published relationships relating site Modified Mercalli Intensity to magnitude and peak ground acceleration are inappropriate for the low magnitude earthquakes experienced at the Geysers. A site intensity attenuation function was derived from published empirically determined relationships between intensity and felt area in California.

Static stress modeling calculations indicate that Geysers induced seismicity should not increase the risk of larger earthquakes on nearby faults.

9 ACKNOWLEDGEMENTS

The authors wish to thank Unocal Geothermal Division for generous cooperation in providing all data utilized herein concerning geothermal wells (locations and operational histories), U-N-T hypocentral data, and lease unit boundaries within the Unocal leasehold. Dr. Robert Simpson of the U.S. Geological Survey generously provided computational support concerning stress changes due to Geysers earthquakes.

Acknowledgment is also given to Dr. Bruce R. Julian, Seismology Section, U. S. Geological Survey, Menlo Park, and Dr. Ernest L. Majer, Earth Sciences Division, Lawrence Berkeley National Laboratory, Berkeley, and William B. Cumming, Unocal seismologist, who performed detailed technical reviews of the draft report. Dr. David H. Oppenheimer of the U. S. Geological Survey and Dr. Anthony Mossop, Stanford University, reviewed and critiqued the methodology utilized in the study.

APPENDIX A

TABLES

Table 5.1

Average Historical and Forecast Induced Seismicity in the Geysers Geothermal Field

AVERAGE HISTORICAL

Magnitude	b-slope	Annual Number of Earthquakes
≥ 0.7	——[1]	2168
≥ 2.0	1.07	155
≥ 3.3	1.83[2]	5

SANTA ROSA WASTEWATER SCENARIO

Magnitude	b-slope	Annual Number of Earthquakes
≥ 0.7	——[1]	1660
≥ 2.0	1.07	166
≥ 3.3	1.83[2]	7

LACOSAN WASTEWATER SCENARIO

Magnitude	b-slope	Annual Number of Earthquakes
≥ 0.7	——[1]	2050
≥ 2.0	1.28	11
≥ 3.3	1.83[2]	.24

1 Not determined because of incomplete detection for M < 1.4

2 Approximate due to insufficient data for M > 3.9

Table 7.1

Model Seismicity Parameters

Source	Type	Parameters[1]				
		R_{min} (km)	L (km)	M_{min}	M_{max}	N / yr
Region - Natural						
San Andreas	Fault	56	420	6.0	7.8	.008
Rodgers Creek	Fault	27	58	3.25	7.0	.08
Maacama	Fault	16	136	2.5	7.5	9
Green Valley-Bartlett Springs	Fault	18	180	2.5	7.5	8
Collayomi	Fault	.2	20	2.0	6.5	.8
Konocti Bay	Fault	10	13	2.0	6.0	3
Big Valley	Fault	15	8	2.5	5.5	1
Mt. Hannah	Area	5	5	2.0	5.0	.6
Induced[2]						
GGF-small	Area	3.3	6.8	2.0	3.3	146
GGF-large	Area	3.3	6.8	3.3	5.0	6
LACOSAN-small	Area	5.1	3.7	2.0	3.3	11
LACOSAN-large	Area	5.1	3.7	3.3	5.0	.24
SRWW-small	Area	4.5	4.9	2.0	3.3	166
SRWW-large	Area	4.5	4.9	3.3	5.0	7

1 R_{min} - minimum distance from Cobb
L - fault length (for area, width of annular zone)
M_{min} - minimum magnitude
M_{max} - maximum magnitude
N - annual number of events in range M_{min} to M_{max}
- b-slope is 0.9 for all natural sources

2 Using a bilinear curve, with b = 1.07 (but 1.28 for LACOSAN) for M 2.0-3.3 and b = 1.83 for M 3.3-5.0

GGF: Geysers Geothermal Field
LACOSAN: Lake County Sanitation District wastewater injection project
SRWW: Santa Rosa wastewater injection scenario

Table 7.2

Historic Intensity Reports for Cobb, 1906–1985

REGIONAL EVENTS

MMI	YR	MO	DA	LAT	LON	MAG	Location
V	06	4	18	38.00	123.00	8.3	San Andreas
IV	38	9	12	40.25	125.00	5.5	Cape Mendocino
VI	54	12	21	40.82	124.08	6.6	Eureka
IV	56	4	5	38.53	122.52	4.8	St. Helena
III	57	3	22	37.67	122.47	5.3	Daly City
V	62	6	6	39.08	123.07	5.2	Lakeport
III	66	12	23	38.70	122.80	3.7	Jimtown
IV	68	4	25	38.48	122.72	4.6	Santa Rosa
IV	69	10	2	38.47	122.69	5.6	Santa Rosa
IV	74	3	21	38.60	122.66	3.8	Cloverdale
IV	77	9	11	38.70	122.80	4.0	Jimtown
III	77	9	22	38.60	122.76	4.0	Windsor
II	78	9	8	38.64	121.91	4.4	Healdsburg
III	80	12	12	38.96	122.69	3.9	S. Clear Lake
II	82	6	14	38.78	122.92	3.0	Boggs Lake

Recurrence Intervals 1954–1985

MMI	CUM #	T(yr)
II	13	2
III	11	3
IV	7	5
V	2	16
VI	1	32
ALL	13	2.5

MMI: Modified Mercalli Intensity reported for Cobb vicinity
YR: Year of earthquake
MO: Month of earthquake
DA: Day of earthquake
LAT: North latitude of earthquake epicenter
LON: West longitude of earthquake epicenter
MAG: Magnitude
CUM #: cumulative number events >= MMI value shown
T: average recurrence interval, MMI >= value shown

Table 7.2 (continued)

Historic Intensity Reports for Cobb, 1906–1985

GEYSERS GEOTHERMAL FIELD EVENTS

MMI	YR	MO	DA	LAT	LON	MAG	Location
IV	73	11	29	38.82	122.80	2.3	GGF
IV	73	11	28	38.80	122.80	3.2	GGF
II	76	3	4	38.79	122.75	3.1	GGF
II	76	3	6	38.83	122.83	2.9	GGF
II	79	12	20	38.80	122.80	3.0	GGF
III	80	7	24	38.81	122.79	2.9	GGF
III	80	8	23	38.81	122.78	2.8	GGF
II	81	10	31	38.81	122.81	3.1	GGF
II	81	12	10	38.80	122.79	3.3	GGF
IV	82	3	25	38.80	122.80	3.4	GGF
V	82	5	29	38.80	122.82	4.3	GGF
II	82	5	29	38.84	122.83	2.9	GGF
IV	82	12	26	38.81	122.78	3.1	GGF
V	83	6	11	38.80	122.82	3.4	GGF
II	83	4	19	38.79	122.81	2.8	GGF
II	83	6	20	38.82	122.79	3.2	GGF
II	83	4	19	38.83	122.80	2.9	GGF
II	83	10	1	38.79	122.84	3.0	GGF
II	84	10	4	38.83	122.78	2.8	GGF
II	84	3	2	38.81	122.79	3.0	GGF
V	84	9	22	38.80	122.81	4.2	GGF
IV	85	3	30	38.82	122.82	3.3	GGF
II	85	7	26	38.80	122.80	3.5	GGF
II	85	7	26	38.79	122.79	3.8	GGF

Recurrence Intervals 1980–1985

MMI	CUM #	T(yr)
II	17	0.4
III	8	0.8
IV	6	1.0
V	3	2.0
VI	0	
ALL	17	0.4

MMI: Modified Mercalli Intensity reported for Cobb vicinity
YR: Year of earthquake
MO: Month of earthquake
DA: Day of earthquake
LAT: North latitude of earthquake epicenter
LON: West longitude of earthquake epicenter
MAG: Magnitude
CUM #: cumulative number events >= MMI value shown
T: average recurrence interval, MMI >= value shown
GGF: Geysers Geothermal Field

Table 7.3

Summary of Predicted Earthquake Effects at Cobb
(See text concerning uncertainties in these data)

7.3-A Recurrence Intervals for Intensity and Peak Ground Acceleration[1]

MMI ≥	**R**	**R+G**	**R+G+S**	**R+G+L**	**R+G+L+S**
III	210 da	14 da	6.1 da	13 da	6.0 da
IV	510 da	73 da	33 da	70 da	33 da
V	3.6 yr	1.6 yr	.94 yr	1.6 yr	.93 yr
VI	13 yr	10 yr	8.4 yr	10 yr	8.3 yr
VII	80 yr	80 yr	80 yr	80 yr	80 yr
VIII	900 yr	900 yr	900 yr	900 yr	900 yr
PGA(g) ≥					
.025	74 da	4.5 da	2.1 da	4.2 da	2.1 da
.05	360 da	17 da	8.0 da	16 da	7.8 da
.10	8 yr	.46 yr	.22 yr	.44 yr	.22 yr
.20	76 yr	11 yr	5.4 yr	10 yr	5.3 yr
.30	300 yr	91 yr	51 yr	89 yr	50 yr
.40	850 yr	424 yr	270 yr	418 yr	270 yr

7.3-B Probable Maximum Intensity and Peak Acceleration[1,2]

Recurrence Interval (years)	**R**	**R+G**	**R+G+S**	**R+G+L**	**R+G+L+S**
	MMI				
1	III	IV	V–	IV	V–
10	V	V+	VI–	V+	VI–
50	VI	VI	VI	VI	VI
	PGA(g)				
1	.05	.12	.14	.12	.14
10	.11	.20	.22	.20	.22
50	.17	.27	.30	.27	.30

1 Model seismicity sources:
R - Regional background
G- Geysers geothermal field, current
L - Induced seismicity projected for LACOSAN injection
S - Induced seismicity projected for Santa Rosa wastewater scenario, average annual injection

2 Values listed have a 63% chance of being exceeded in the stated recurrence interval (Gumbel 1958)

MMI: Modified Mercalli Intensity
PGA: Peak Ground Acceleration

Table 7.4

Modified Mercalli Intensity Scale of 1931

I.	Not felt except by a very few under especially favorable circumstances.
II.	Felt only by a few persons at rest, especially on upper floor of buildings. Delicately suspended objects may swing.
III.	Felt quite noticeably indoors, especially on upper floors of buildings, but many people do not recognize it as an earthquake. Standing motorcars may rock slightly. Vibration like passing truck. Duration estimated.
IV.	During the day felt indoors by many, outdoors by few. At night some awakened. Dishes, windows, and doors disturbed; walls make cracking sound. Sensation like heavy truck striking building. Standing motorcars rocked noticeably.
V.	Felt by nearly everyone; many awakened. Some dishes, windows, etc., broken; a few instances of cracked plaster; unstable objects sometimes overturned. Disturbance of trees, poles, and other tall objects sometimes noticed. Pendulum clocks may stop.
VI.	Felt by all; many frightened and run outdoors. Some heavy furniture moved; a few instances of fallen plaster or damaged chimneys. Damage slight.
VII.	Everybody runs outdoors. Damage negligible in buildings of good design and construction; slight to moderate in well built ordinary structures; considerable in poorly built or badly designed structures. Some chimneys broken. Noticed by persons driving motorcars.
VIII.	Damage slight in specially designed structures; considerable in ordinary substantial buildings, with partial collapse; great in poorly built structures. Panel walls thrown out of frame structures. Fall of chimneys, factory stacks, columns, monuments, walls. Heavy furniture overturned. Sand and mud ejected in small amounts. Changes in well water. Persons driving motorcars disturbed.
IX.	Damage considerable in specially designed structures; well-designed frame structures thrown out of plumb; great in substantial buildings, with partial collapse. Buildings shifted off foundations. Ground cracked conspicuously. Underground pipes broken.
X.	Some well-built wooden structures destroyed; most masonry and frame structures destroyed with foundations; ground badly cracked. Rails bent. Landslides considerable from river banks and steep slopes. Shifted sand and mud. Water splashed (slopped) over banks.
XI.	Few, if any (masonry), structures remain standing. Bridges destroyed. Broad fissures in ground. Underground pipelines completely out of service. Earth slumps and land slips in soft ground. Rails bent greatly.
XII.	Damage total. Waves seen on ground surfaces. Lines of sight and level distorted. Objects thrown upward into the air.

Reference: Wood and Neumann (1931)

APPENDIX B

FIGURES

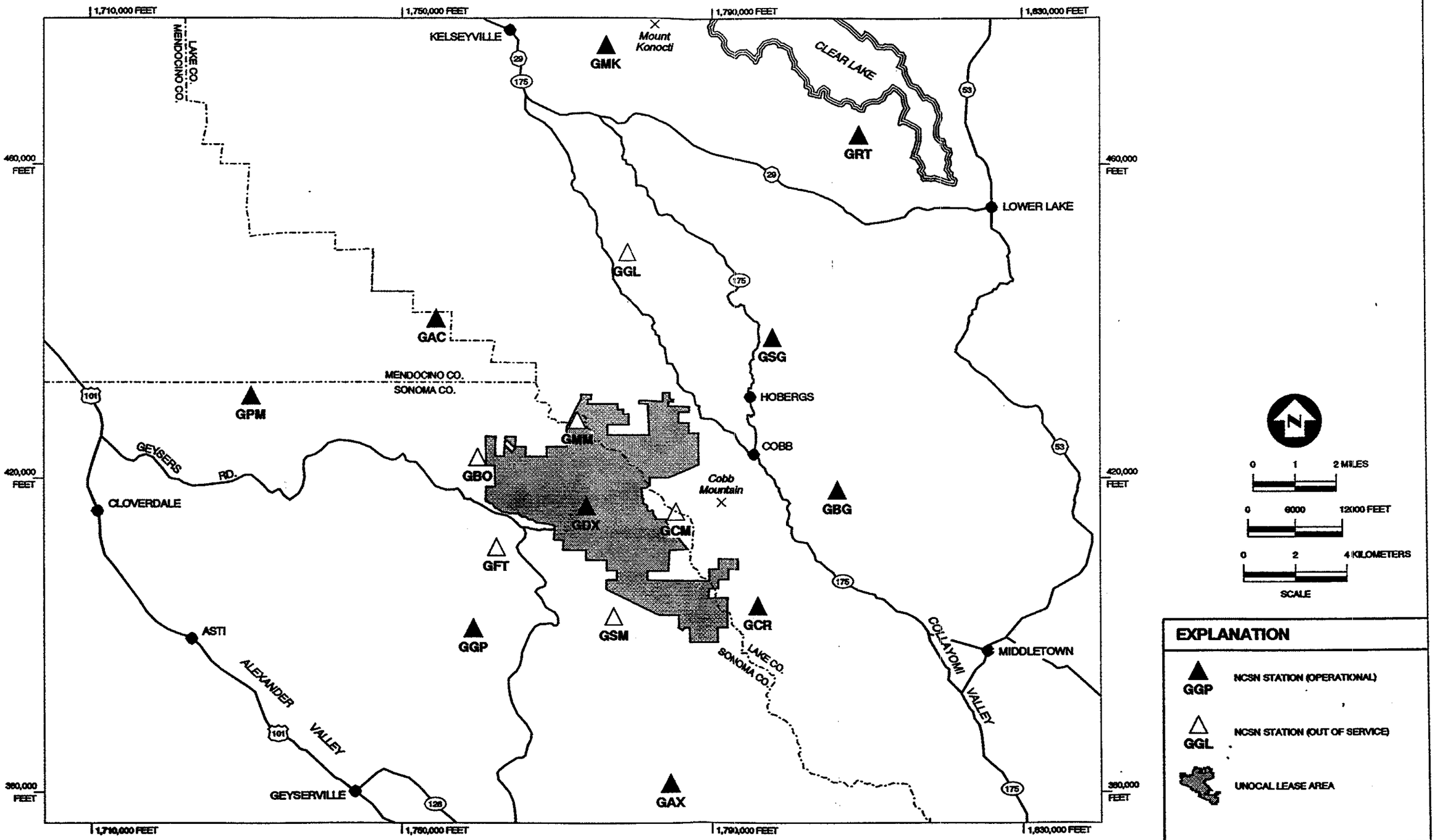

Santa Rosa
Subregional Long-Term Wastewater Project

SEISMOGRAPH STATION LOCATIONS
NCSN (USGS) NETWORK
GEYSERS INDUCED SEISMICITY STUDY

FIGURE 1.1

REV. 3 SR406-01.DWG 02/13/98

PARSONS ENGINEERING SCIENCE, INC.

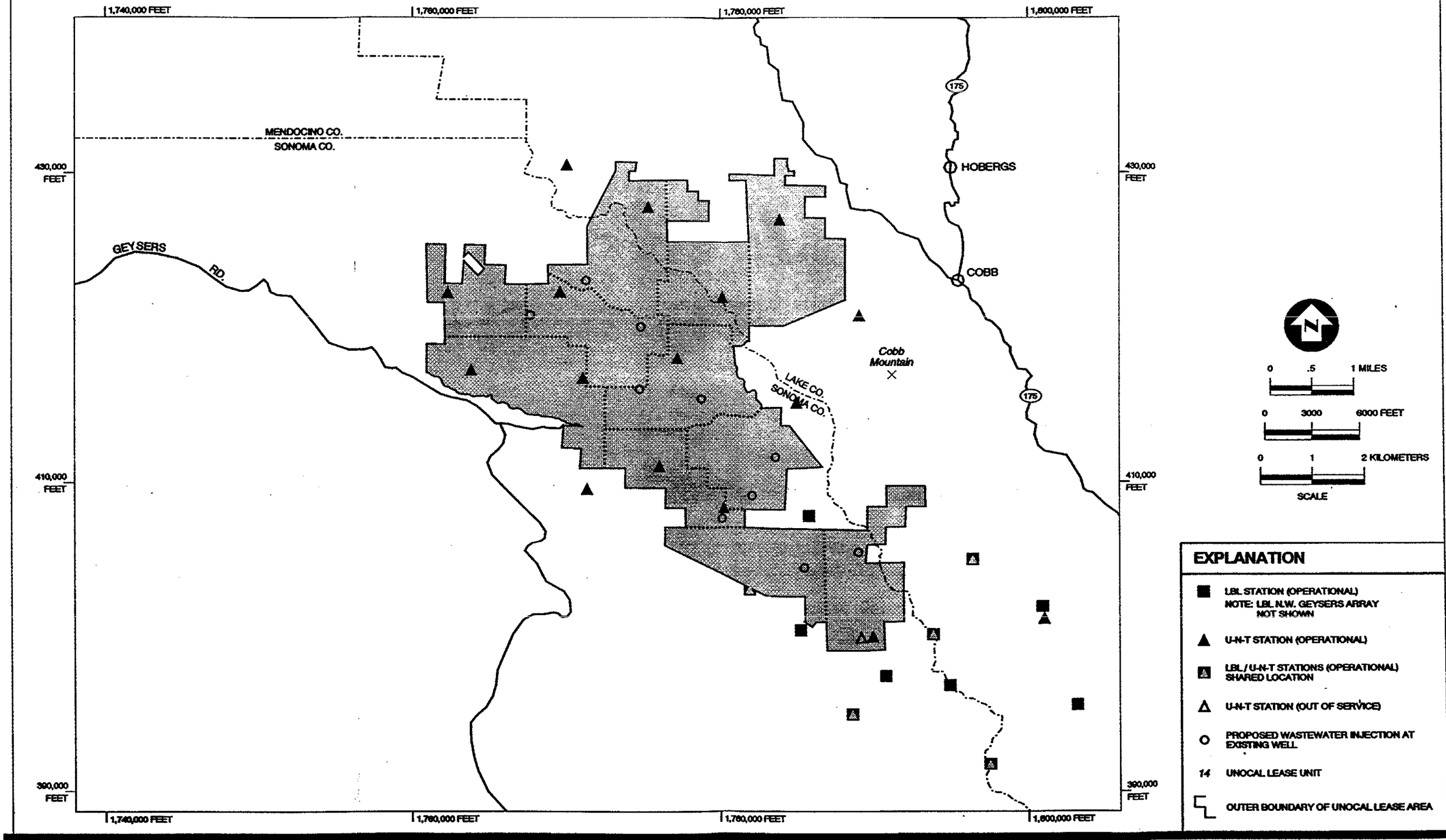

Santa Rosa
Subregional Long-Term Wastewater Project

SEISMOGRAPH STATION LOCATIONS
LBL AND U-N-T NETWORKS
GEYSERS INDUCED SEISMICITY STUDY

FIGURE 1.2

REV. 3 SR406-02.DWG 02/13/96

PARSONS ENGINEERING SCIENCE, INC.

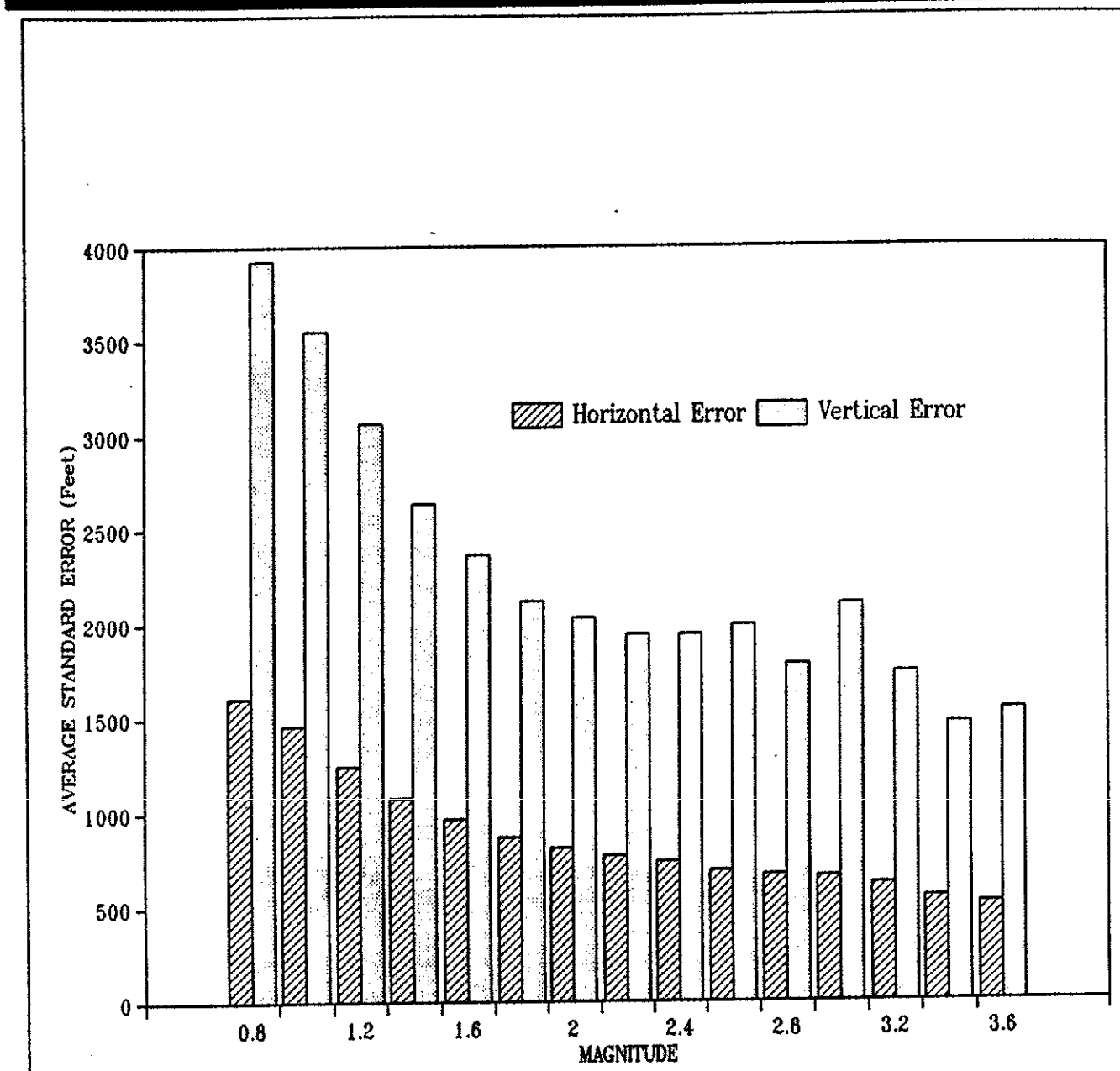

Subregional Long-Term Wastewater Project

STANDARD ERROR IN NCSN HYPOCENTERS
ENTIRE UNOCAL AREA
JANUARY 1976 THROUGH MAY 1995
GEYSERS INDUCED SEISMICITY STUDY

FIGURE 2.1

REV. 2 SR408-95.DWG 01/10/96

PARSONS ENGINEERING SCIENCE, INC.

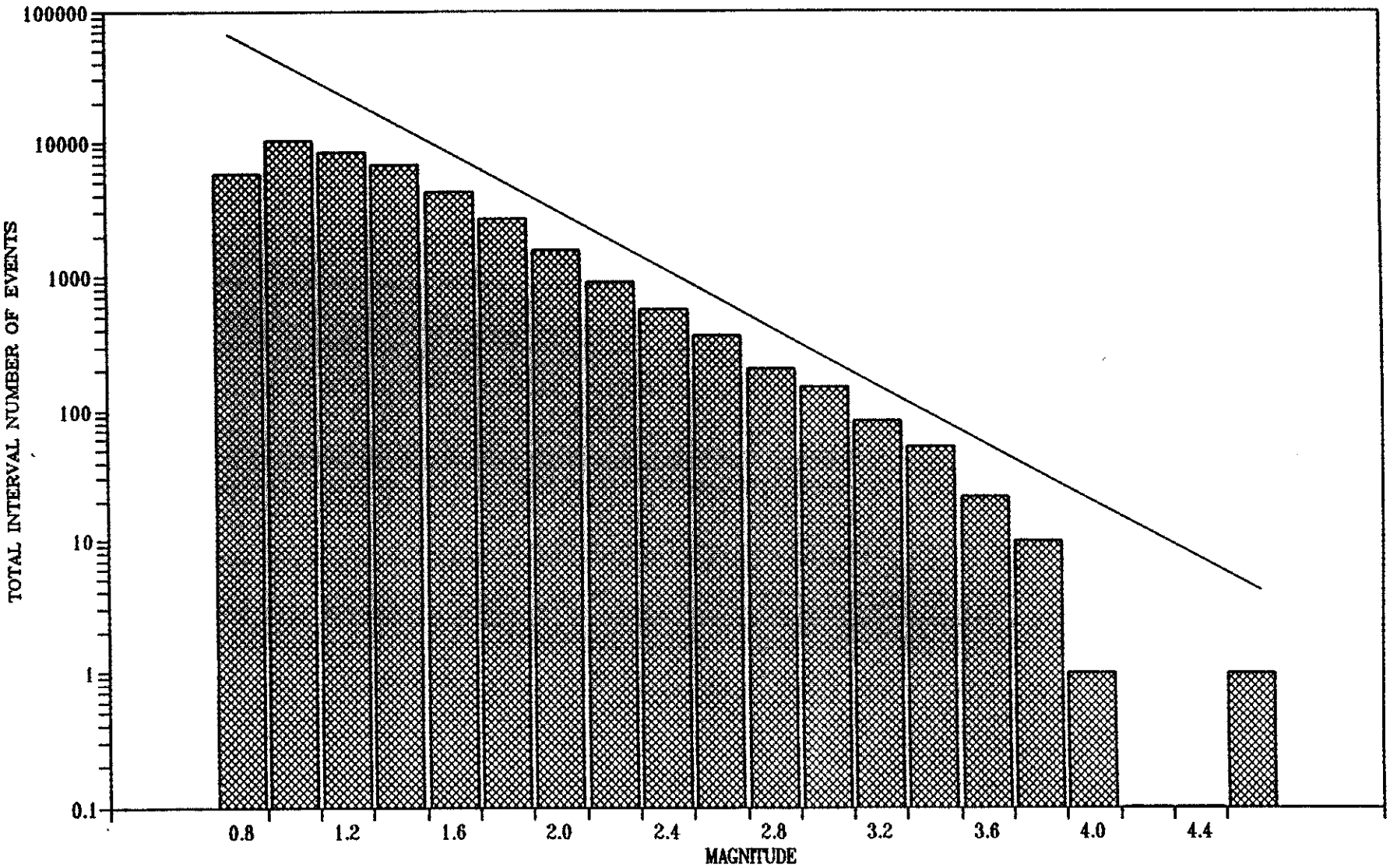

Santa Rosa
Subregional Long-Term Wastewater Project

INTERVAL FREQUENCY VS. MAGNITUDE
ENTIRE UNOCAL AREA, JANUARY 1976 THROUGH MAY 1995
GEYSERS INDUCED SEISMICITY STUDY

FIGURE 2.2

REV. 2 SR409-07.DWG 01/10/96

PARSONS ENGINEERING SCIENCE, INC.

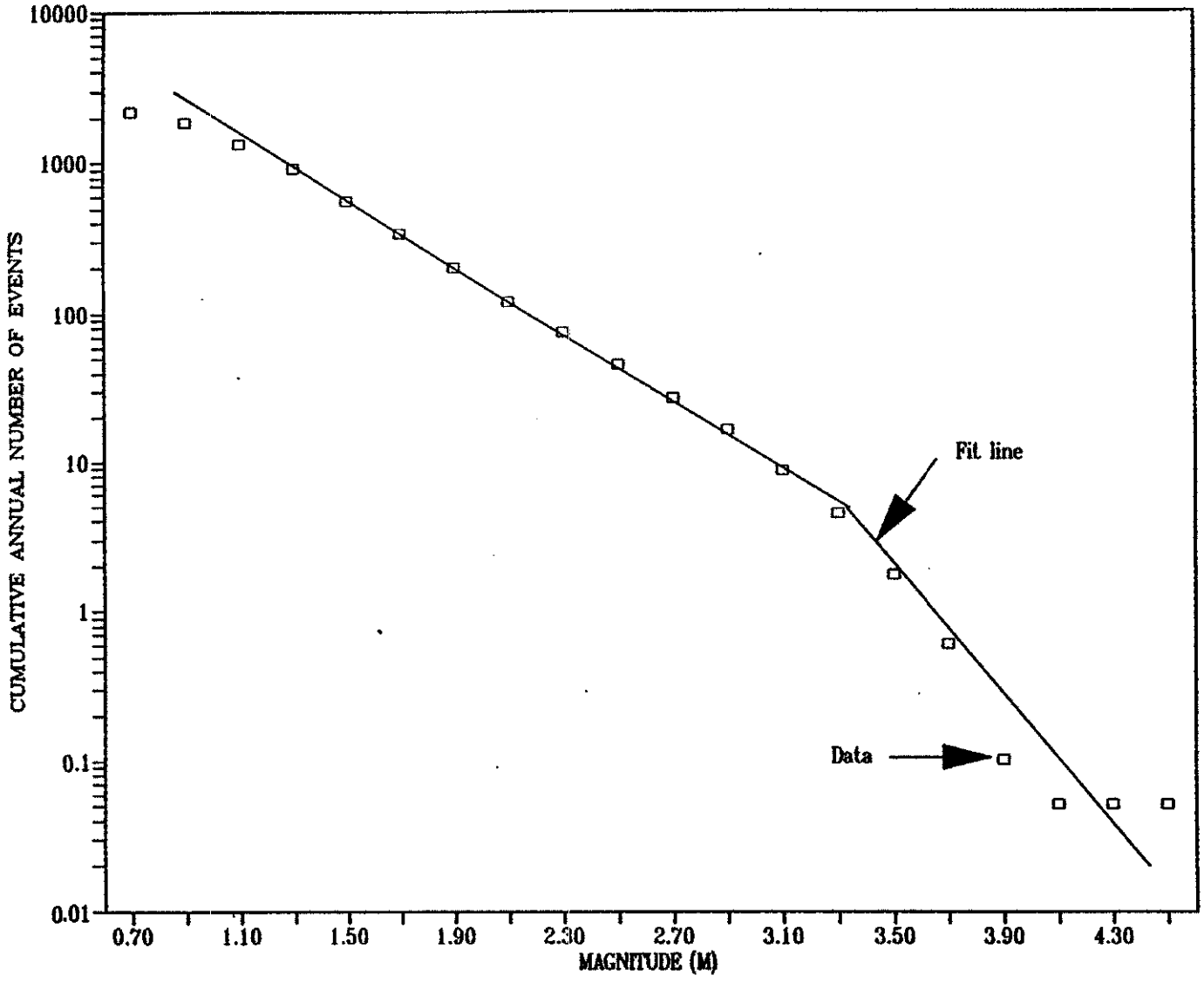

Subregional Long-Term Wastewater Project

CUMULATIVE ANNUAL FREQUENCY VS. MAGNITUDE, ENTIRE UNOCAL AREA, JANUARY 1976 THROUGH MAY 1995

GEYSERS INDUCED SEISMICITY STUDY

FIGURE 2.3

REV. 2 SR408-08.DWG 01/10/96

PARSONS ENGINEERING SCIENCE, INC.

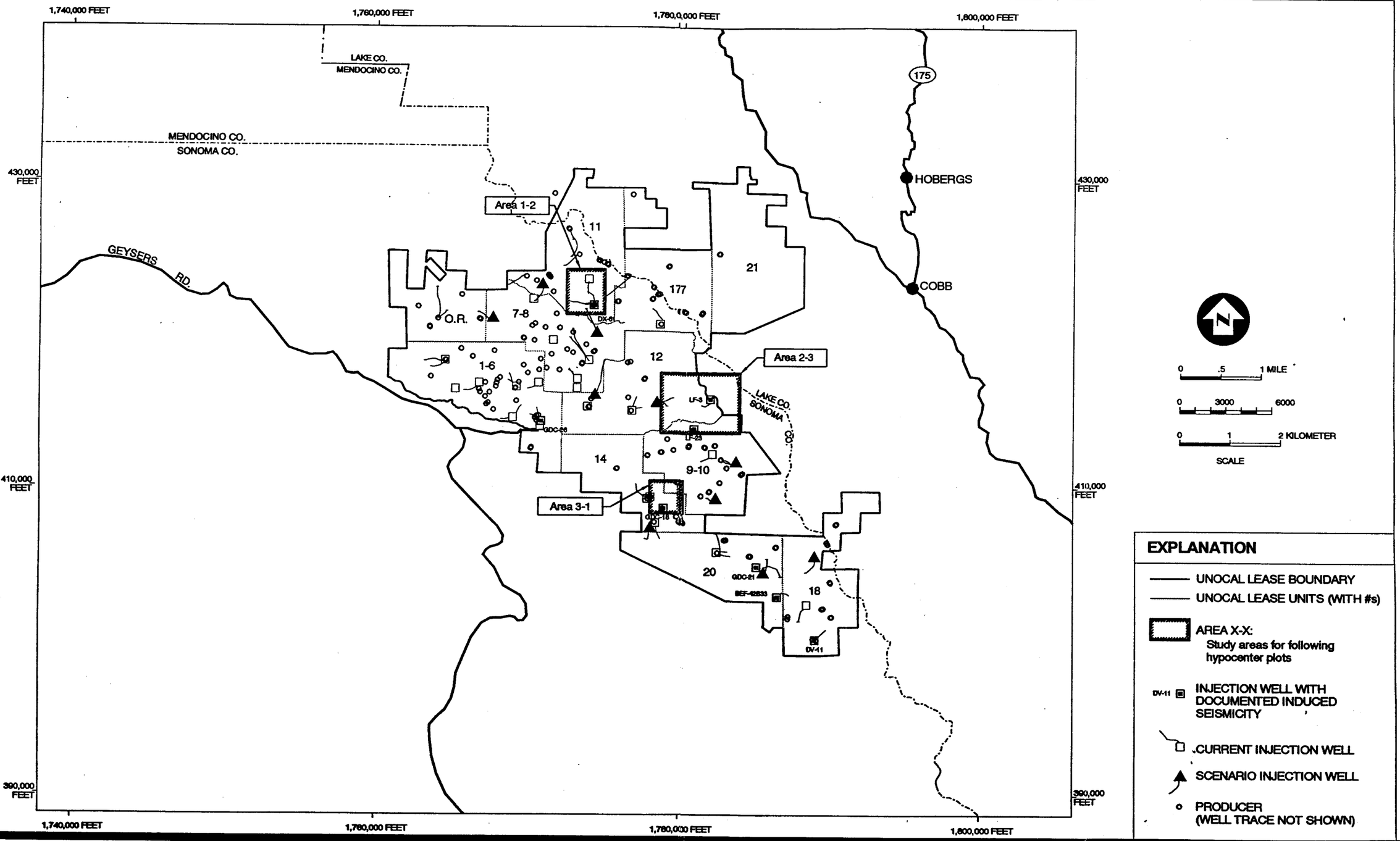

Santa Rosa
Subregional Long-Term Wastewater Project

LOCATIONS OF CURRENT AND SCENARIO INJECTION WELLS AND INJECTORS WITH DOCUMENTED INDUCED SEISMICITY

GEYSERS INDUCED SEISMICITY STUDY

FIGURE 3.1

REV. 4 SR408-05.DWG 02/13/98

PARSONS ENGINEERING SCIENCE, INC.

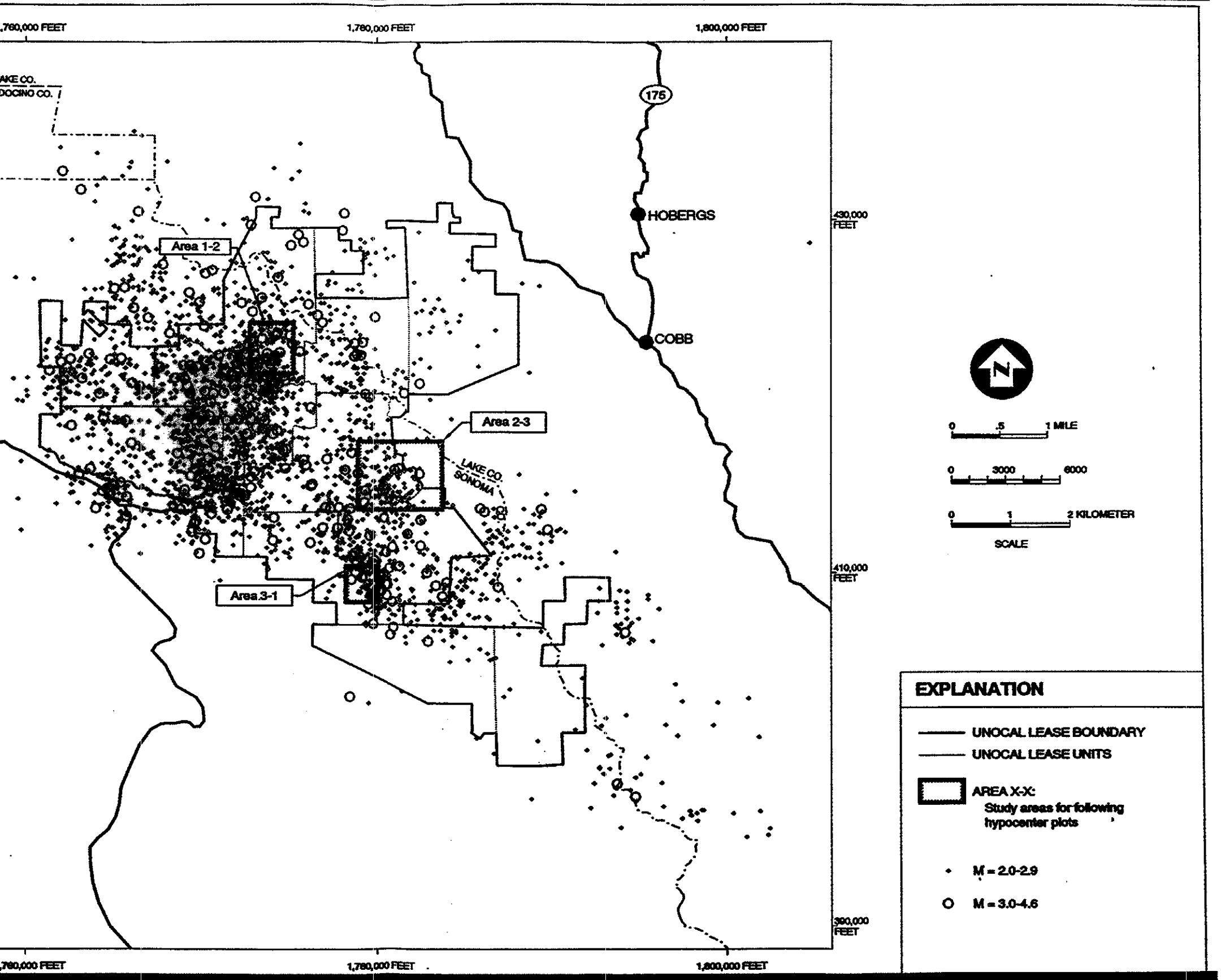

EARTHQUAKES CENTERS (NCSN), M≥ 2.0
1976-1995
GEYSERS INDUCED SEISMICITY STUDY

FIGURE 4.1

PARSONS ENGINEERING SCIENCE, INC.

NCSN Hypocenters

Shown in Figures 4.1 to 4.7

	Average Standard Error (feet)	
Magnitude	**Horizontal**	**Vertical**
0.7 – 2.0	1,600 – 800	4,000 – 2,000
2.0 – 3.0	800 – 700	2,000 – 1,700
3.0 – 4.5	700 – 600	1,700 – 1,500

U-N-T Hypocenters

Shown in Figures 4.8 and 4.9

	Estimated Uncertainty (feet)	
Magnitude	**Horizontal**	**Vertical**
0.7 – 4.5	700	1,300

Subregional Long-Term Wastewater Project

UNCERTAINTIES IN HYPOCENTRAL LOCATIONS FOR FIGURES 4.1 THROUGH 4.9

FIGURE 4.1-A

GEYSERS INDUCED SEISMICITY STUDY

REV. 1 SR408-06.DWG 12/27/95

PARSONS ENGINEERING SCIENCE, INC.

PLAN VIEW

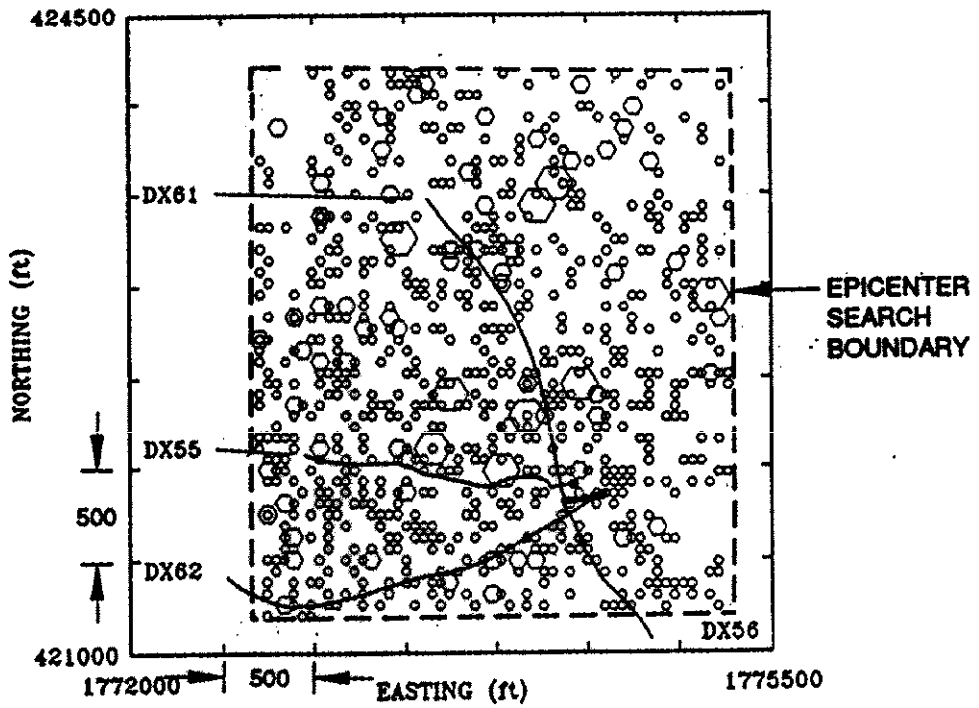

VERTICAL-PLANE PROJECTION

MAGNITUDE	:	0≤M<2	2≤M<3	3≤M<4	4≤M<5
SYMBOL	:	○	○	⬡	✳

see fig. 4.1-A for location error

MAP AND EAST-WEST VERTICAL-PLANE PROJECTION OF EARTHQUAKE HYPOCENTERS, VICINITY OF INJECTION WELL DX-61 (AREA 1-2), JULY 1986 - MAY 1995

FIGURE 4.2

Santa Rosa
Subregional Long-Term Wastewater Project

GEYSERS INDUCED SEISMICITY STUDY

REV. 2 SR408-10.DWG 01/10/96

PARSONS ENGINEERING SCIENCE, INC.

PLAN VIEW

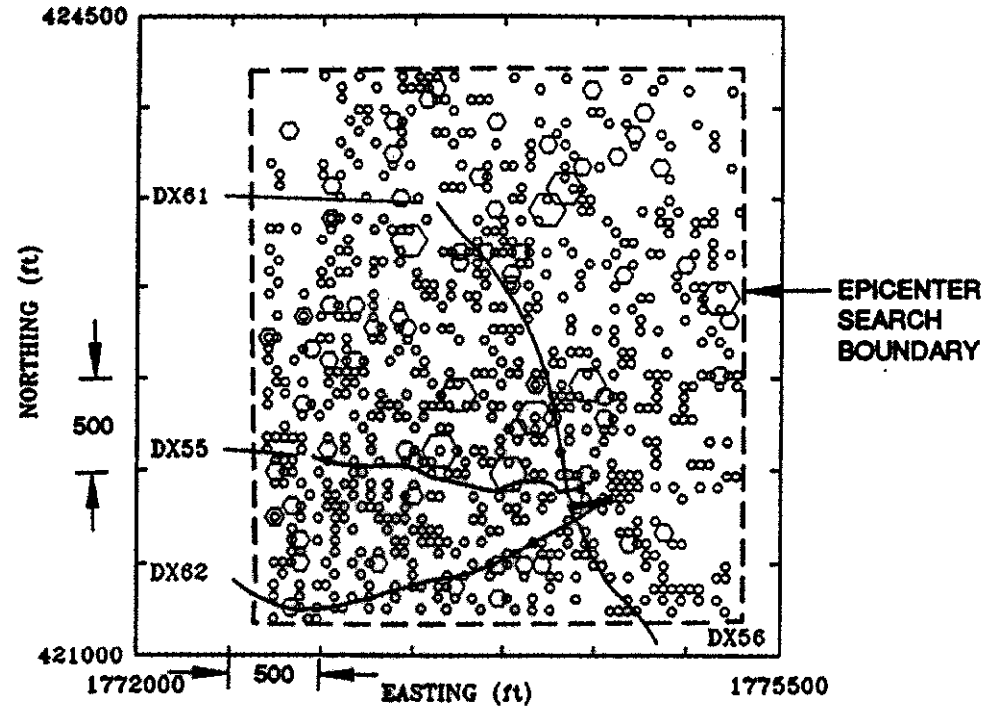

VERTICAL-PLANE PROJECTION

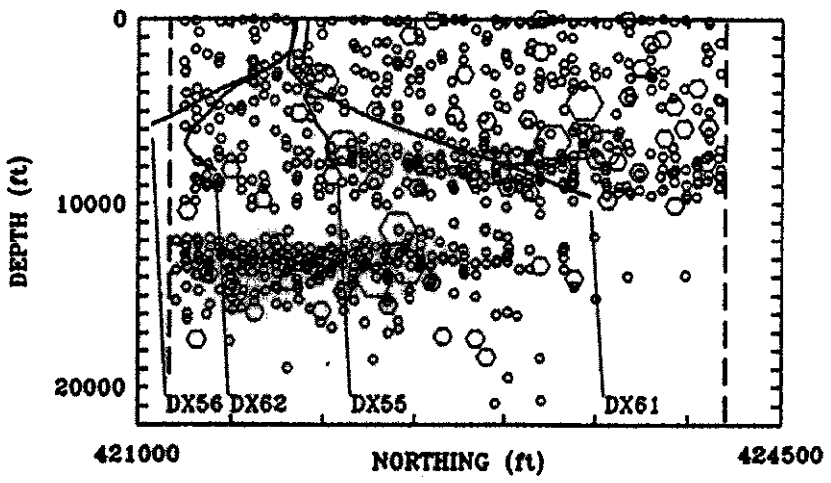

MAGNITUDE :	0≤M<2	2≤M<3	3≤M<4	4≤M<5
SYMBOL :	∘	○	⬡	✳

see fig. 4.1-A for location error

MAP AND NORTH-SOUTH VERTICAL-PLANE PROJECTION OF EARTHQUAKE HYPOCENTERS, VICINITY OF INJECTION WELL DX-61 (AREA 1-2), JULY 1986 - MAY 1995

FIGURE 4.3

Subregional Long-Term Wastewater Project

GEYSERS INDUCED SEISMICITY STUDY

REV. 2 SR406-11.DWG 01/11/96

PARSONS ENGINEERING SCIENCE, INC.

PLAN VIEW

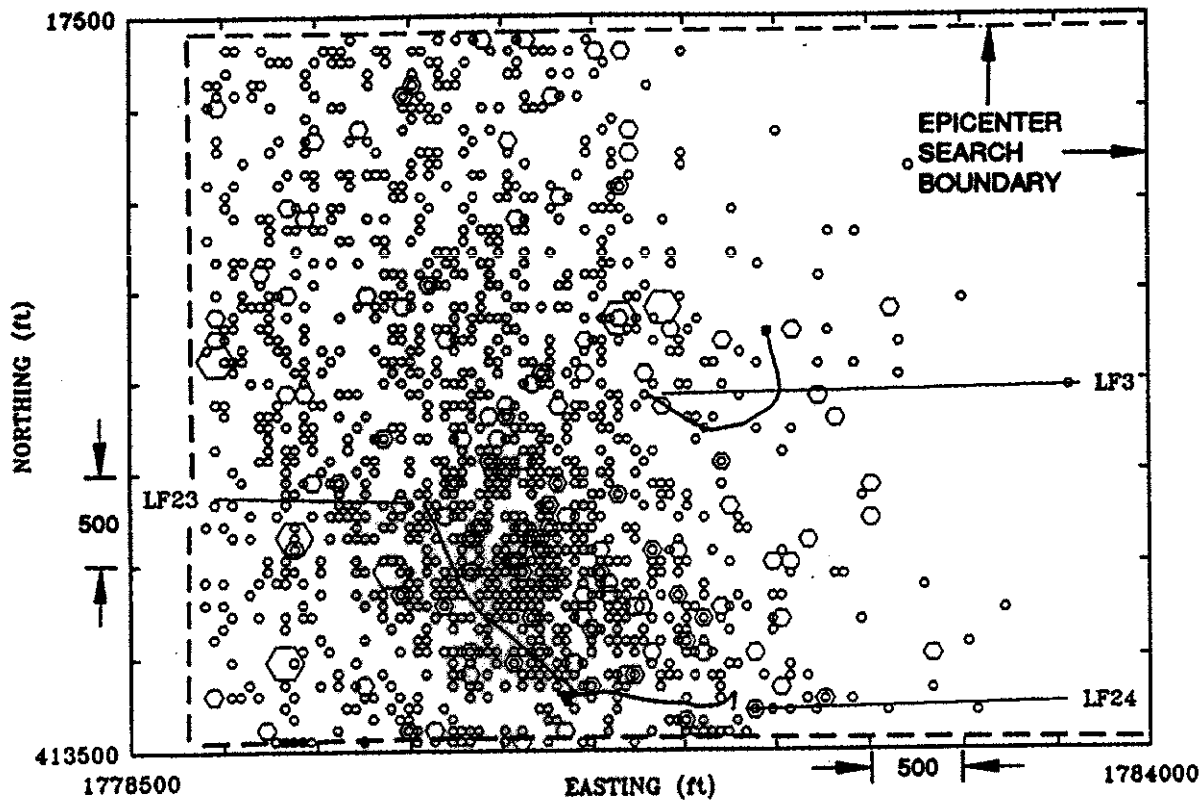

VERTICAL–PLANE PROJECTION

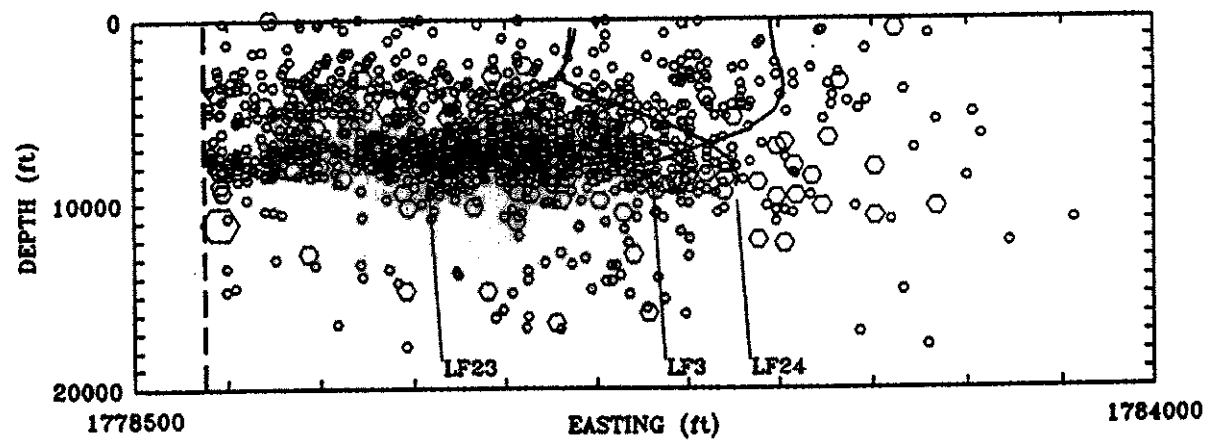

MAGNITUDE	:	0≤M<2	2≤M<3	3≤M<4	4≤M<5
SYMBOL	:	○	○	⬡	✳

see fig. 4.1–A for location error

MAP AND EAST-WEST VERTICAL-PLANE PROJECTION OF EARTHQUAKE HYPOCENTERS, VICINITY OF INJECTION WELLS LF-3 AND LF-23 (AREA 2-3), APRIL 1979 - MAY 1995

FIGURE 4.4

Santa Rosa
Subregional Long-Term Wastewater Project

GEYSERS INDUCED SEISMICITY STUDY

REV. 2 SR406-12.DWG 01/10/96

PARSONS ENGINEERING SCIENCE, INC.

PLAN VIEW

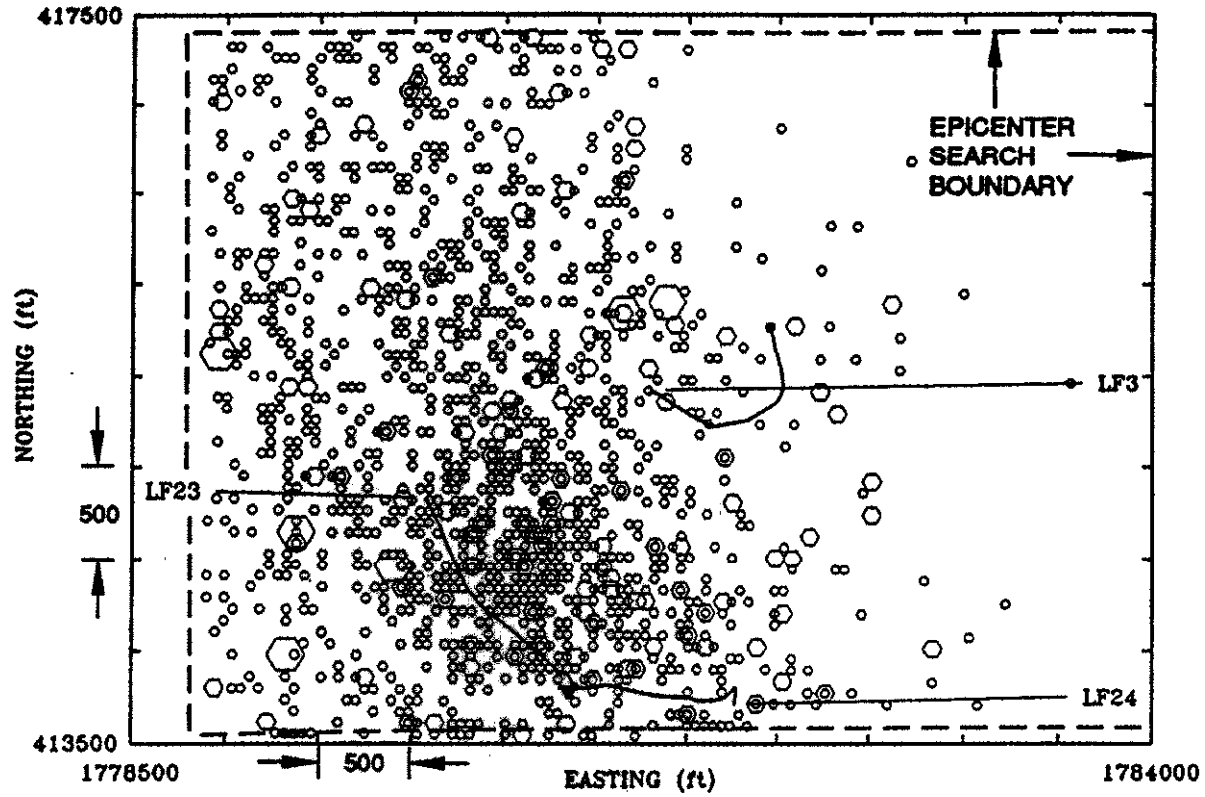

VERTICAL-PLANE PROJECTION

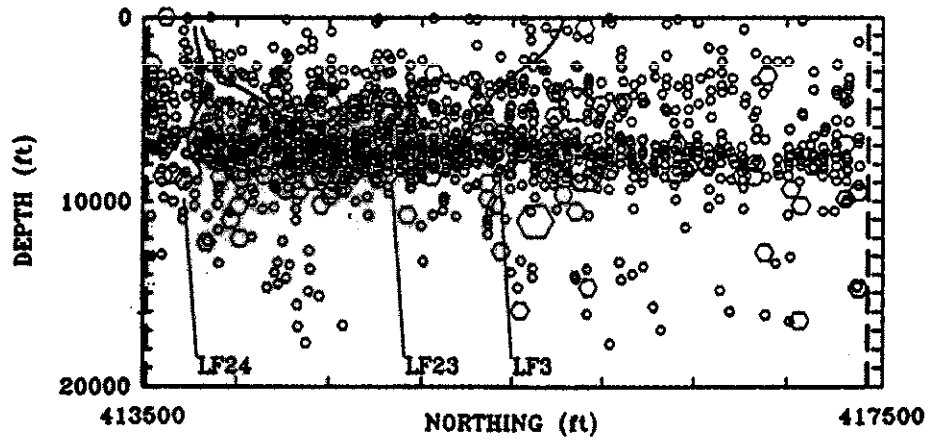

MAGNITUDE :	0≤M<2	2≤M<3	3≤M<4	4≤M<5
SYMBOL :	○	○	⬡	✳

see fig. 4.1-A for location error

MAP AND NORTH-SOUTH VERTICAL-PLANE PROJECTION OF EARTHQUAKE HYPOCENTERS, VICINITY OF INJECTION WELLS LF-3 AND LF-23 (AREA 2-3), APRIL 1979 - MAY 1995

FIGURE 4.5

Subregional Long-Term Wastewater Project

GEYSERS INDUCED SEISMICITY STUDY

REV. 2 SR408-13.DWG 01/10/96

PARSONS ENGINEERING SCIENCE, INC.

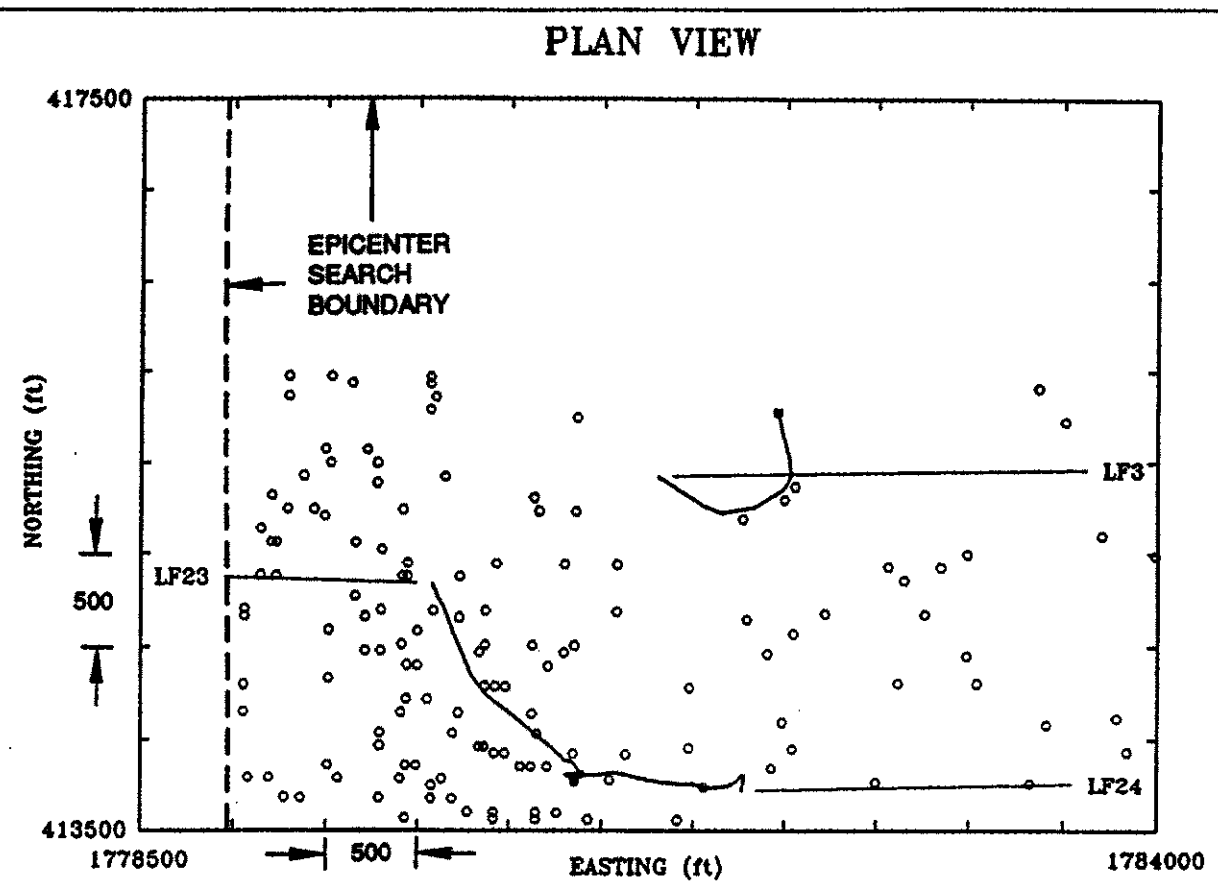

MAP AND EAST-WEST VERTICAL-PLANE PROJECTION OF EARTHQUAKE HYPOCENTERS, VICINITY OF INJECTION WELLS LF-3 AND LF-23 (AREA 2-3), MARCH 10, 1992 - JULY 16, 1992

GEYSERS INDUCED SEISMICITY STUDY

FIGURE 4.6

Subregional Long-Term Wastewater Project

REV. 2 SR408-14.DWG 01/10/96

PARSONS ENGINEERING SCIENCE, INC.

PLAN VIEW

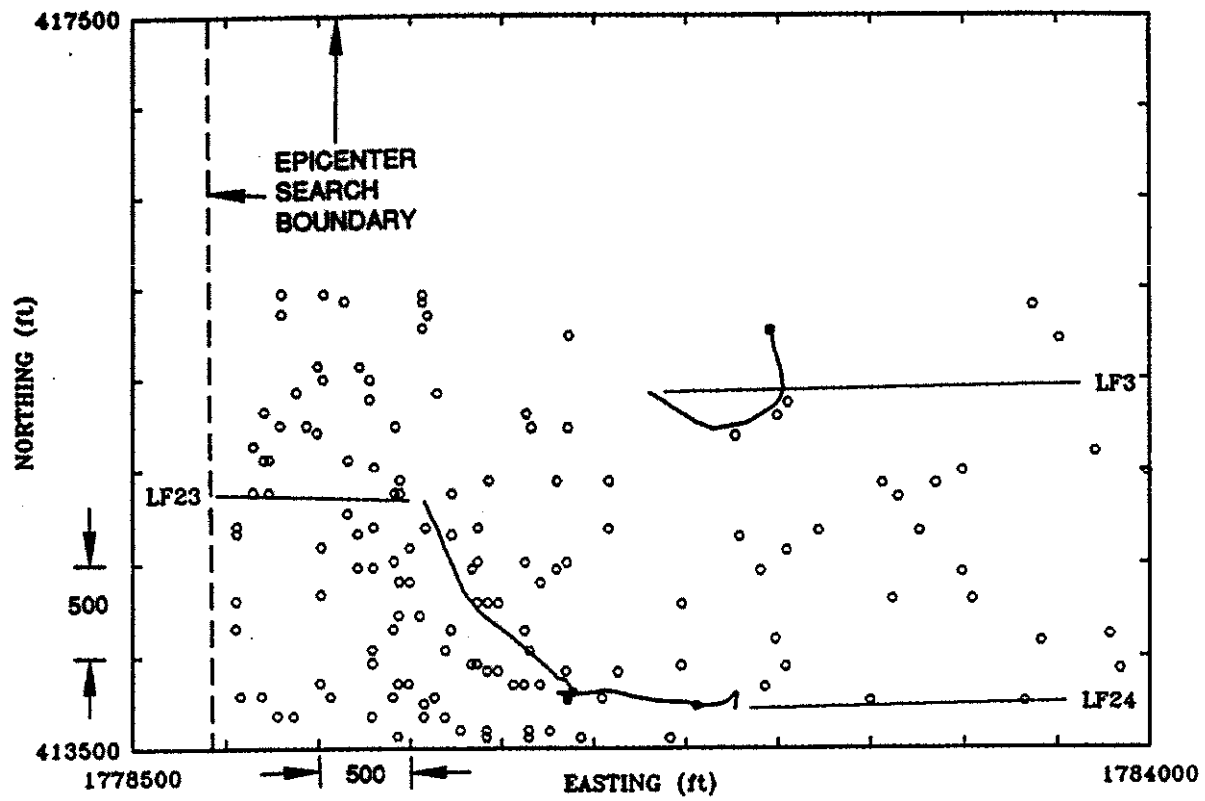

VERTICAL-PLANE PROJECTION

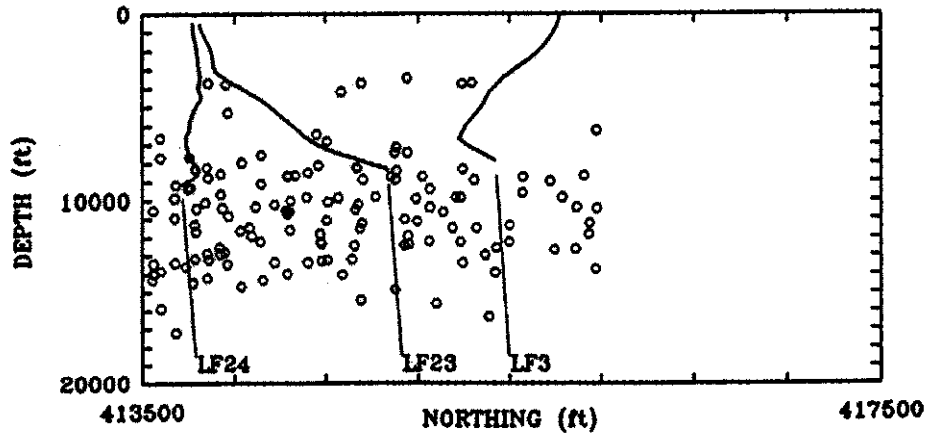

MAGNITUDE :	0≤M<2	2≤M<3	3≤M<4	4≤M<5
SYMBOL :	○	○	⬡	✳

see fig. 4.1-A for location error

MAP AND NORTH-SOUTH VERTICAL-PLANE PROJECTION OF U-N-T HYPOCENTERS, VICINITY OF INJECTION WELLS LF-3 AND LF-23 (AREA 2-3), MARCH 10, 1992 - JULY 16, 1992

GEYSERS INDUCED SEISMICITY STUDY

FIGURE 4.7

Subregional Long-Term Wastewater Project

REV. 2 SR408-15.DWG 01/10/96

PARSONS ENGINEERING SCIENCE, INC.

PLAN VIEW

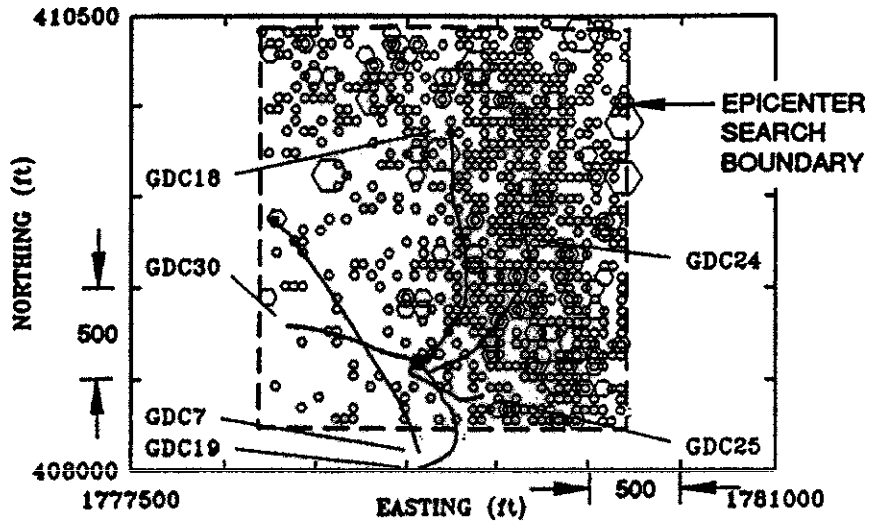

VERTICAL-PLANE PROJECTION

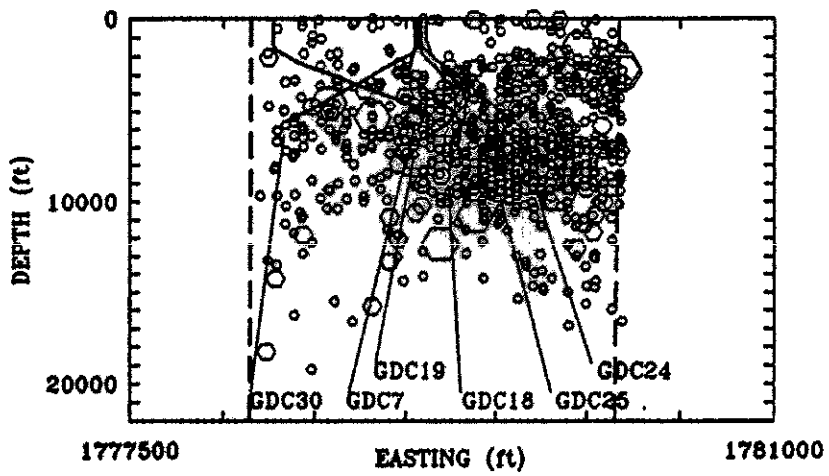

MAGNITUDE :	0≤M<2	2≤M<3	3≤M<4	4≤M<5
SYMBOL :	∘	○	⬡	✳

see fig. 4.1-A for location error

Subregional Long-Term Wastewater Project

MAP AND EAST-WEST VERTICAL-PLANE PROJECTION OF EARTHQUAKE HYPOCENTERS, VICINITY OF INJECTION WELL GDC-18 (AREA 3-1), JANUARY 1983 - MAY 1995

GEYSERS INDUCED SEISMICITY STUDY

FIGURE 4.8

PLAN VIEW

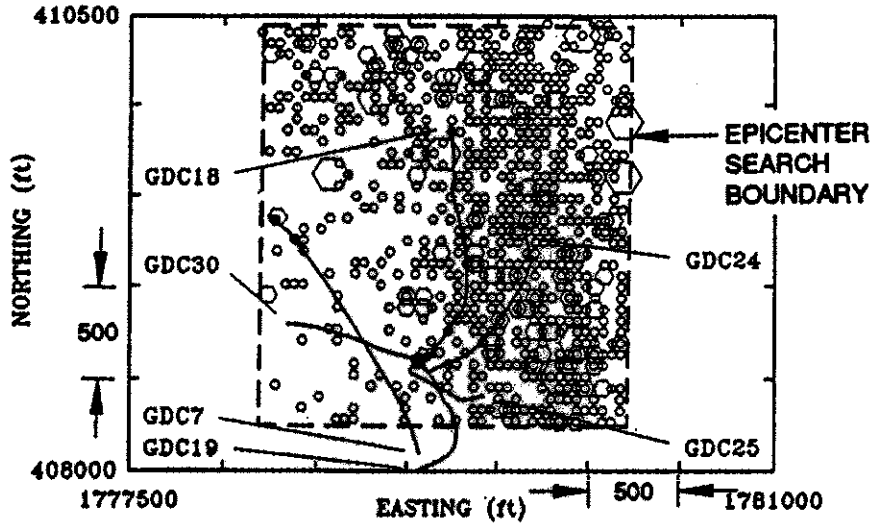

VERTICAL-PLANE PROJECTION

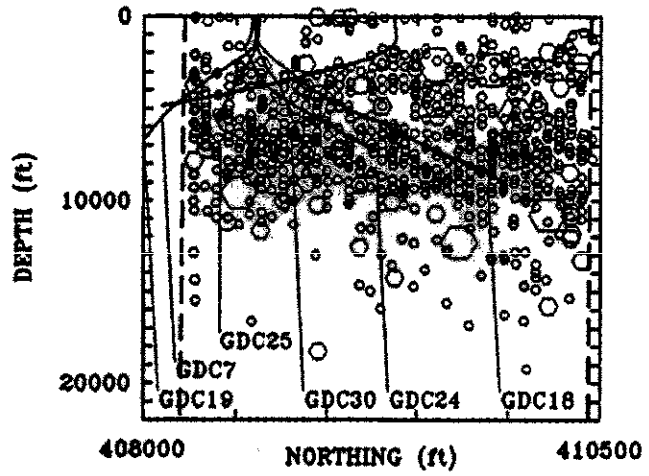

MAGNITUDE :	0≤M<2	2≤M<3	3≤M<4	4≤M<5
SYMBOL :	∘	○	⬡	✳

see fig. 4.1-A for location error

MAP AND NORTH-SOUTH VERTICAL-PLANE PROJECTION OF EARTHQUAKE HYPOCENTERS, VICINITY OF INJECTION WELL GDC-18 (AREA 3-1), JANUARY 1983 - MAY 1995

GEYSERS INDUCED SEISMICITY STUDY

FIGURE 4.9

Santa Rosa
Subregional Long-Term Wastewater Project

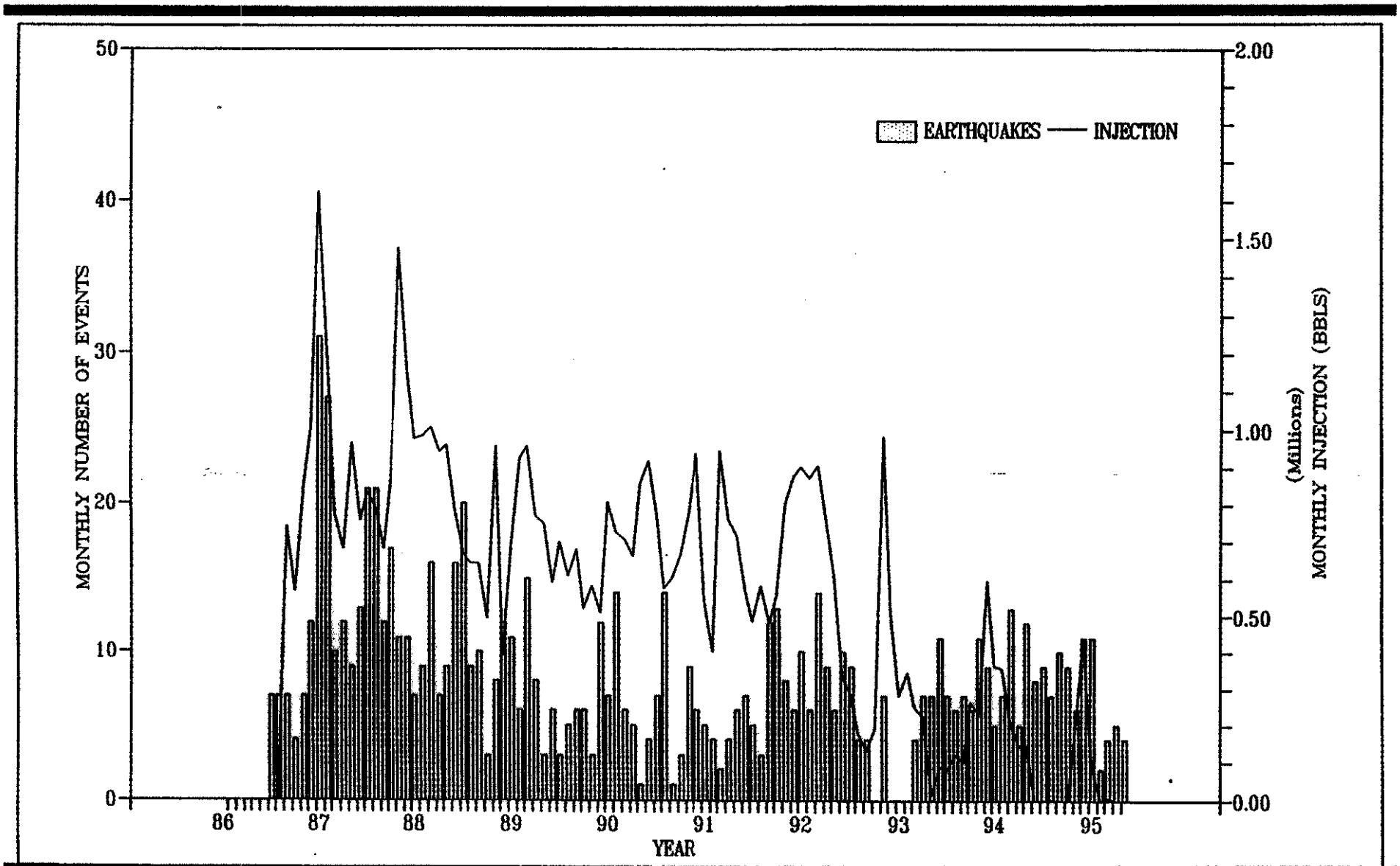

Subregional Long-Term Wastewater Project

EARTHQUAKES AND INJECTION
VICINITY OF WELL DX-61, AREA 1-2
GEYSERS INDUCED SEISMICITY STUDY

FIGURE 4.10

REV. 2 SR408-16.DWG 01/10/96

PARSONS ENGINEERING SCIENCE, INC.

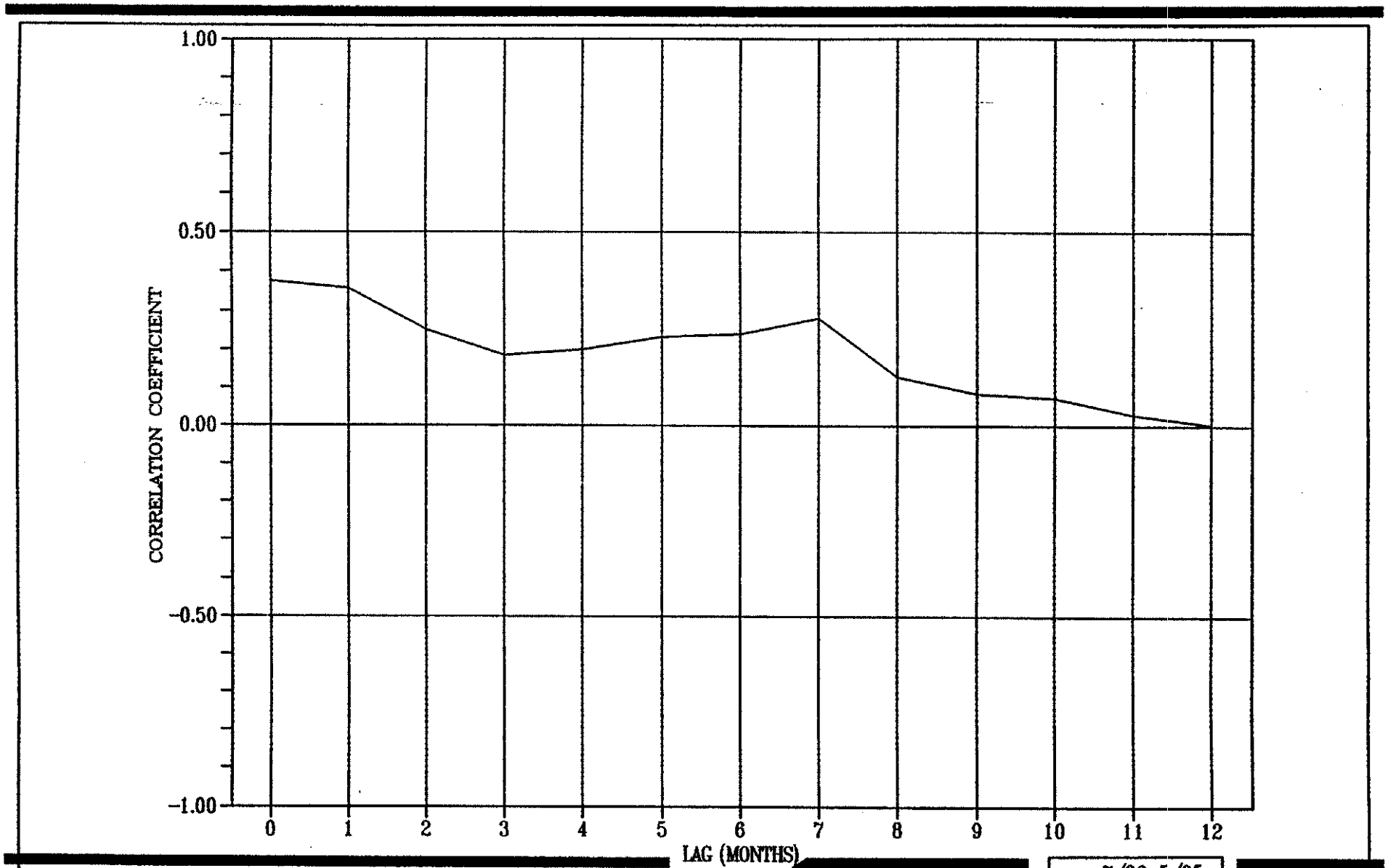

Subregional Long-Term Wastewater Project

CROSS CORRELATION, EARTHQUAKES AND INJECTION, VICINITY OF WELL DX-61, AREA 1-2

GEYSERS INDUCED SEISMICITY STUDY

FIGURE 4.11

REV. 1 SR408-18.DWG 12/27/95

PARSONS ENGINEERING SCIENCE, INC.

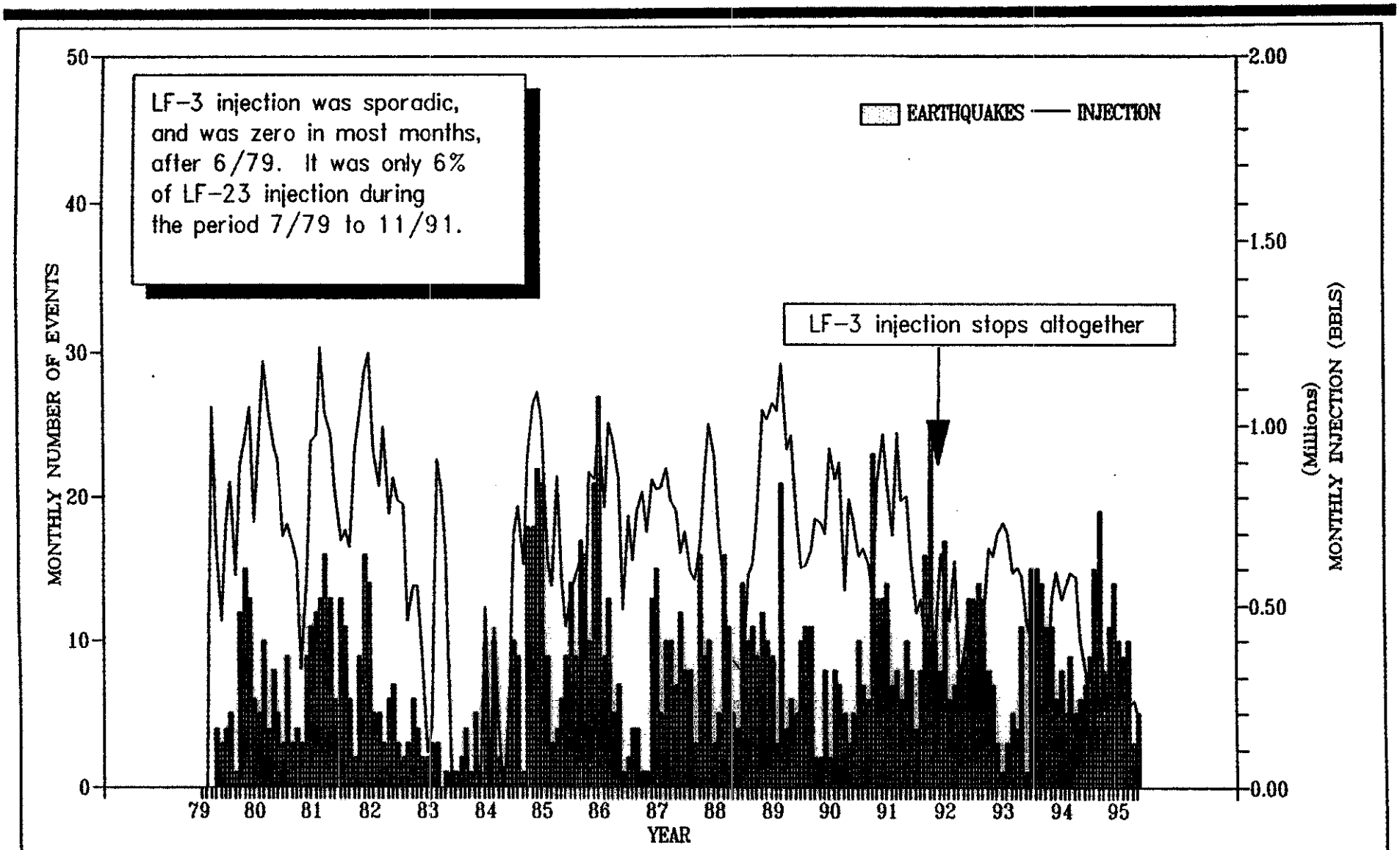

Santa Rosa
Subregional Long-Term Wastewater Project

EARTHQUAKES AND INJECTION
VICINITY OF WELLS LF-3 AND LF-23, AREA 2-3
GEYSERS INDUCED SEISMICITY STUDY

FIGURE 4.12

REV. 2 SR408-20.DWG 01/10/96

PARSONS ENGINEERING SCIENCE, INC.

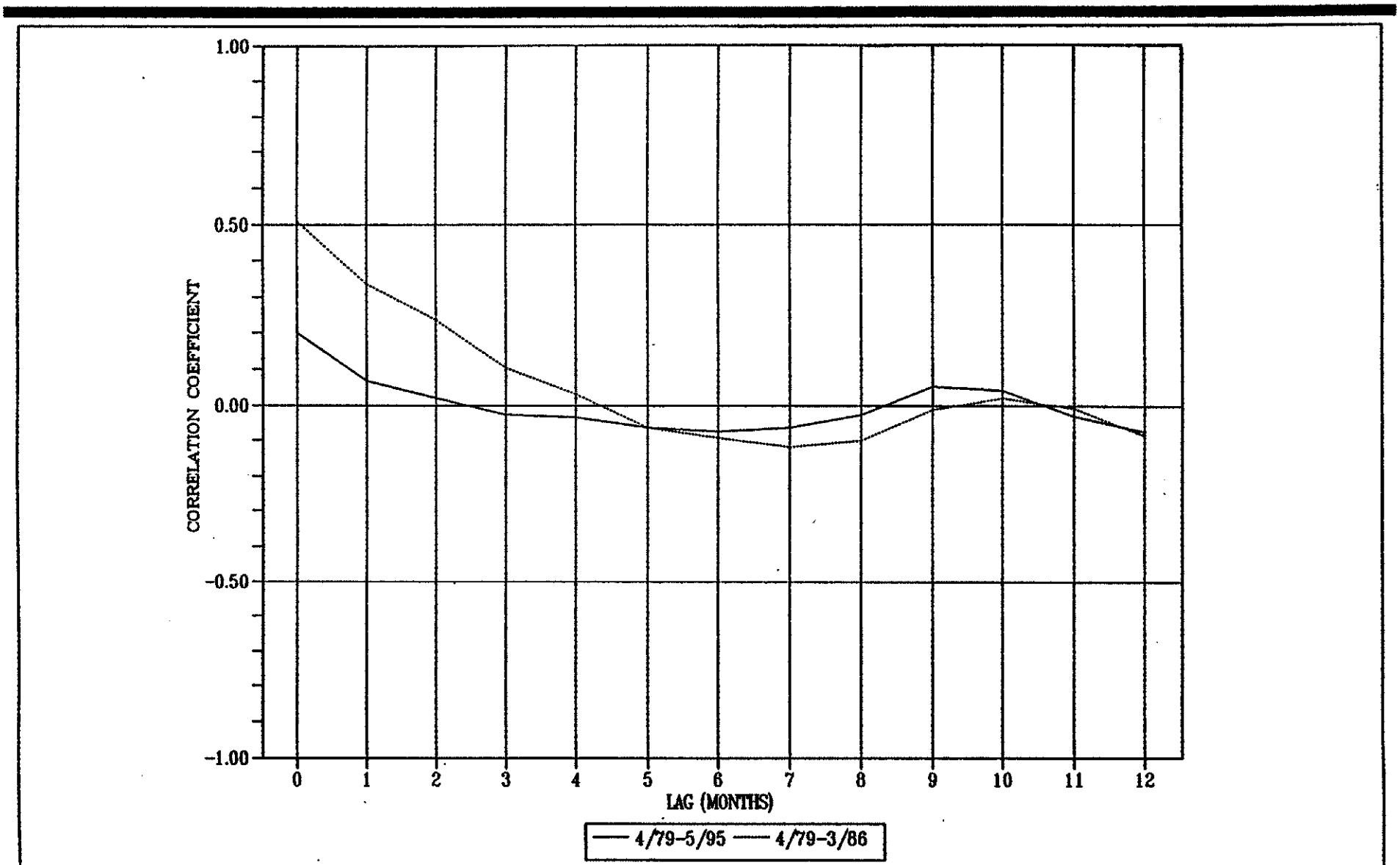

Subregional Long-Term Wastewater Project

CROSS CORRELATION, EARTHQUAKES AND INJECTION VICINITY OF WELLS LF-3 AND LF-23, AREA 2-3

GEYSERS INDUCED SEISMICITY STUDY

FIGURE 4.13

REV. 2 SR408-21.DWG 01/10/96

PARSONS ENGINEERING SCIENCE, INC.

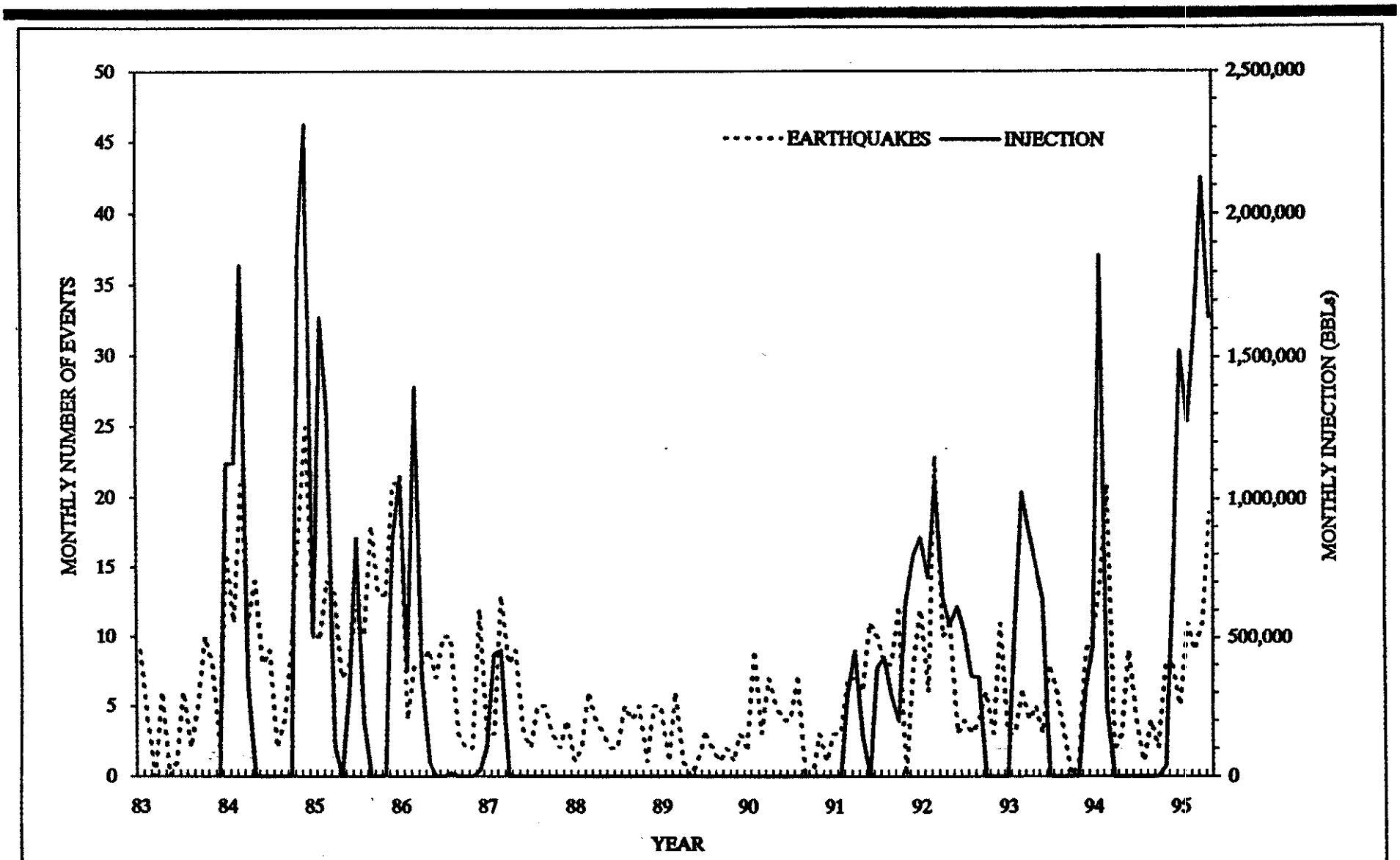

Subregional Long-Term Wastewater Project

EARTHQUAKES AND INJECTION VICINITY OF WELL GDC-18, AREA 3-1

GEYSERS INDUCED SEISMICITY STUDY

FIGURE 4.14

REV. 2 SR408-22.DWG 01/10/96

PARSONS ENGINEERING SCIENCE, INC.

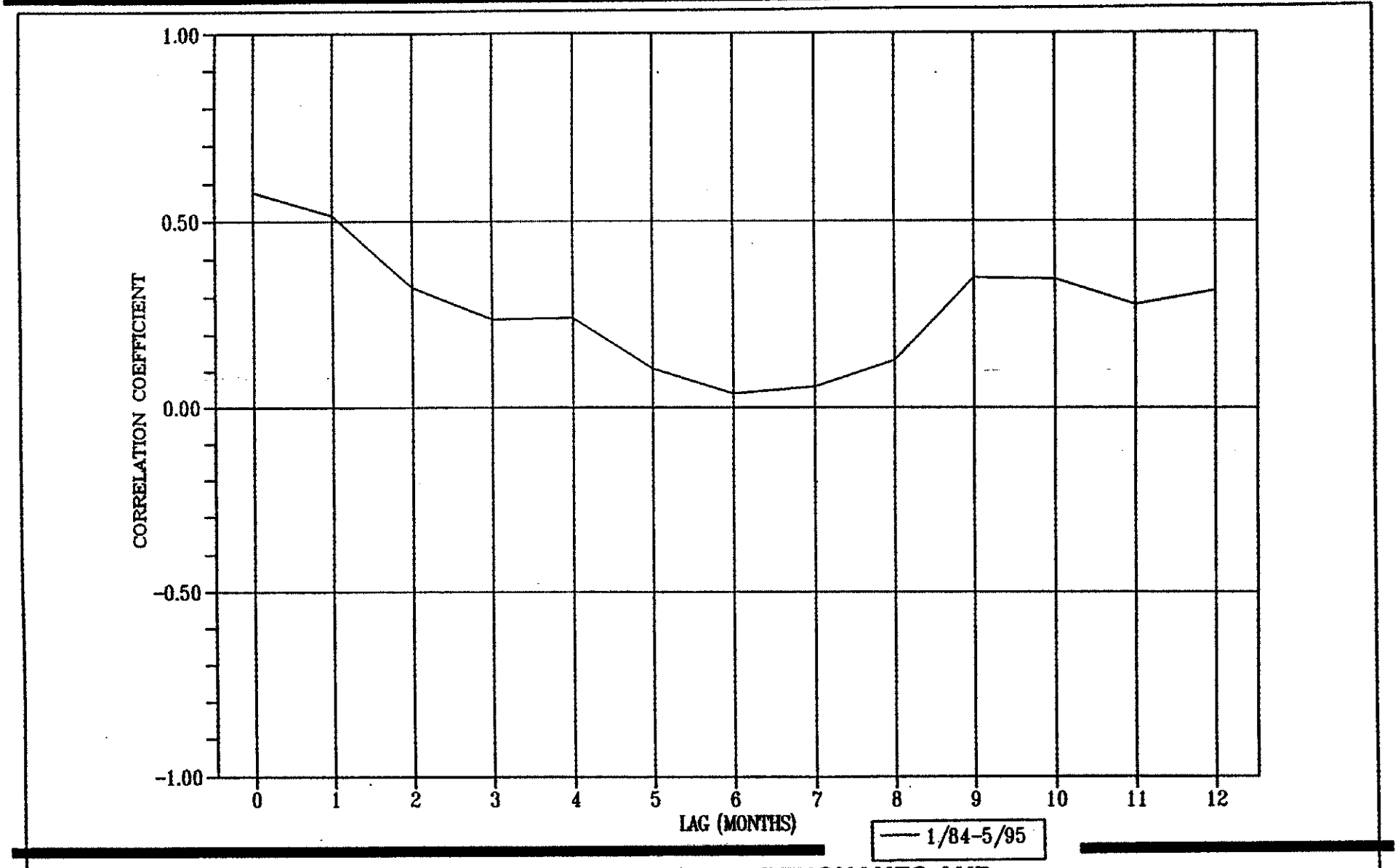

Subregional Long-Term Wastewater Project

CROSS CORRELATION, EARTHQUAKES AND INJECTION, VICINITY OF WELL GDC-18, AREA 3-1

GEYSERS INDUCED SEISMICITY STUDY

FIGURE 4.15

REV. 2 SR408-23.DWG 01/11/96

PARSONS ENGINEERING SCIENCE, INC.

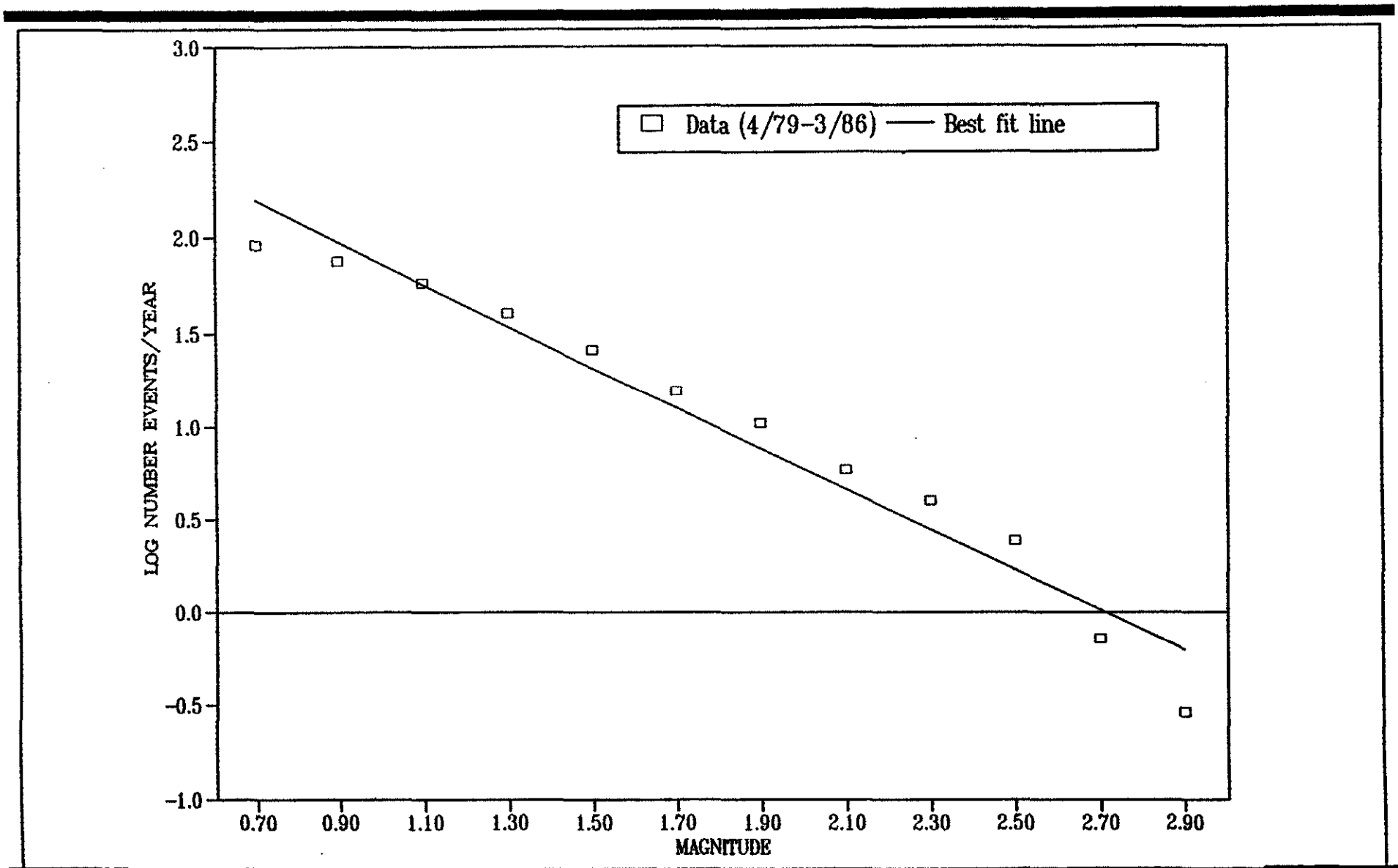

Santa Rosa
Subregional Long-Term Wastewater Project

FREQUENCY-MAGNITUDE DATA
VICINITY OF WELL DX-61, AREA 1-2
GEYSERS INDUCED SEISMICITY STUDY

FIGURE 4.16

REV. 2 SR408-24.DWG 01/10/86

PARSONS ENGINEERING SCIENCE, INC.

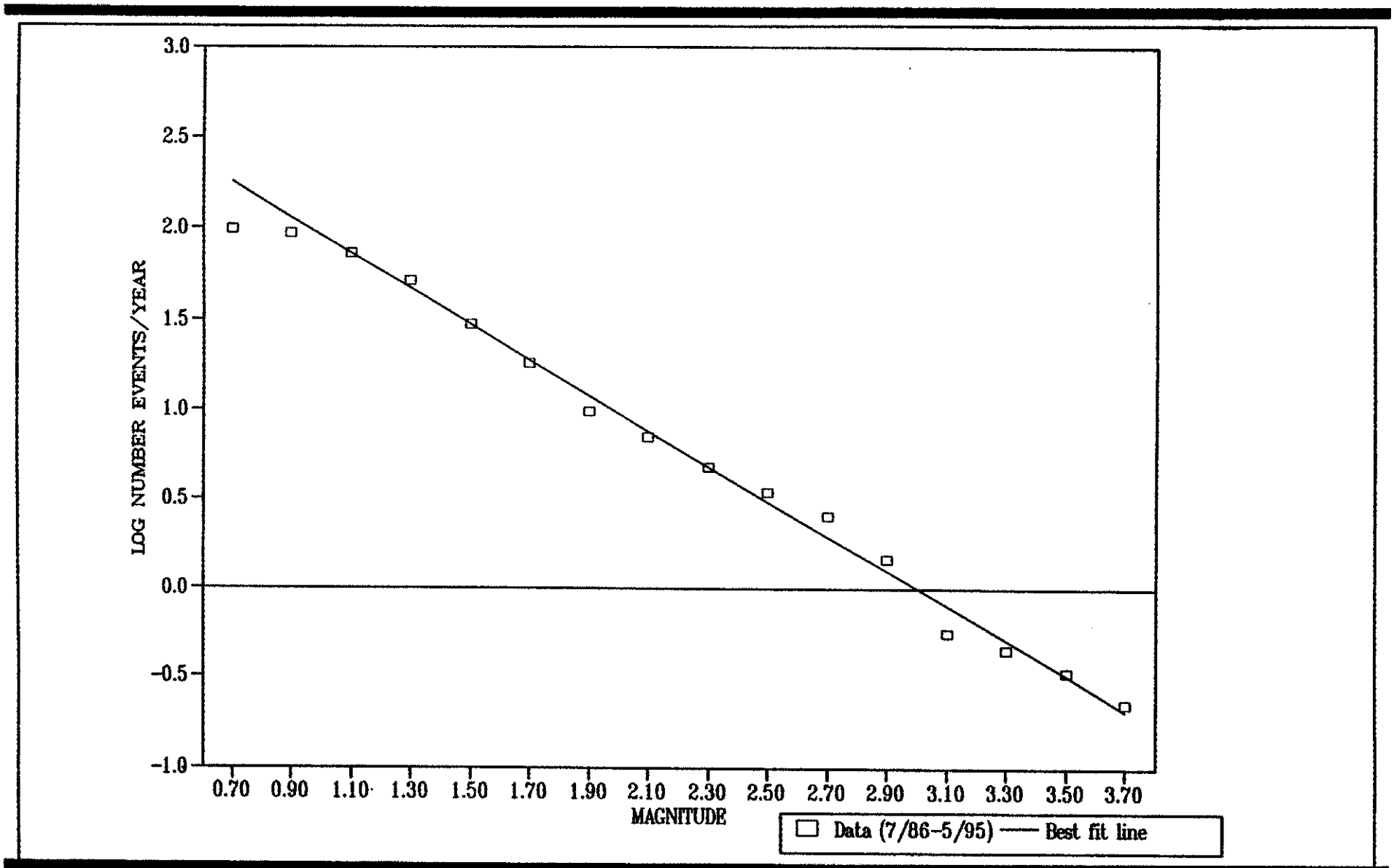

Subregional Long-Term Wastewater Project

FREQUENCY-MAGNITUDE DATA
VICINITY OF WELLS LF-3 AND LF-23, AREA 2-3
GEYSERS INDUCED SEISMICITY STUDY

FIGURE 4.17

REV. 2 SR408-25.DWG 01/10/96

PARSONS ENGINEERING SCIENCE, INC.

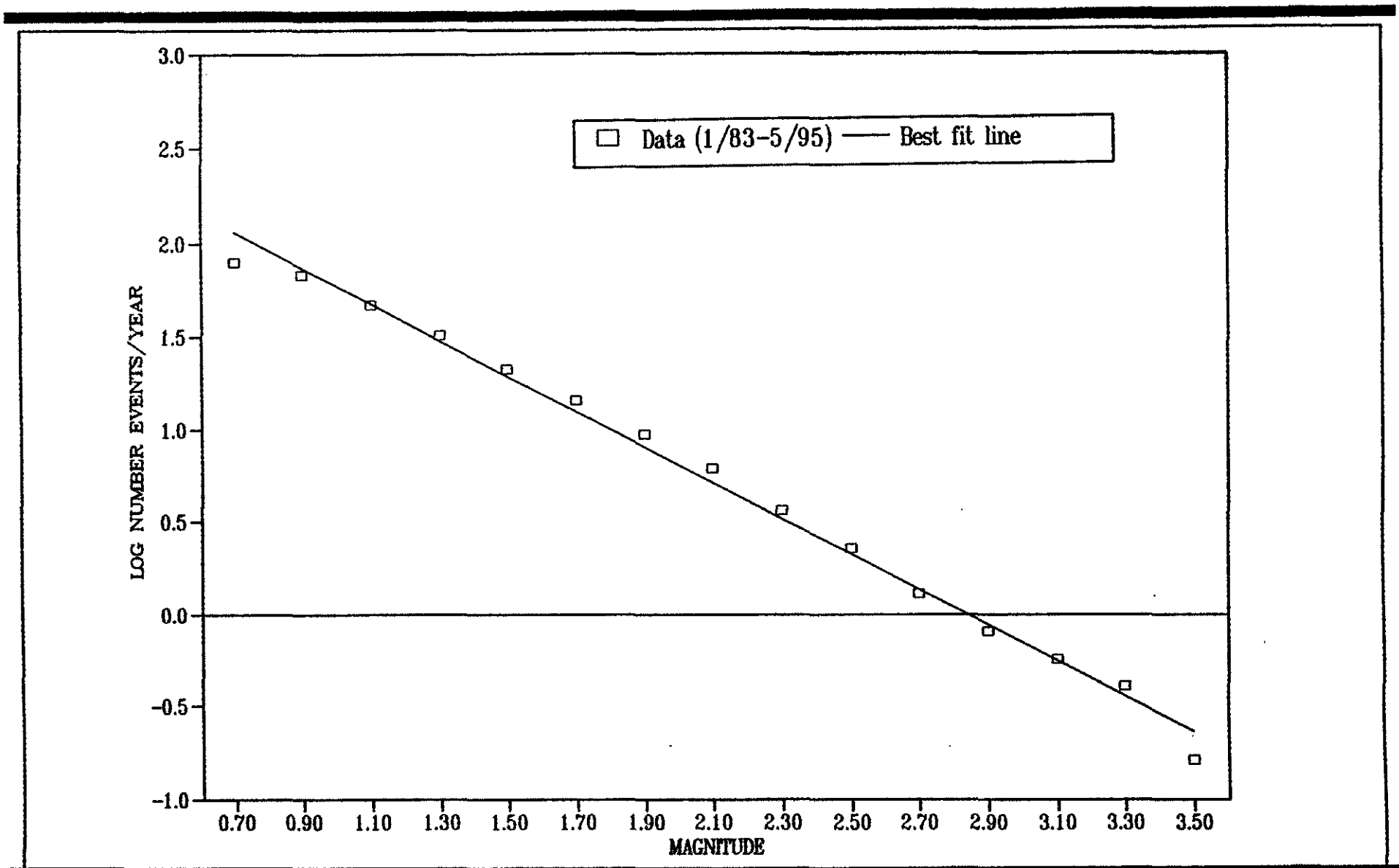

Subregional Long-Term Wastewater Project

FREQUENCY-MAGNITUDE DATA
VICINITY OF WELL GDC-18, AREA 3-1
GEYSERS INDUCED SEISMICITY STUDY

FIGURE 4.18

REV. 2 SR409-27.DWG 01/10/96

PARSONS ENGINEERING SCIENCE, INC.

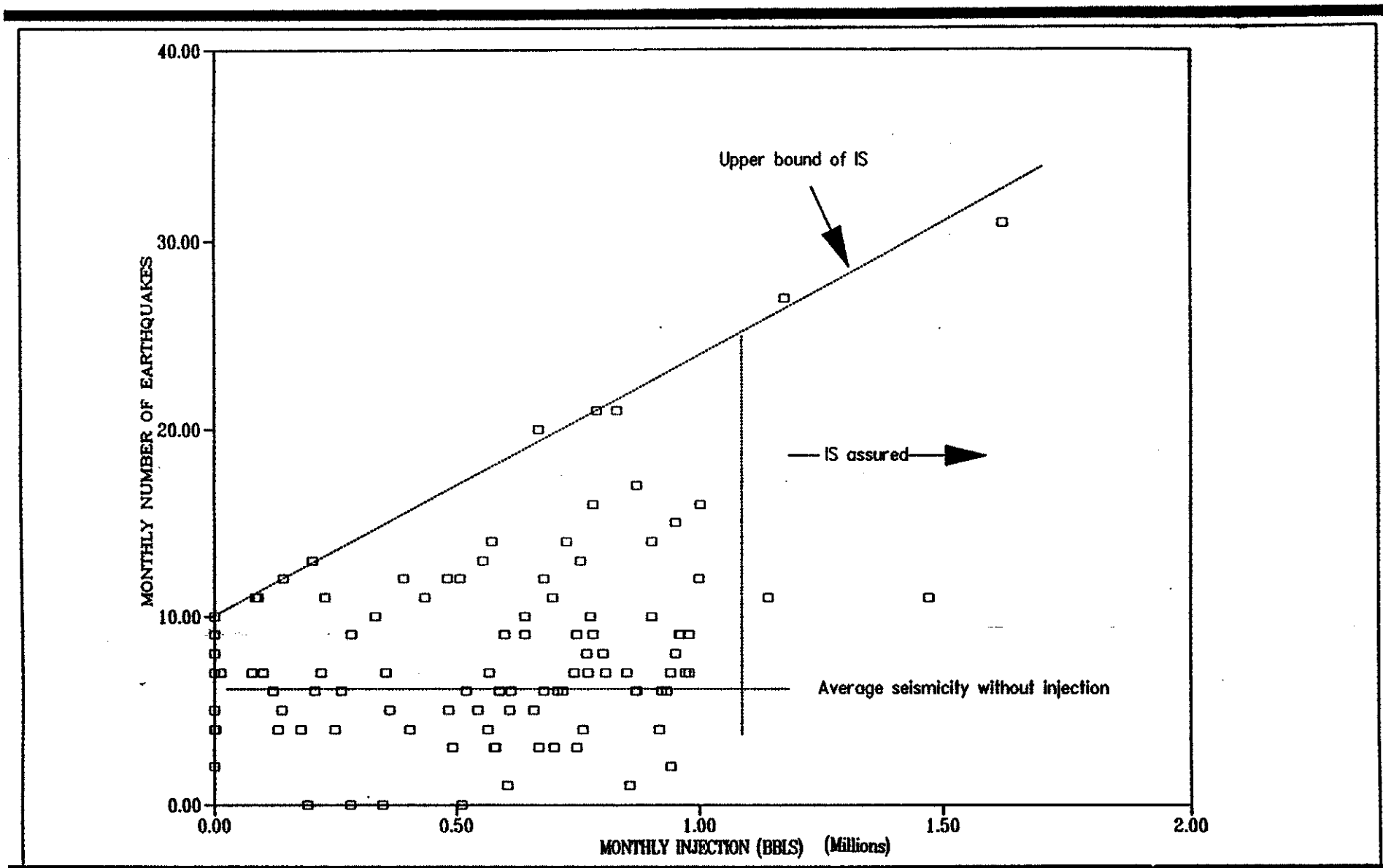

Subregional Long-Term Wastewater Project

EARTHQUAKES VERSUS RATE OF INJECTION VICINITY OF WELL DX-61, AREA 1-2

GEYSERS INDUCED SEISMICITY STUDY

FIGURE 4.19

REV. 2 SR408-28.DWG 01/10/96

PARSONS ENGINEERING SCIENCE, INC.

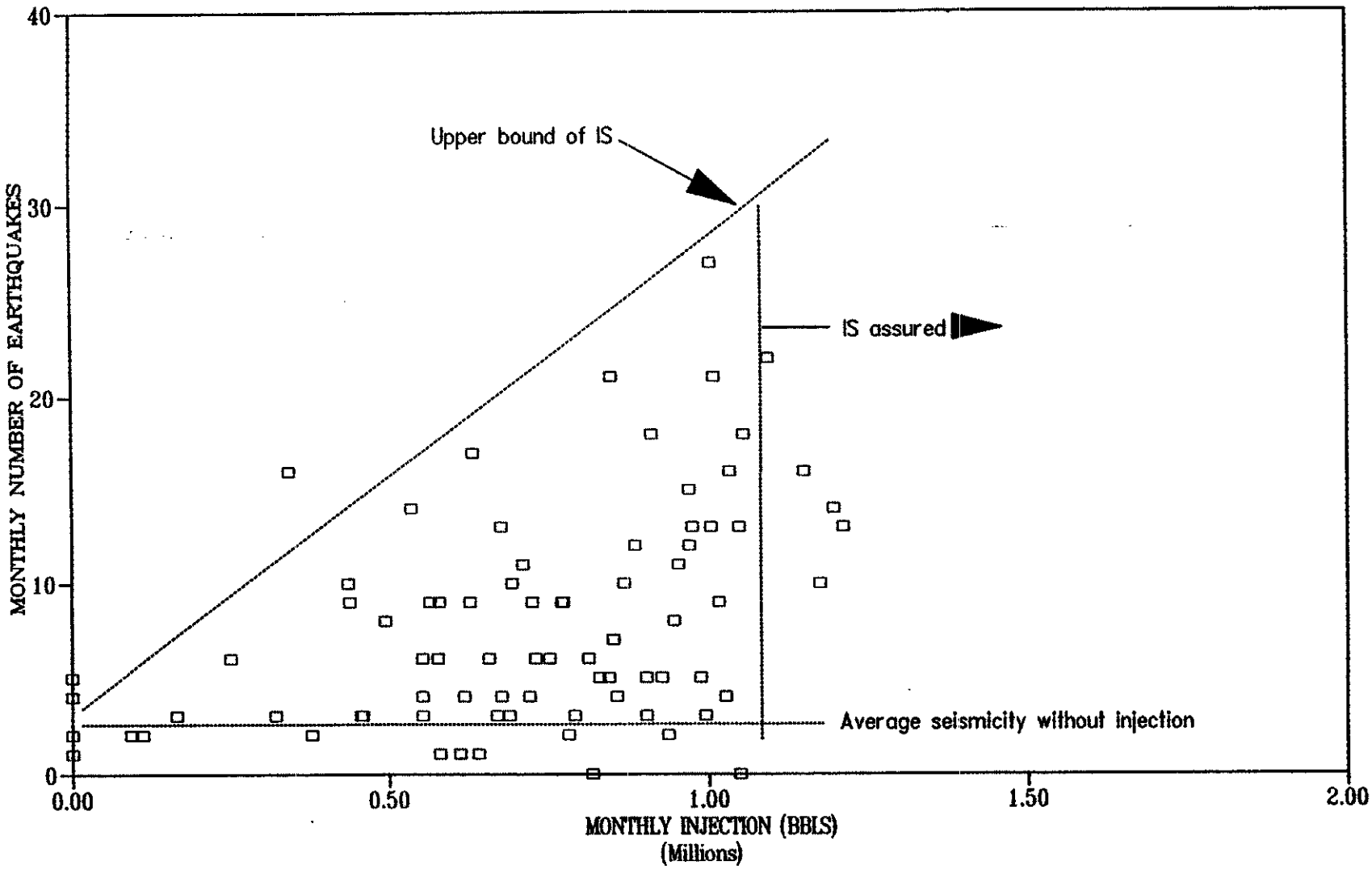

Subregional Long-Term Wastewater Project

EARTHQUAKES VERSUS RATE OF INJECTION VICINITY OF WELLS LF-3 AND LF-23, AREA 2-3

GEYSERS INDUCED SEISMICITY STUDY

FIGURE 4.20

REV. 1 SR406-30.DWG 01/11/96

PARSONS ENGINEERING SCIENCE, INC.

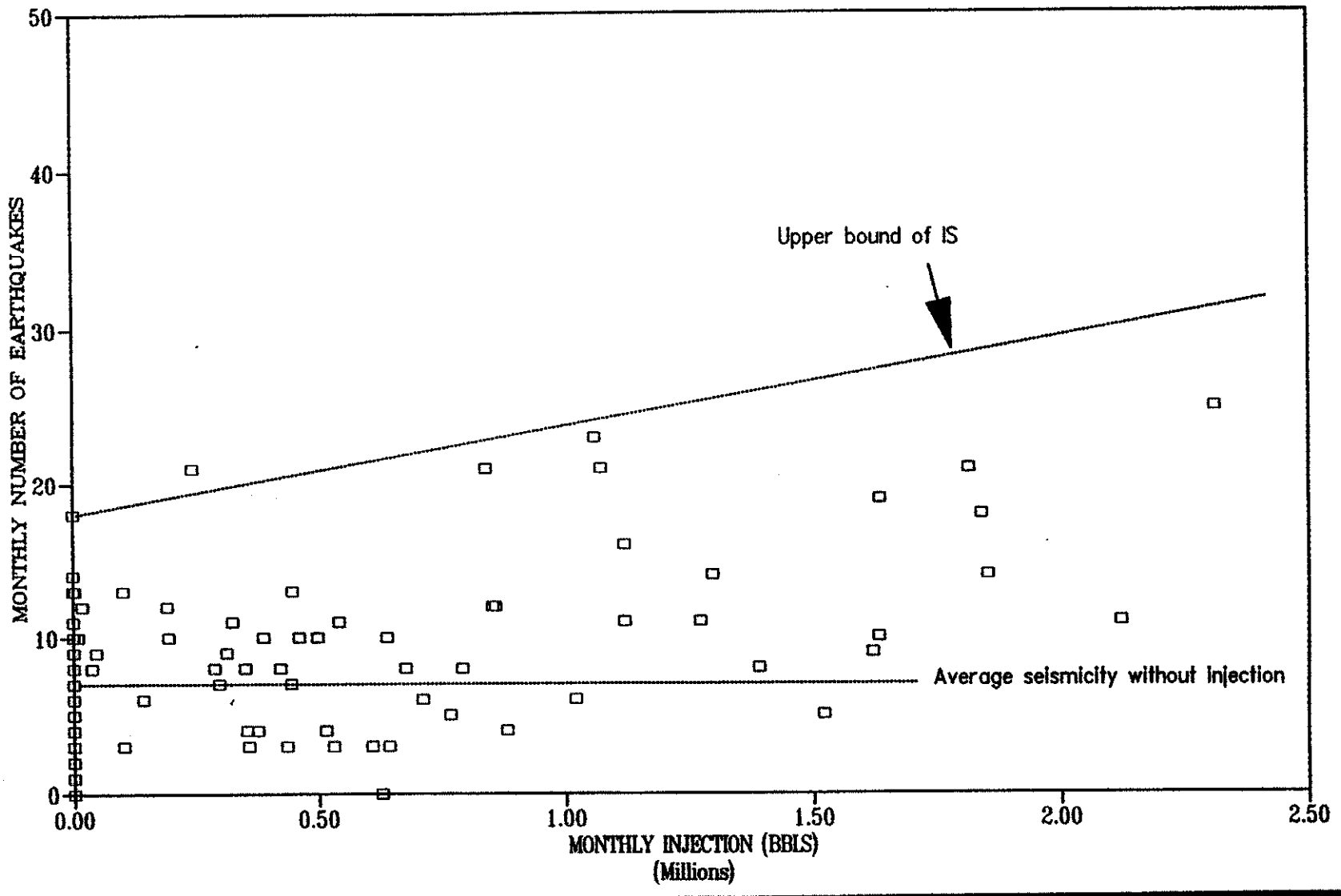

Subregional Long-Term Wastewater Project

EARTHQUAKES VERSUS RATE OF INJECTION VICINITY OF WELL GDC-18, AREA 3-1

GEYSERS INDUCED SEISMICITY STUDY

FIGURE 4.21

REV. 2 SR408-28.DWG 01/10/96

PARSONS ENGINEERING SCIENCE, INC.

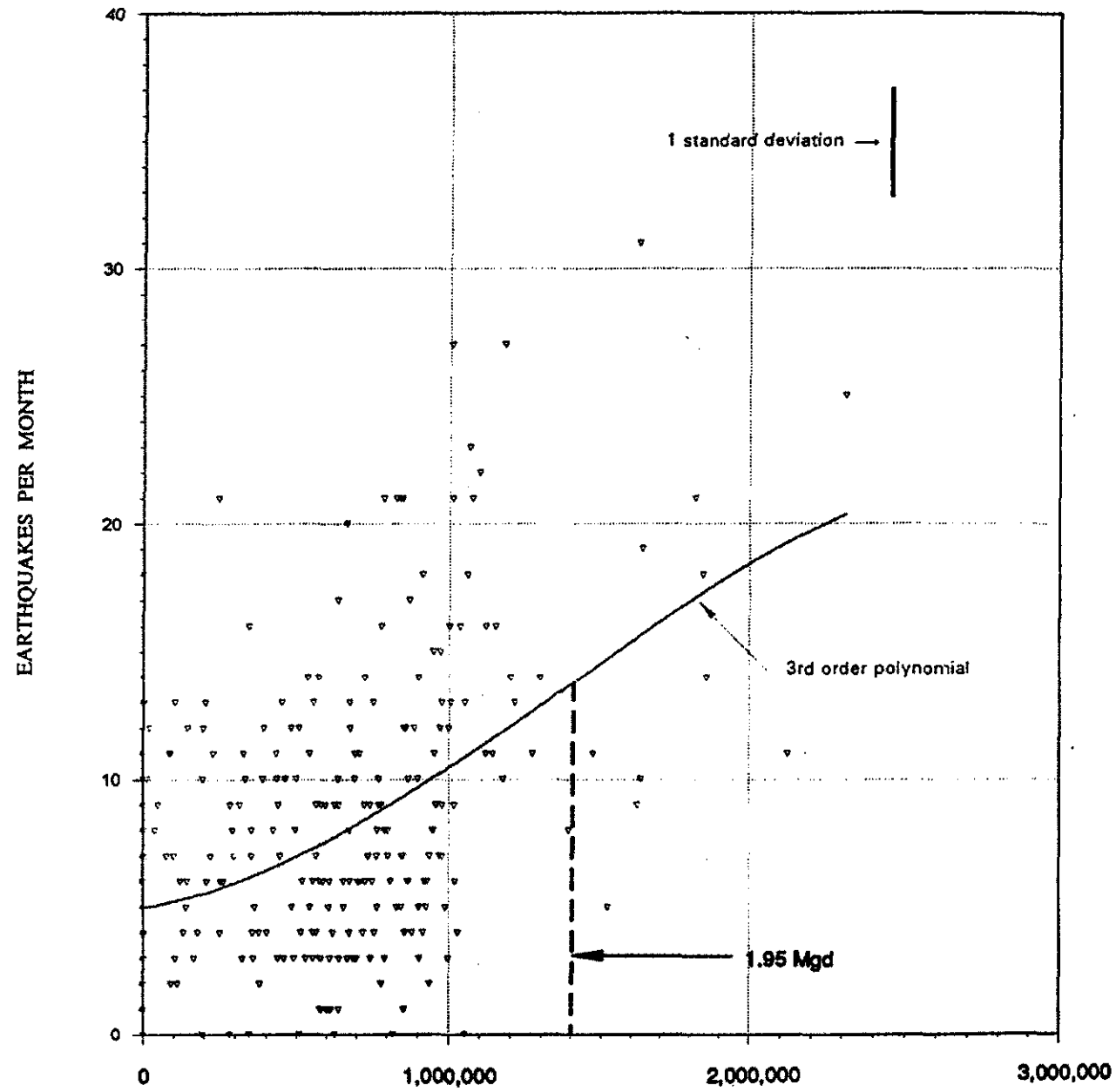

Subregional Long-Term Wastewater Project

REGRESSION FIT, IS VS. INJECTION FOR ONE WELL (DATA FROM ALL STUDY AREAS.)

FIGURE 4.22

GEYSERS INDUCED SEISMICITY STUDY

REV. 1 SR408-30.DWG 12/27/95

PARSONS ENGINEERING SCIENCE, INC.

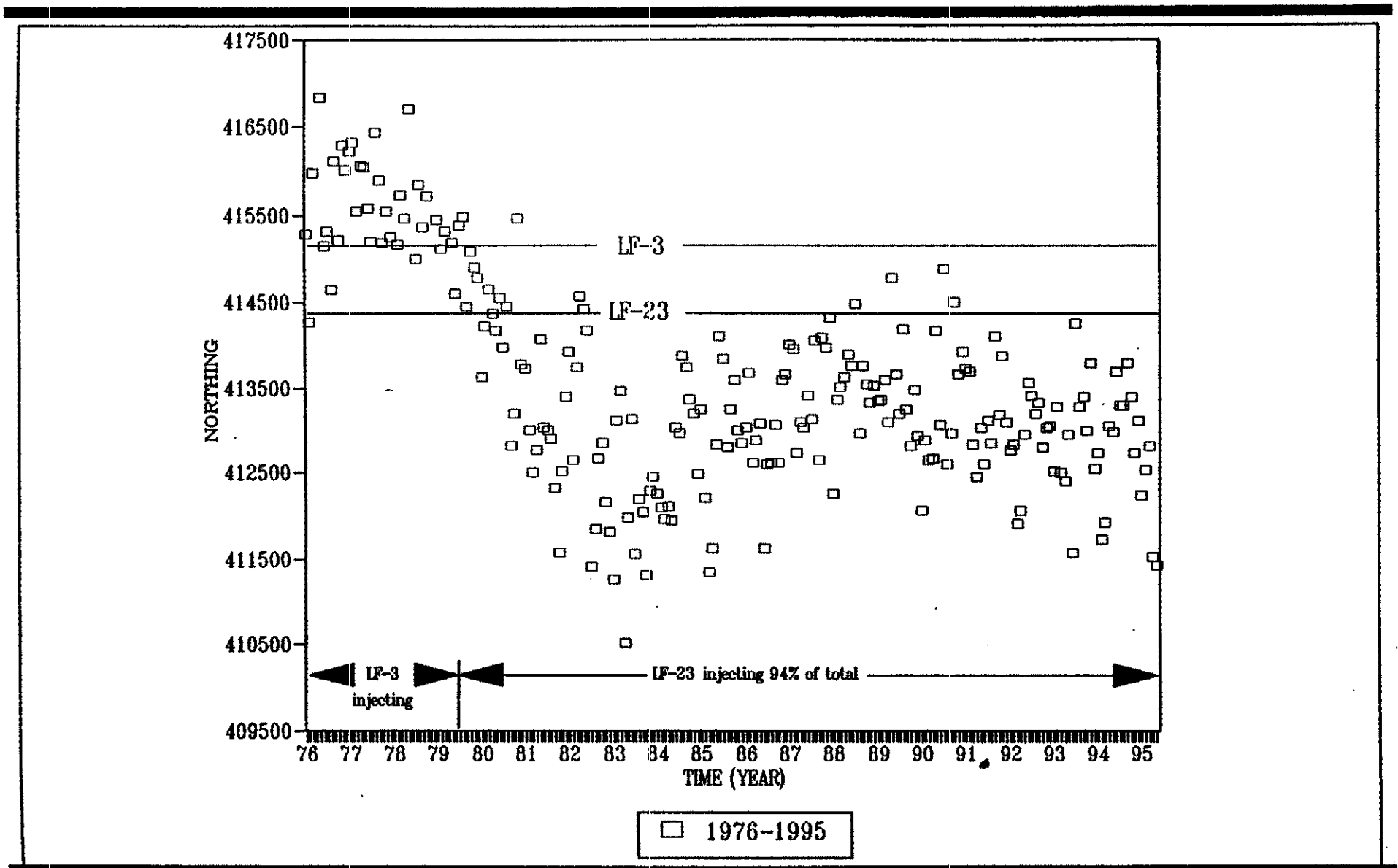

Subregional Long-Term Wastewater Project

EPICENTER NORTHING VS. TIME, VICINITY OF WELLS LF-3 AND LF-23, (AREA 2-1 EXTENDED 4000 FEET SOUTHWARD)

GEYSERS INDUCED SEISMICITY STUDY

FIGURE 4.23

REV. 1 SR406-31.DWG 12/27/95

PARSONS ENGINEERING SCIENCE, INC.

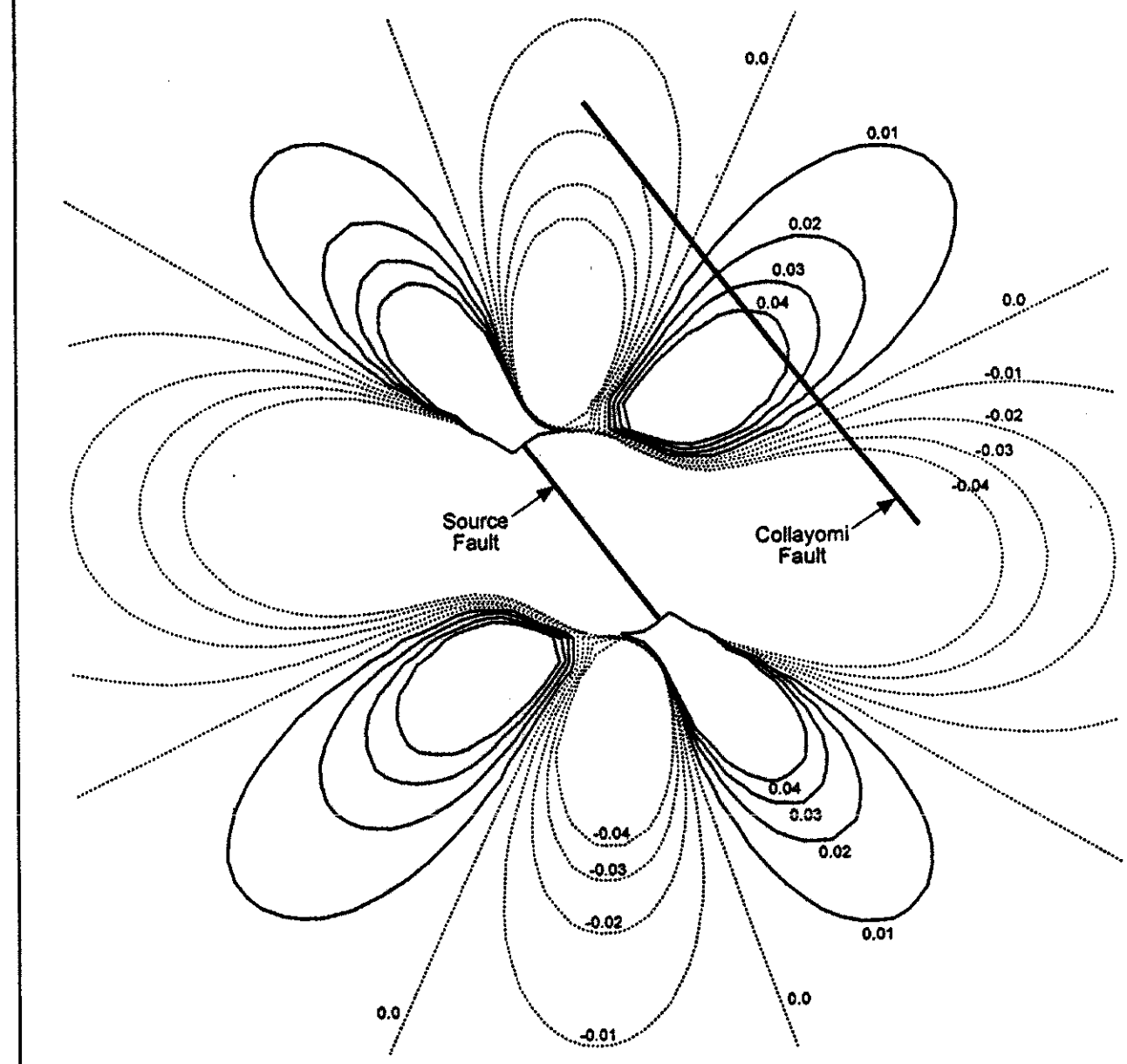

NOTE: COURTESY OF ROBERT SIMPSON, U.S. GEOLOGICAL SURVEY

Subregional Long-Term Wastewater Project

COULOMB STRESS CHANGES (IN BARS) ON THE COLLAYOMI FAULT DUE TO AN M_L =4.5 EARTHQUAKE IN THE GGF

GEYSERS INDUCED SEISMICITY STUDY

FIGURE 6.1

REV. 2 SR406-32.DWG 01/10/96

PARSONS ENGINEERING SCIENCE, INC.

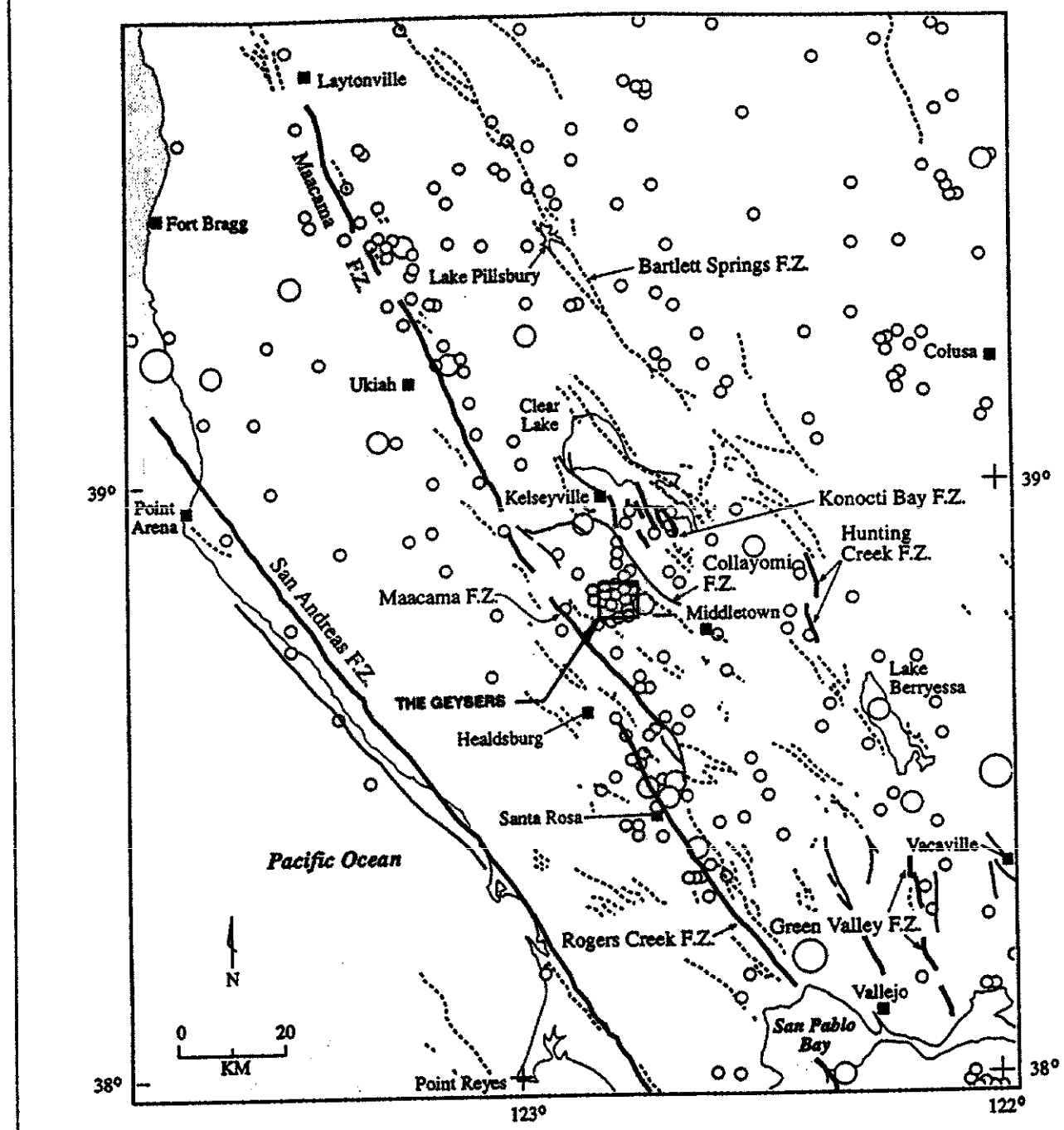

SOURCE: EPICENTERS FROM GOTER, 1988; FAULTS AFTER JENNINGS, 1992

Subregional Long-Term Wastewater Project

REGIONAL CAPABLE FAULTS AND SEISMICITY
$M_L \geq 3.0$ (1808-1987)

FIGURE 7.1

GEYSERS INDUCED SEISMICITY STUDY

REV. 2 SR408-33.DWG 01/10/96

PARSONS ENGINEERING SCIENCE, INC.

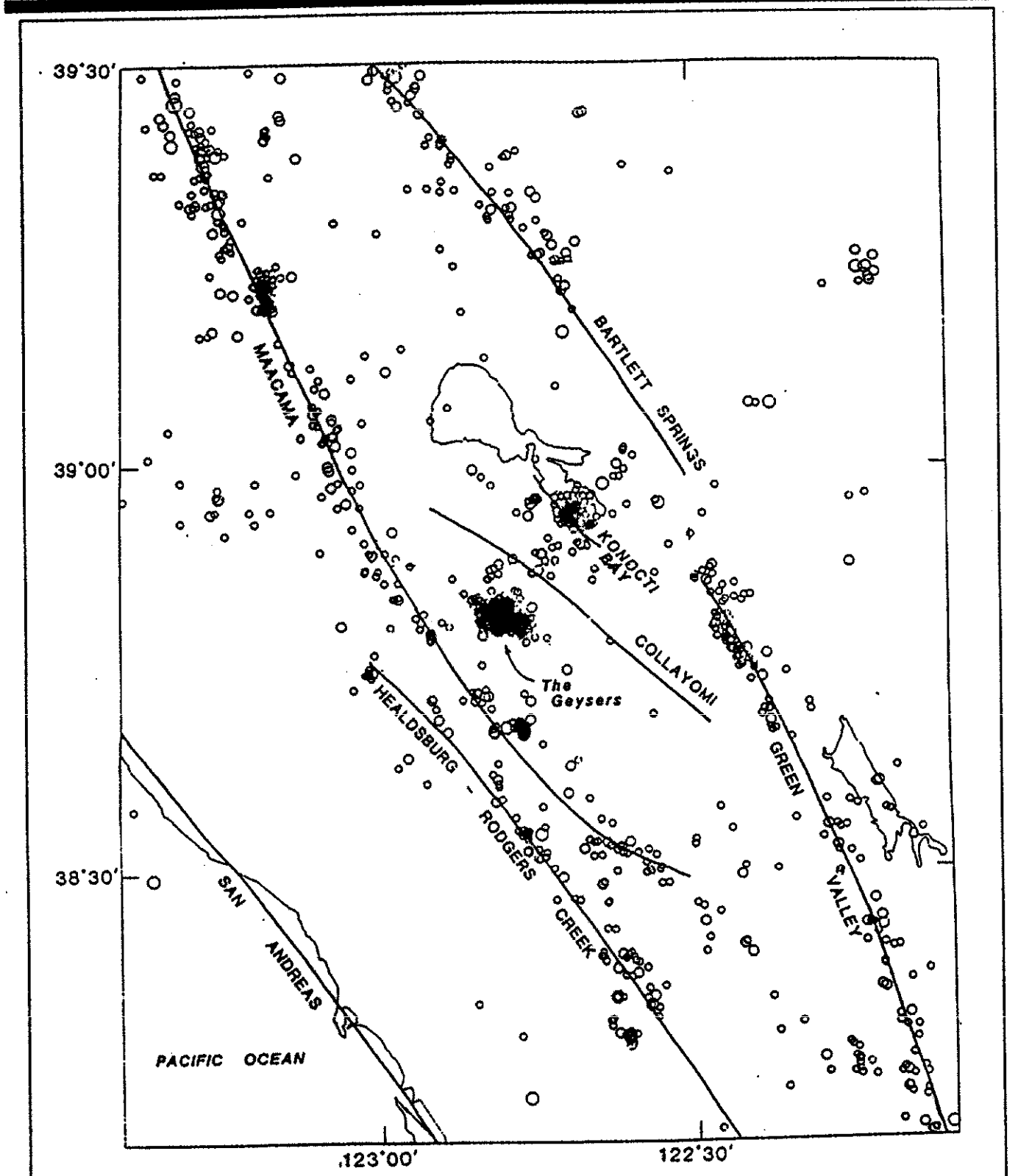

SOURCE: ADAPTED FROM EBERHART-PHILLIPS, 1988

Subregional Long-Term Wastewater Project

REGIONAL FAULTS AND SEISMICITY
$M_L \geq 1.5$, MARCH 1972-DECEMBER 1981

FIGURE 7.2

GEYSERS INDUCED SEISMICITY STUDY

REV. 2 SR408-34.DWG 01/10/96

PARSONS ENGINEERING SCIENCE, INC.

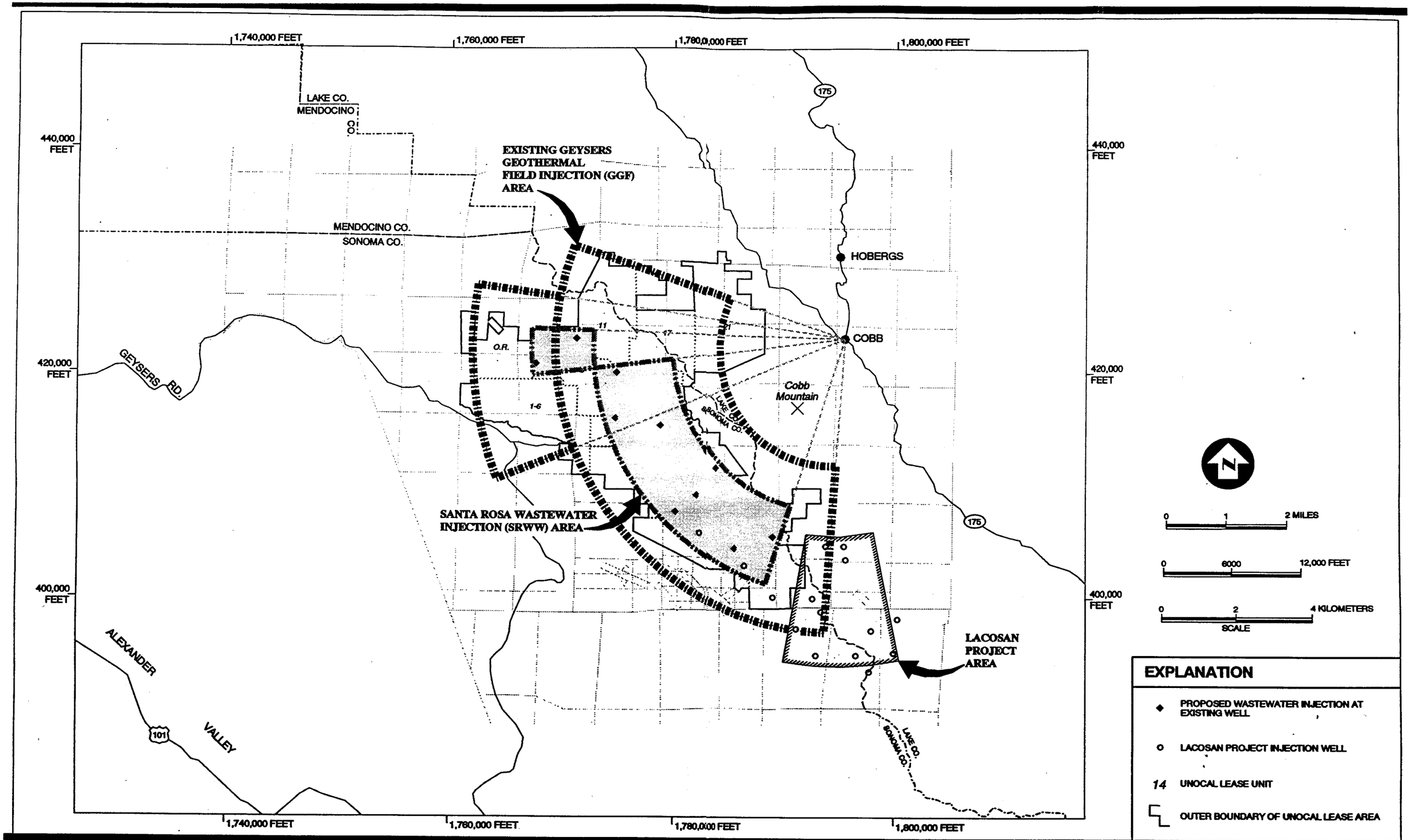

Santa Rosa
Subregional Long-Term Wastewater Project

MODEL GEOMETRY OF INDUCED SEISMICITY SOURCES

GEYSERS INDUCED SEISMICITY STUDY

FIGURE 7.3

REV. 2 SR406-04.DWG 01/10/96

PARSONS ENGINEERING SCIENCE, INC.

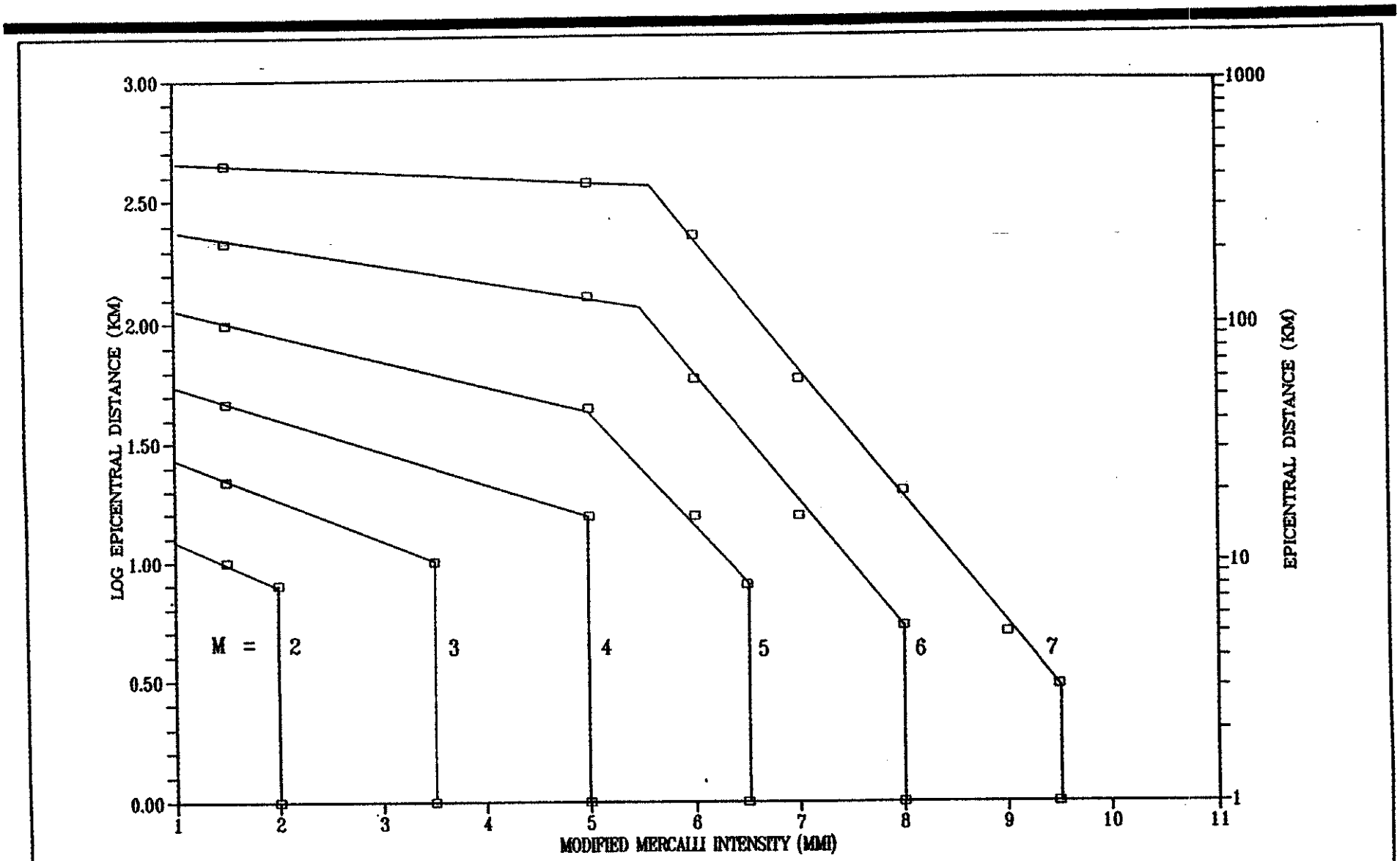

NOTE: CALCULATED FROM EQUATIONS BY TOPPOZADA, 1975

Subregional Long-Term Wastewater Project

MMI VS MAGNITUDE AND EPICENTRAL DISTANCE BASED ON FELT AREAS

GEYSERS INDUCED SEISMICITY STUDY

FIGURE 7.4

REV. 2 SR408-35.DWG 01/10/96

PARSONS ENGINEERING SCIENCE, INC.

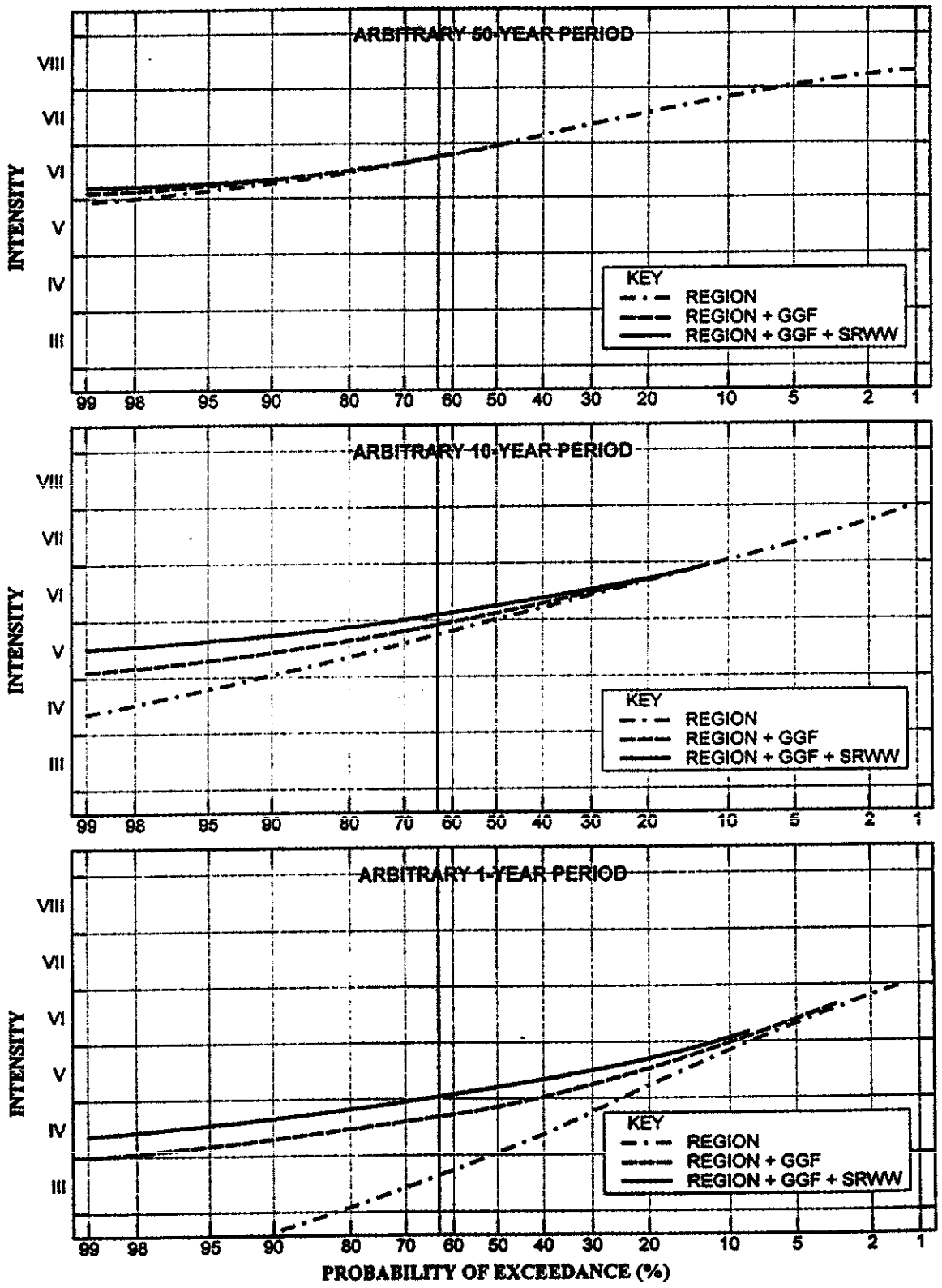

Subregional Long-Term Wastewater Project

INTENSITY VS. PROBABILITY OF EXCEEDANCE

FIGURE 7.5

GEYSERS INDUCED SEISMICITY STUDY

REV. 1 SR406-36.DWG 12/27/95

PARSONS ENGINEERING SCIENCE, INC.

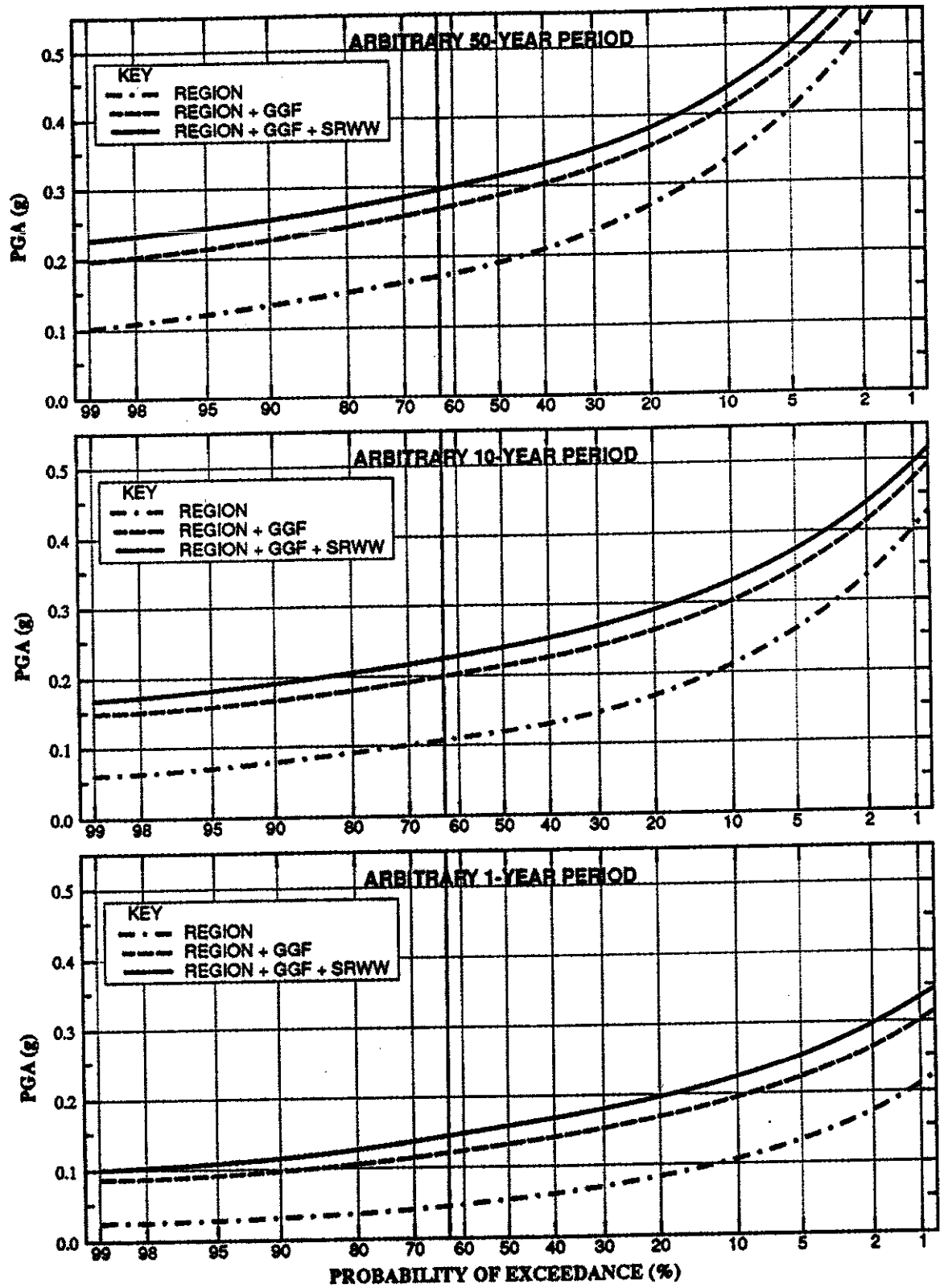

Santa Rosa
Subregional Long-Term Wastewater Project

PEAK GROUND ACCELERATION VS. PROBABILITY OF EXCEEDANCE

FIGURE 7.6

GEYSERS INDUCED SEISMICITY STUDY

REV. 3 SR408-37.DWG 02/13/96

PARSONS ENGINEERING SCIENCE, INC.

APPENDIX C

GLOSSARY

GLOSSARY

Aseismic	Condition of no seismicity (seen under **Seismicity**)
Coda	Latter part of an earthquake wave train.
Coefficient of friction	The shear stress required to induce slippage across a fracture divided by the normal stress (perpendicular to the fracture).
Confining pressure	Tends to close fractures; see under **Normal stress**.
Creep	Plastic deformation, not accompanied by seismicity; contrasts with elastic deformation, which may result in brittle failure and seismicity.
Effective/failure stress	Effective stress is lithostatic stress reduced by the pore pressure; failure stress is that stress required to produce brittle failure.
Epicenter	Point on earth's surface directly above earthquake *focus* (*hypocenter*).
Fault	A fracture surface along which two blocks of the earth's crust have experienced relative movement.
Focal depth	See under **Epicenter**
Focal mechanism	The type of fault rupture causing an earthquake; determined by analysis of seismograms recorded at many seismograph stations.
Focus	Initial point of seismic fault rupture.
Geodetic/geodetic strain	Refers to precise land surveys which, when repeated can measure tectonic strain (see under **Tectonic strain)**.
Holocene	Latest epoch of geologic time — the past 10,000 years; latest epoch of the Quaternary Period (last 2 million years).
Hydrostatic pressure/stress	Pressure or stress in a fluid or pore fluid (e.g., in a rock mass).
Hypocenter	See under **Focus**.
Intensity	See under **Modified Mercalli Intensity**
Lithostatic pressure/stress	Pressure or stress in the solid particles of a rock mass; distinct from the *hydrostatic* stress (see under **Hydrostatic stress).**
Magnitude	A measure of the intrinsic size of an earthquake, *not* to be confused with *intensity*, which rates *effects* at particular

	places. A unit-increase in magnitude represents a 30-fold increase in elastic wave energy radiated by an earthquake. There are several methods of calculating magnitude: Richter or local (M_l), coda-length (M_c), and others. For $M < 7$ they all they yield similar numbers; for $M < 5$, M_c and M_l agree within about 0.2 units.
Modified Mercalli Intensity (MMI)	One of several scales used to qualitatively rate earthquake *effects* on people, structures, objects, and the ground surface. The MMI scale has been the accepted standard in North America and Europe since 1931. It can be considered a quasi-quantitative ranking of the energy of earthquake ground shaking.
Microearthquake	Earthquake with $M \leq 3.0$; so-called because few of these are ever felt by persons.
Microseismicity	See under **Seismicity**.
Moment	A measure of radiated energy (usually in dyne-cm); the logarithm of moment is linearly related to magnitude.
Normal stress	Compressive stress acting across a fracture (tending to close it and prevent slippage); see under **Confining pressure**.
Peak Ground Acceleration (PGA)	Maximum acceleration amplitude of earthquake ground shaking, usually expressed as a fraction of the acceleration (weight-force) due to gravity (1 g). [A vertical acceleration over 1 g will cause free objects to leave the ground.]
Quaternary	Latest geologic period (last 2 million years).
Poisson's Ratio	A parameter of elasticity.
Pore Pressure	Fluid pressure in the pore volume of a (rock) mass.
Pressure axis of stress	Maximum principal stress; see under **Principal stress**.
Principal extension	Strain directed along the axis of greatest extension (least principal strain) of the strain tensor.
Principal stress	Stress directed along one of the three axes of the stress tensor (*maximum, minimum, and intermediate* principal stresses/axes).
Seismicity	Rate of occurrence and magnitude distribution of earthquakes in any selected region; *microseismicity* refers to earthquakes with $M \leq 3.0$.
Seismic moment	A measure of the size of an earthquake, based on the product of fault rupture area and amount of slip.

Shear modulus	The rigidity of a material, calculated as shear stress divided by shear strain.
Shear stress	Stress which produces shear strain; capable of causing slippage along a fracture.
Strain rate	Change of strain with time; see **Tectonic strain**.
Tectonic	Pertaining to deformation of the earth's crust and upper mantle; may be quantified in terms of stress or strain, or strain rate.
Tectonic stress/strain	Elastic stress/strain in a given block of the earth's crust or upper mantle.
Tension axis of stress	Minimum principal stress; see under **Principal stress**.
Volumetric contraction	Volumetric strain; changes of dimension are the same for all orientations.

APPENDIX D

REFERENCES CITED

REFERENCES CITED

Allis, R.G. 1981, Comparison of mechanisms proposed for induced seismicity at The Geysers geothermal field, In: *Proceedings of the 3rd New Zealand Geothermal Workshop*, Auckland NZ, pp. 57-61.

Barker, B.J., et al. 1991, Geysers Reservoir Performance, In: *Geothermal Resources Council, Monograph on The Geysers Geothermal Field, Special Report No. 17*, pp. 167-177.

Barker, B.J., Koenig, B.A., and Stark, M.A. 1995, Water injection management for resource maximization: observations from 25 years at The Geysers, California, In: *Proceedings of the World Geothermal Congress*, Florence, Italy, May 1995.

Batini, F., Console, R., and Luongo, G. 1985, Seismological study of the Larderello-Travale geothermal area, *Geothermics* 14:255-272.

Bendat, J.S. and A.G. Piersol 1966, *Measurement and Analysis of Random Data*, John Wiley, New York.

Benjamin, J.R., and Cornell, C.A. 1971, *Probability, Statistics, and Decisions for Civil Engineers*, McGraw Hill, New York, 864 pp.

Bromley, C.J., Pearson, C.F., and Rigor, D.M. 1987, Microearthquakes at the Puhagan geothermal field, Philippines; a case of induced seismicity, *Journal of Volcanology and Geothermal Research* 31:293-311.

Bromley, C.J., and Rigor, D.M. 1983, Microseismic studies in Tongonan and Southern Negros, In: *Proceedings of the 5th New Zealand Geothermal Workshop*, Geothermal Institute, University of Auckland.

Bufe, C.G. and Ludwin, R.S. 1980, Continued Seismic Monitoring of The Geysers, California Geothermal Area, *U.S. Geological Survey, Open File Report 80-60.*

Bufe, C.G. et al. 1981, Seismicity of the Geysers-Clear Lake region, In: Research in The Geysers-Clear Lake Geothermal Area, Northern California, *U.S. Geological Survey Professional Paper 1141*, pp. 129-137.

Campbell, K.W. 1989, The dependence of peak horizontal acceleration on magnitude, distance, and site effects for small-magnitude earthquakes in California and eastern North America, *Bulletin of the Seismological Society America* 79:1311-1335.

Crow, E.L., Davis, F.A., and Maxfield, M.W. 1960. *Statistics Manual*, Dover Publications, New York.

Cumming, W.B. 1996, Comments on the Geysers induced seismicity study for the Santa Rosa Wastewater Project (SRWP), *Unocal internal memorandum to D.S. Hackley*, January 11, 1996.

Eberhart-Phillips, D. 1988, Seismicity in the Clear Lake area, California, In: *Geological Society America, Special Paper 214*, pp. 195-206.

Eberhart-Phillips, D., and Oppenheimer, D. 1984, Induced seismicity in The Geysers geothermal area, California, *Journal of Geophysical Research* 89:1191-1207.

Ellsworth, W.L. 1990, Earthquake history, In: The San Andreas Fault System, California, *U.S. Geological Survey Professional Paper 1515*, pp. 153-188.

Enedy, S.L., Enedy, K.L., and Maney, J. 1991, Reservoir response to injection in the southeast Geysers, In: *Geothermal Resources Council, Monograph on The Geysers Geothermal Field, Special Report No. 17*, pp. 211-219.

ESA (Environmental Science Associates) 1994, *Southeast Regional Wastewater Treatment Plant Facilities Improvements Project and Geysers Effluent Pipeline Project Draft EIR/EIS*. Appendix B: GeothermEx, Inc., Analysis of Geothermal Reservoir Effects and Induced Seismicity.

Fabriol, H., et al. 1992, Microseismic monitoring during production and reinjection tests in the Chipilapa geothermal field (El Salvador), *Geothermal Resources Council Transactions* 16:221-225.

Goter, S.K. 1988, Seismicity of California, 1808-1987, *U.S. Geological Survey, Open-File Report 88-286*.

Greensfelder, R.W. 1993, New evidence of the causative relationship between well injection and microseismicity in The Geysers geothermal field, *Geothermal Resources Council Transactions* 17:243-247.

Gumbel, E.J. 1958, *Statistics of Extremes*, Columbia University Press, New York.

Gutenberg, B., and Richter, C.F. 1956, Earthquake magnitude, intensity, energy, and acceleration, *Bulletin of the Seismological Society America* 32:163-191.

Hamilton, R.M., and Muffler, L.J.P. 1972, Microearthquakes at The Geysers geothermal area, California, *Journal of Geophysical Research* 77:2081-2086.

Hubbert, M.K., and Rubey, W.W., 1959, Role of fluid pressure in mechanics of overthrust faulting, *Geological Society of America Bulletin* 70:115-166.

Hunt, T.M., et al. 1990, Results of a 13-month reinjection test at Wairakei geothermal field, New Zealand, *Geothermal Resources Council Transactions* 14: Pt II.

Jennings, C.W. 1992, Preliminary Fault Activity Map of California, *California Division Mines & Geology, Open-File Report 92-03.*

King, G.C.P., Stein, R.S., and Lin, J. 1995, Static stress changes and the triggering of earthquakes, *Bulletin of the Seismological Society America* 84:935-953.

Klein, C. and Enedy, S.L. 1991, Effect of condensate injection on steam chemistry at the Geysers field, *Geothermal Resources Council, Monograph on The Geysers Geothermal Field, Special Report No. 17*, pp. 167-177.

Kirkpatrick, A., Peterson, J.E., and Majer, E.L. 1995, Microearthquake monitoring at the southeast Geysers using a high-resolution digital array, In: *Proceedings of the 20th Annual Geothermal Workshop*, Stanford, February 1995.

McLaughlin, R.J. 1981, Tectonic setting of pre-Tertiary rocks and its relation to geothermal resources in the Geysers-Clear Lake area, In: *U.S. Geological Survey Professional Paper 1141*, pp. 3-24.

National Academy of Sciences and National Academy of Engineering (NAS/NAE) 1972, Earthquakes Related to Reservoir Engineering, In: *Report by the joint panel on problems concerning seismology and rock mechanics.*

Oppenheimer, D.H. 1986, Extensional tectonics at The Geysers geothermal area, California, *Journal of Geophysical Research* 91:11,463-11,476.

Prescott, W.H., and Yu, S. 1986, Geodetic measurement of horizontal deformation in the northern San Francisco Bay region, California, *Journal Geophysical Research* 91:7475-7484.

Romero, A.E. et al. 1994, Seismic monitoring at The Geysers geothermal field, *Geothermal Resources Council Transactions* 18:331-338.

Stark, M.A. 1990, Imaging injected water in the Geysers reservoir using microearthquake data, *Geothermal Resources Council Transactions* 14:1697-1704.

Sherburn, S. 1984, Seismic monitoring during a cold-water injection experiment, Wairakei geothermal field: preliminary results, In: *Proceedings of the 6th New Zealand Geothermal Workshop,* Geothermal Institute, University of Auckland.

Sherburn, S., Allis, R., and Clotworthy, A. 1990, Microseismic activity at Wairakei and Ohaaki geothermal fields, In: *Proceedings of the 12th New Zealand Geothermal Workshop*, Geothermal Institute, University of Auckland.

Talwani, P. 1981, Earthquake prediction studies in South Carolina, In: *Earthquake Prediction-an International Review*, American Geophysical Union, Maurice Ewing Series 4, pp. 381-393.

Thompson, R.C. and Gunderson, R.P. 1991, The orientation of steam-bearing fractures at the Geysers geothermal field, *Geothermal Resources Council, Monograph on The Geysers Geothermal Field, Special Report No. 17*, pp. 65-68.

Toppozada, T.R. 1975, Earthquake magnitude as a function of intensity data in California and western Nevada, *Bulletin of the Seismological Society America* 65:1223-1238.

Trifunac, M.D., and Brady, A.G. 1975, On the correlation of seismic intensity scales with the peaks of recorded strong ground motion, *Bulletin of the Seismological Society America* 75:139-162.

Walter, M.A., and Combs, J. 1991, Heat flow in The Geysers-Clear Lake geothermal area of northern California, U.S.A., *Geothermal Resources Council, Monograph on The Geysers Geothermal Field, Special Report No. 17*, pp. 43-53.

U.S. Geological Survey 1990, Probabilities of Large Earthquakes in the San Francisco Bay Region, California, *U.S. Geological Survey Circular 1053*.

Voge, E., et al. 1991, Initial findings of the Geysers Unit 18 cooperative injection project, In: *Proceedings of Annual Fall Meeting, Geothermal Resources Council*, 1994.

Wood, H.O., and Neumann, F. 1931, Modified Mercalli intensity scale of 1931, *Bulletin of the Seismological Society America* 21:277-283.